TÉCNICO LISBOA

Simultaneous separation of impurities and exchange of surrounding media in Nanolignin suspensions

Rita Caiado Gaspar

Thesis to obtain the Master of Science Degree in

Chemical Engineering

Supervisors: Professor Anton Friedl (TU Wien)

Professor Maria Norberta Correia de Pinho (IST)

Examination Committee

Chairperson: Professor Henrique Matos (IST)

Supervisor: Professor Anton Friedl (TU Wien)

Member of the Committee: Professor Ana Clara Marques (IST)

November 2018

Acknowledgements

I would like to address a special thanks to Professor Maria Norberta de Pinho, as a supervisor, for the opportunity to carry out this work abroad, for the knowledge transmitted and for its essential suggestions.

This master thesis has been performed at the Institute of Chemical, Environmental and Bioscience Engineering, TU Wien, in Vienna (Austria) which I would like to thank everyone at the department for the friendly and supportive environment during my presence in Vienna, especially to my supervisor Professor Anton Friedl for the opportunity to carry this work at TU Wien, for receiving me, treating and providing me everything so kindly while I was staying in Vienna. The experimental work and the suggestions for improving my thesis could not have been conducted without the support from Stefan Beisl and Dr. Martin Miltner to which I am very grateful. **Works by the master student are based on a technology TU Wien has applied international patent protection for (priority application: Austria, A 51180/2016 and A 50527/2018).**

Finally, I am also very grateful to my closest friends and family who have supported me during all this time.

Abstract

Lignin is a source of low value products which comes from pulp and paper industry or from cellulosic biorefineries. The production of nanolignin particles with a larger surface area than standard lignin, enhance the properties of this molecule, originating more applications.

The aim of this work was to evaluate the performance of an ultrafiltration in diafiltration mode operation by using membranes with different MWCO for the separation and purification of nanolignin particles from a suspension made of wheat straw extract, produced by an Organosolv Pre-treatment. The suspension was filtrated in a laboratory scale cross-flow system.

A particle size evaluation of all the ultrafiltration permeates, revealed that no nanolignin particles exist in the permeates which means that all the lignin nanoparticles are retained by the chosen membranes.

For a TMP of 8 bar and 0.7 L/min of feed flow-rate, the membrane which showed the most promising results to separate nanolignin particles from the other impurities present in the suspension was the 30 kDa membrane, showing a percentage of removal efficiency of dissolved components of approximately 47%, which means that this membrane is more efficient at separating and purifying the nanolignin particles, for the indicated operating conditions.

The 30 kDa membrane was then used to optimize the operating conditions to reduce the fouling effect, by varying the TMP and the feed flow-rate. For the optimization experiments using the 30 kDa membrane, 4 bar of transmembrane pressure and a feed flow-rate of 0.7 L/min showed a removal efficiency of dissolved components of 61%.

Keywords: ultrafiltration, wheat straw, nanolignin, purification, diafiltration, Organosolv.

Resumo

A lenhina é uma fonte de produtos de baixo valor proveniente da indústria da pasta e papel ou de bio refinarias. A produção de partículas de nanolenhina com uma área superficial superior à da lenhina padrão amplia as propriedades dessa molécula, aumentando as aplicações em que pode ser usada.

O objetivo desta tese foi avaliar o desempenho de uma operação de ultrafiltração em modo de diafiltração utilizando membranas com diferentes limites de exclusão molecular para a separação e purificação de partículas de nanolenhina a partir de uma suspensão feita de palha de trigo, produzida através de um pré-tratamento Organosolv. A suspensão foi filtrada num sistema de filtração tangencial em escala laboratorial.

Uma análise do tamanho das partículas em todas as amostras de permeado demonstrou que todas as nanopartículas são retidas pelas membranas.
Ao utilizar membranas de ultrafiltração com diferentes limites de exclusão molecular com uma pressão transmembranar de 8 bar e um fluxo de alimentação de 0.7 L/min, a membrana que apresentou os resultados mais promissores para separar as partículas de nanolenhina das outras impurezas presentes na suspensão foi a membrana de 30 kDa, com uma percentagem de remoção dos componentes dissolvidos de 47%.
Para os ensaios de otimização com a membrana de 30 kDa, a pressão transmembranar e o fluxo de alimentação foram alterados para reduzir o efeito do fouling. A experiência com uma pressão transmembranar de 4 bar e um fluxo de alimentação de 0.7 L/min mostrou os melhores resultados com uma percentagem de componentes dissolvidos da suspensão inicial de 61%.

Palavras-chave: ultrafiltração, palha de trigo, nanolenhina, purificação, diafiltração, Organosolv.

Table of contents

List of Acronyms and Nomenclature

Acronyms

Buna-N- acrylonitrile butadiene rubber

EDTA- *Ethylenediamine tetraacetic acid*

KL – Kraft Lignin

MF – microfiltration

MWCO – molecular weight cut-off

NF – nanofiltration

OL – Organosolv Lignin

PES – Polyethersulphone

PESH – Hydrophilic Polyethersulphone

PSU – Polysulphone

RO – reverse osmosis

SEM – Scanning Electron Microscopy

SL – soda Lignin

TF – Transmembrane Flux

TMP – Transmembrane Pressure

UF – ultrafiltration

Nomenclature

A_m - membrane active area

C_f - feed concentration

C_p - permeate concentration

C_m - concentration on the membrane

D - diffusion coefficient

DM – Dry Matter

$DM_{sample\ bef.centri.}$ - dry matter concentration of the sample before centrifugation

$\mathrm{DM}_{\mathrm{sample\ after\ centri.}}$ - dry matter concentration of the sample after centrifugation

$DM_{initial\ suspension}$ - DM amount of the initial suspension

DM_{W2R2} - DM amount of the final retentate (W2R2)

$DM_{samples}$ - DM amount of each of the samples taken

$DM_{permeates}$ - DM amount of each of the collected permeates

$DM_{permeate}$ - DM amount in each permeate

$DM_{initial}$ - DM amount of dissolved components in the initial suspension

J - permeate flux

k - mass transfer coefficient

LC - nanolignin particles concentration

L_p- hydraulic permeability

$M_{dry\ sample}$ - mass of sample after being dried

$M_{inital\ sample}$ - mass of initial sample taken

ΔP - transmembrane pressure

Re - Reynolds Number

R- Retention coefficient

RE- Removal Efficiency

Sc – Schmidt Number

Sh – Sherwood Number

TMS - total mass of the system at each time

$TMS_{initial}$ - initial mass of nanolignin suspension

TNL_{sample} - total nanolignin particles in the sample taken

$TOC\ nanolignin\ particles$ -TOC associated with nanolignin in the solution

$TOCsample$ - TOC of retentate sample before centrifugation

$TOCethanol$ - TOC associated with ethanol in the solution

$TOCdis.components$ - TOC of other dissolved components in the solution

$\mathrm{TOC}_{\mathrm{supernatant}}$ -TOC of supernatant of retentate sample after centrifugation

TNL_{sample} - total nanolignin particles in the sample taken

$TOC_{initial\ suspension}$ - TOC amount of the initial suspension

TOC_{W2R2} -TOC amount of the final retentate (W2R2)

$TOC_{samples}$ - TOC amount of each of the samples taken

$TOC_{permeates}$ - TOC amount of each of the collected permeates

$TOC_{permeate}$ = TOC amount in each permeate

v- linear speed

μ_s - viscosity of the solvent (pure water in this case)

$\Delta\pi$ - average osmotic pressure

R- retention coefficient

δ - boundary layer thickness

η - dynamic viscosity

List of Figures

List of Tables

1 Introduction

Lignin is the second most abundant biopolymer on earth, after cellulose. It confers rigidity, resistance and impermeability to plant cell walls (Rastogi and Dwivedi 2008). Normally, lignin is a by-product of paper and pulp industry and for the past years, the goal was to remove as much lignin as possible from cellulose to produce high quality paper. This delignification process brings environmental concerns and produces a lignin that is a low added-value product. This lignin is mainly incinerated and used to produce energy (Mohan, Pittman, and Steele 2006).

In a near future, the need to maximize the paper industry by-products valorization and the increase of biorefinery projects, will produce a great amount of lignin. The problem with most biorefineries is that the main concern is the valorization of cellulose and hemicellulose, while lignin is still considered a low-value by-product (FitzPatrick et al. 2010). Lignin is produced as a compound with a complex structure and has uncertain reactivity, which limits its wide-scale use in biorefineries. Roughly, the factors that prevent the use of technical lignin as a high-value-added product are similar for all different types of lignin (Vishtal and Kraslawski 2011).

One of the ways to fractionate lignocellulosic raw materials is by using an Organosolv pre-treatment, which applies organic solvent/water mixtures, at elevated temperatures, to break the plant structure into its different components (cellulose, hemicellulose and lignin). By using an Organosolv process to separate the plant components, the result is a less modified lignin molecule, with less chemical changes than the lignin from lignosulphonates or alkali lignin (Lora 2008).

To maximize lignin valorization, it is possible to produce nanolignin particles which have a different and wide variety of applications than standard lignin, mainly because these nanoparticles have a higher specific surface area (Xu et al. 2007). As researchers find more and more applications for nanolignin particles (Beisl, Friedl, and Miltner 2017), it becomes necessary to find a way of isolating and purifying this particles, to eventually produce them in an industrial scale. The main problem with isolating and purifying these nanoparticles is to separate them from the other components in the suspension, such as cellulose, hemicellulose and dissolved lignin.

2 Literature Review

2.1 Lignin

The main components of plant cell wall structure are cellulose, hemicellulose and lignin. Cellulose can be hydrolyzed into the monomer Glucose. The major use of cellulose is in pulp and paper industry and smaller quantities are used to in other applications such as biofuels (cellulosic ethanol).

Lignin is a complex macromolecule which consists mainly of phenylpropane units from three different aromatic alcohols (p-coumaryl, coniferyl and sinapyl alcohols) (Gordobil et al. 2016). Basically, lignins from different sources have different percentages of these aromatic alcohols. Usually, three different types of lignin can be identified: softwood lignins, which comprise mostly coniferyl, hardwood lignins made of coniferyl and sinapyl alcohols and grass lignins, which comprise the three different alcohols (Gellerstedt and Henriksson 2008). The percentage of the main components of different plants is shown on Table 1.

Table 1. Main components % in different plants (Ragauskas et al. 2014)(del Río, Rencoret, and Prinsen 2013).

Feedstock	% Cellulose	% Hemicellulose	% Lignin
Miscanthus	45-52	24-33	9-13
Switchgrass	37-32	26-33	17-18
Corn Stover	37	31	18
Poplar	42-48	16-22	21-27
Eucalyptus	39-46	24-28	29-32
Wheat Straw	35-45	20-30	15
Pine	46	23	28

Furthermore, lignin can also be divided in two different groups, the first is the lignin recovered before carbohydrate conversion and the second one is lignin recovered after carbohydrates conversion. The second one is usually used for low-added value products while the first one has less structural changes and can be used to high-added value products. Lignin that is recovered before the carbohydrate conversion can be pre-treated in several different ways.

2.1.1 Lignocellulosic biomass pre-treatments

There are several pre-treatments to lignocellulosic biomass, which differ in the type of raw material used, as well as the process conditions. Different lignocellulosic raw materials and different conditions produce different types of lignin macromolecules which can be classified in to Kraft Lignin (KL), Soda Lignin (SL), lignosulphonates (LS), Organosolv Lignin (OL) and enzymatic hydrolysis lignin (EHL) (Vishtal and Kraslawski 2011).

The Organosolv lignin (OL) process uses a solution of an organic solvent with water and with or without a catalyst, at specific conditions to separate Lignin and Hemicelluloses. There are several solvents available for this purpose, which includes alcohols (methanol, ethanol, ethylene glycol, butanol, etc.), organic acids (formic and acetic) and ketones (acetone and other ketones) among others (Xu et al. 2006).

Organosolv lignin is known for its high purity, reactivity towards modification and low and uniform molecular weight (Lora and Glasser 2002). At the same time, the Organosolv process is more environmental responsible, as the solvents are usually recovered by distillation, which decreases water pollution and eliminates the odor associated with other lignin recovery processes such as, Kraft process.

Several experiments using different organic solvents were performed over the years to isolate lignin, but, using ethanol as the organic solvent for the recovery of OL, shows some advantages. To begin with, numerous experiments were made showing the efficiency of the separation by using this solvent (Gordobil et al. 2016). On the other hand, ethanol is available easily and at low costs. The usage of ethanol for the Organosolv process requires operation temperatures of 160-180 ºC and, as ethanol is highly volatile and creates a higher vapor pressure than water it is required a high-pressure reactor (Yebo and Khanal 2016).

2.1.2 Nanolignin particles production

One of the ways to overcome the complexity and the lack of homogeneity of the lignin particles, is to produce nanolignin particles. The production of nanoparticles has an advantage when compared with standard size particles because nanoparticles have a larger surface area. So far, there are several methods to produce this type of particles which differ on the size of the particles formed and the materials and conditions of the experiments. As for the particle size, the particles vary from a range of a few dozens to a few thousand nanometers. The next figure, Figure 1, summarizes the methods found in literature to produce micro and nano size lignin particles.

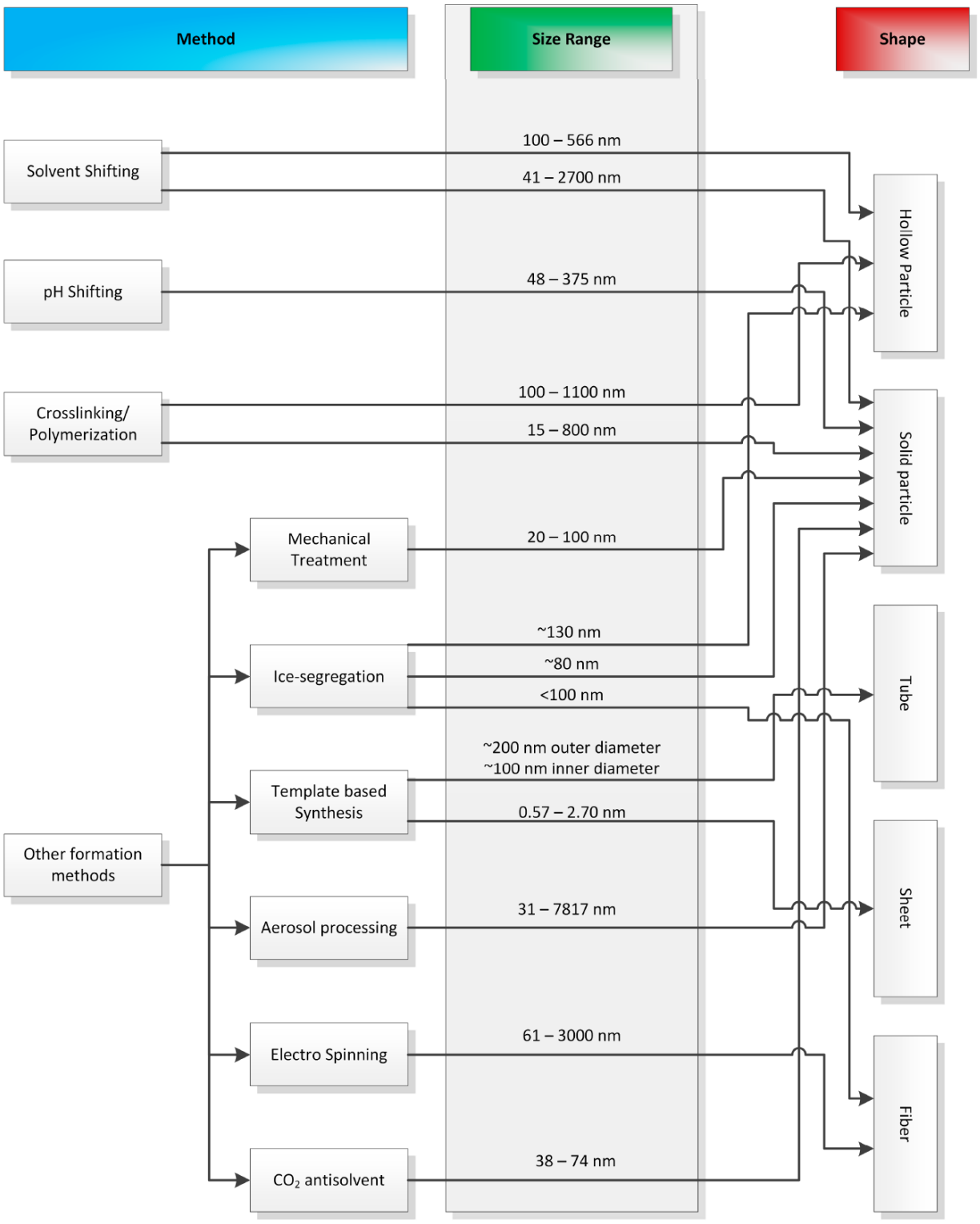

Figure 1. Nano and micro size lignin production methods (Beisl, Friedl, and Miltner 2018).

Solvent Shifting

Solvent shifting includes the addition of an excess of water to a solution of an organic compound in a water soluble organic solvent. The addition of water decreases the solubility of the particles making them precipitate and forming the nanoparticles. The major limitation of this method is the low solid content. (around 1 wt%), which can be obtained. By varying the conditions used in the solvent shifting method, different sizes and shapes of particles are obtained. For example, using water as an anti-solvent, and different solvents, such as tetrahydrofuran (THF), acetone/water and dimethyl sulfoxide (DMSO), produced nanolignin particles with a size range between 41 and 2700 nm. On the other hand, it is also possible to produce hollow particles with a size range between 100-566 nm by changing the solvent and antisolvent conditions (Beisl, Friedl, et al. 2018). Several other methods have already been used to produce nanoparticles, but the research of using these methods to produce the nanolignin particles is still in its early stages.

2.1.3 Nanolignin particles production from wheat straw

Wheat straw is an agricultural waste that has a great potential as a source of biorefineries feedstock because it is available worldwide and at a low cost. Wheat straw world production was estimated to be around 680 million tons in 2011 (del Río et al. 2013). The wheat straw is composed of approximately 38.2% cellulose, 21.2 % hemicellulose, 23.4 % lignin and 17.2 % other components. (Mosier et al. 2005).

The wheat straw structure can be ruptured at high temperatures and under pressure by doing an Organosolv pre-treatment. By changing the organic solvent and the temperature and pressure conditions, different wheat straw extracts are produced. The extract produced using the Organosolv pre-treatment is a complex mixture of components, in which lignin is included. The main components of this mixture are lignin, water and the organic solvent. Cellulose, hemicellulose and other components that exist in the wheat straw extract at low concentrations, are considered impurities. The precipitation of Organosolv Lignin (OL), can be affected by several factors, for example, the nanolignin particles can agglomerate with themselves or with the impurities causing the precipitation of unwanted particles of bigger sizes.

A paper on the production of nanolignin particles from wheat straw was found in the literature. Other methods exist to produce nanoparticles of lignin from wheat straw, but direct precipitation of lignin nanoparticles reduces the solvent consumption, which is an economical and environmental concern (Beisl, Loidolt, et al. 2018). These experiments used an Organosolv Pre-treatment with a 60 w/w % aqueous ethanol solution at 180 ºC to produce wheat straw extract.

2.1.4 Micro and Nanolignin Particles Applications

The production of nanoparticles can be done by several methods, which include solvent shifting. The production on nanolignin particles originated from dissolved lignin particles from lignocellulosic biomass has been studied before. Depending of the size and the shape of the produced particles, they can be used in different applications.

Lignin is known for its UV absorption, high stiffness, ability to retard oxidation reactions and its resistance to decay and biological attacks. By producing micro or nanolignin particles, these characteristics of the lignin macromolecule can be enhanced and used for a great variety of applications. The next figure, Figure 2, resumes the applications found in literature for nano and micro lignin particles.

Figure 2. Micro and nanolignin applications found in literature (Beisl et al. 2017).

2.2 Membranes

2.2.1 Pressure Driven Membrane Processes

One of most common membrane processes are the ones which are based on pressure difference between the feed and the permeate. This type of membrane processes includes Ultrafiltration (UF), Microfiltration (MF), Nanofiltration (NF) and Reverse Osmosis (RO). The next table, Table 2, summarizes the pressure driven membrane processes characteristics and Figure 3 shows the common applications for each of these processes.

Table 2. Pressure Driven membrane Processes(Strathmann 1986).

Membrane Process	Membrane type	Transmembrane Pressure	Mechanism
Reverse Osmosis (RO)	Asymmetric composite with homogeneous skin	High (20-100 bar)	Solution-diffusion
Nanofiltration	Asymmetric composite with homogeneous skin	High (10-40 bar)	Solution-diffusion
Ultrafiltration (UF)	Asymmetric microporous	Low (0.5- 8 bar)	Size exclusion and electrostatic interactions
Microfiltration (MF)	Symmetric and asymmetric microporous	Low (0.1-1 bar)	Size exclusion

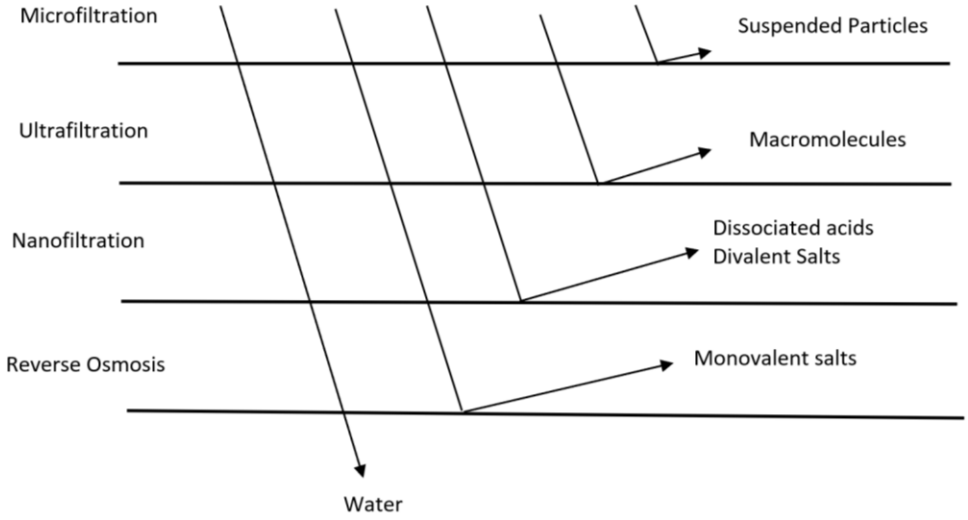

Figure 3. Pressure driven membrane applications adapted from (Luque, Gómez, and Álvarez 2008).

Ultrafiltration

Due to the size of the molecules and particles that compose the nanoparticles suspension from wheat straw, the most indicated pressure driven membrane process to use is Ultrafiltration (UF). This membrane process has been used since the last century for concentration and purification in laboratory scale experiments. The problem with the first ultrafiltration membranes was the low chemical and mechanical resistance and the high permeabilities required for applications in industrial scale. In the early 1960's the development of asymmetric reverse osmosis membranes by Loed and Sourirajan changed this situation, as this new membranes could also be used for ultrafiltration processes (Strathmann 1986). The

ultrafiltration process separation is distinguished from microfiltration and reverse osmosis basically by the size of the particles that is possible to retain. UF membranes can retain particles from a molecular weight of 500 g/mol to colloidal particles with a diameter of 0.2 μm.

2.2.2 Membrane Classification

The membrane structure for ultrafiltration membranes is an asymmetric structure made by the Loeb-Sourirajan method. This membrane type is used mainly because it allows high permeation fluxes and high selectivity. An asymmetric membrane (Figure 4) is made of a thin surface layer supported by a thicker and porous substructure (Baker 2001). This kind of membranes are commonly produced by using the Phase Inversion method. This technique allows the formation of a two layer membrane, where the upper layer is thin and dense while the lower layer is porous and only responsible for giving the membrane mechanical resistance, by using a casting solution. The Phase Inversion method revolutionized the production of asymmetric membranes as it permits the use of a great variety of polymers and casting solutions, which can be adapted to suppress the need of each different separation (Strathmann 1986). In Figure 5, is represented an example of a membrane prepared by the phase inversion method.

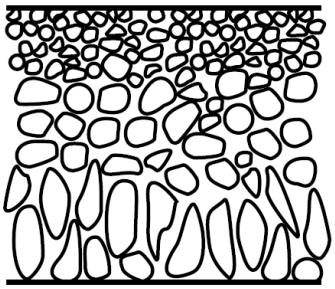

Figure 4. Loeb- Sourirajan Asymmetric membrane (Baker 2001).

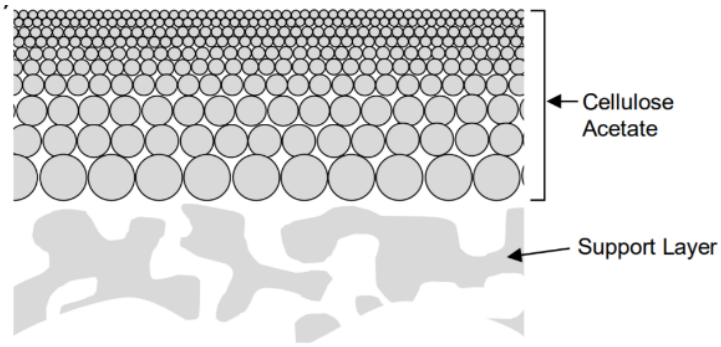

Figure 5. Cellulose acetate membrane prepared by phase inversion with a support layer made of a different material (Microdyn-Nadir 2017).

Asymmetric membranes can be made of two different materials, a supporting material which function is to support and the active layer responsible for the particle separation. The support material should be porous, allowing the membrane to have more mechanical and chemical resistance (Microdyn-Nadir

2017). On the other hand, the active layer can still be prepared with Phase inversion method, which will transform the membrane in to an apparent three layer membrane.

2.2.3 Membrane Material

The great amount of different processes that use membranes as a separation process justifies the wide variety of membrane materials that exist nowadays. Membrane materials are usually divided in three types, inorganic, which includes glass, ceramic and metallic materials, natural polymers, the ones derived from cellulose and synthetic polymers, which includes polyamide, Polysulphone, polypropylene, etc. (Nunes and K.-V. 2001).

The most frequently polymers to produce this type of membranes are Polysulfone (PSU) and Polyethersulfone (PES). PSU exhibits resistance to extreme pH conditions and a higher thermal stability when compared with other membrane materials. A disadvantage of Polysulfone is its high solubility in organic solvents, which does not make this material suitable to use when processing solutions with an organic solvent based feed. Furthermore, PSU and PES membranes have a hydrophobic character, which requires that the membranes are treated with a hydrophobic agent, like glycerin or prevented from drying. This hydrophobic property also affects the separation process as the membranes have a nonspecific adsorption capacity. Recently, new technologies allow PES membranes to be transformed in to hydrophilic membranes by different techniques (Rana et al. 2005).

Another used membrane in the UF processes is Poly (vinylidene fluoride) (PVDF) which is a polymer with a good chemical resistance to aromatic hydrocarbons, alcohols, TDF and halogenated solvents. It is also stable in a great variety of pH range (Liu et al. 2011).

Membranes made of Cellulose, a natural polymer, are used when low fouling features are required. This type of membrane has a regular structure able to form stable hydrogen-bonds between the hydroxy groups, which makes this membrane suitable to use with material almost all solvents. Nowadays, one of the most regular Cellulose membrane types is Cellulose Acetate which is prepared by hydrolysis of asymmetric cellulose acetate membranes (Bhongsuwan and Bhongsuwan 2008).

The selection of the membrane material depends on a variety of factors such as the composition of the feed solution, the separation goals and the operating parameters. Table 3 shows the characterization of different membrane material types.

Table 3. Membrane material characteristics summary (Nunes and K.-V. 2001)(Microdyn-Nadir 2018).

Membrane Material	Properties	pH- range	Maximum Temperature (ºC)

Polyethersulfone (PES/ PESH)	Hydrophilic, high chemical resistance	1-14	95 ºC
Polysulfone (PSUH)	Hydrophilic, high chemical resistance	1-14	95 ºC
Cellulose Acetate (CA)	Extremely hydrophilic	1-10	55 ºC
Polyvinylidenefluoride (PVDF)	High stability against oxidizing agents	2-11	95 ºC

2.2.4 Membrane Characterization

Hydraulic Permeability

For UF and MF membranes, the permeate flux is the flow of permeate per unit of area (J). If the solution is pure water, the transportation of water through the membranes is proportional to the applied pressure and given by (1).

$$J = \frac{L_p}{\mu_s}.(\Delta P - \Delta\pi) \quad (1)$$

Where,

L_p = hydraulic permeability,

μ_s = viscosity of the solvent (pure water in this case)

ΔP = transmembrane pressure

$\Delta\pi$ = average osmotic pressure

For ultrafiltration processes, the average osmotic pressure, $\Delta\pi$, is usually a small value and for that reason the previous equation, (1), can be rewritten as shown in equation (2)

$$\mathrm{J} = \frac{\mathrm{L_p}}{\mu_\mathrm{s}}.\Delta\mathrm{P} \quad (2)$$

The permeate flux, J, is calculated through the next equation, (3), that considers the solution volume V_p, over time (t) per membrane active area, A_m.

$$\mathrm{J} = \frac{\mathrm{V_p}}{\mathrm{t}.\mathrm{A_m}} \quad (3)$$

For this type of membranes, the permeate flux over time has usually a linear response. This linearity disappears when different solutions instead of pure solvents go through the membrane. For solutions, the

increase of the operation pressure increases the permeate flux. From a determined operation pressure, that changes with every solution used, the permeate flux stabilize at a certain permeate flux, known as limit flux of permeation, J_∞.

Retention Coefficient

One of the possible ways to qualify the performance of an ultrafiltration membrane is to calculate the retention coefficient. This coefficient indicates the percentage of a certain solute that was retained by the membrane. This method to evaluate the performance of a membrane is based on equation (4).

$$\mathrm{R} = \frac{(\mathrm{C_f} - \mathrm{C_p})}{\mathrm{C_f}} \tag{4}$$

Where,

$R =$ retention coefficient

$C_f =$ feed concentration

$C_p =$ permeate concentration

Molecular Weight Cut-Off

The molecular weight cut-off (MWCO) is a parameter that indicates the size of the molecules that will be retained by the membrane. This membrane characteristic is usually indicated by the manufactures in the membrane specification sheet of commercial membranes.

The MWCO is measured for each membrane, by passing through the membrane a certain solute with known molecular size and then evaluation the solute retention. The MWCO depends on the experimental conditions applied by the manufacturer. Ultrafiltration membranes are usually in a range between 1 and 500 kDa but, for membranes with MWCO higher than 100 kDa they are usually classified by pore size (Microdyn-Nadir 2018).

Concentration Polarization

The feed solution, under the driving force of pressure, originates a convective flux of mass in the direction of the membrane. Depending on the membrane properties, the solutes existing in the solution, accumulates in the membrane surface while the solvent goes through it (Mulder 1996).

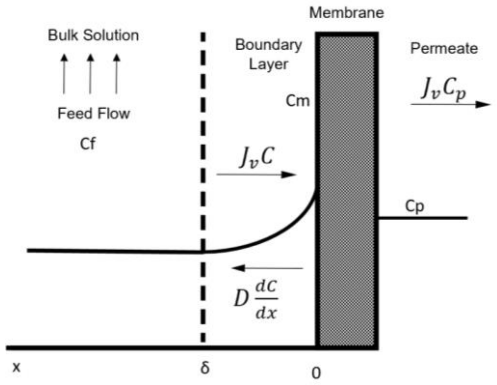

Figure 6. Concentration Profile in the boundary layer of a membrane adapted from Mulder 1996.

The accumulation of solute in the interface membrane/solution produces a diffusive flux in the opposite direction of the convective flux. At a stationary state, the convective flux of solute in the direction of the membrane equals the sum of the permeate flux with the diffusive flux of solute going towards the bulk solution. This creates a concentration profile at the boundary layer (δ) contiguous to the membrane. The concentration profile is shown in Figure 6, where C_m is the concentration in the membrane, C_p is the concentration of the permeate, C_f the concentration of the feed and J_v is the permeate flux.

Considering $D\frac{dC}{dx}$, the diffusive transport in the boundary layer (δ) between the membrane and the bulk solution, the mass balance to the solute is given by (5).

$$\mathrm{J_v C} + \mathrm{D}\frac{\mathrm{dC}}{\mathrm{dx}} = \mathrm{J_v C_p} \tag{5}$$

Knowing that $C = C_m$ to $x = 0$ and $C = C_f$ to $x = \delta$,

And assuming the diffusion coefficient is independent of the concentration and the permeate flux, J_v, is constant, the previous equation, (5) is transformed in to:

$$\ln\left(\frac{\mathrm{C_m} - \mathrm{C_p}}{\mathrm{C_f} - \mathrm{C_p}}\right) = \frac{\mathrm{J_v}\delta}{\mathrm{D}} \tag{6}$$

Based on the theory of the stagnant film, the mass transfer coefficient is given by, $k = \frac{D}{\delta}$. By reorganizing the previous equation (6) the new equation is given by:

$$\frac{\mathrm{C_m} - \mathrm{C_p}}{\mathrm{C_f} - \mathrm{C_p}} = \mathrm{e}^{\frac{\mathrm{J_v}}{\mathrm{k}}} \tag{7}$$

The empirical correlations of Sherwood, Reynolds and Schmidt are related with the mass transfer coefficient. These correlations are found in the literature and depend on the flow regimes and geometries.

$$\mathrm{Sh} = \frac{\mathrm{kd_h}}{\mathrm{D}} = \mathrm{aRe^b Sc^c} \tag{8}$$

Where,

$k =$ mass transfer coefficient

$d_h =$ hydraulic diameter

$D =$ diffusion coefficient

The values for a, b and c depend on the flow regime and geometry. The Reynolds (Re) and Schmidt (Sc) numbers are given by:

$$\mathrm{Re} = \frac{\mathrm{v\rho d_h}}{\eta} \tag{9}$$

$$\mathrm{Sc} = \frac{\eta}{\rho \mathrm{D}} \tag{10}$$

The value of the mass transfer coefficient, k, is then related with the dynamic viscosity, η, of the solution, the diffusion coefficient, D, and with the linear speed, v, of the system.

The Polarization Module, $\frac{C_m - C_p}{C_f - C_p}$, decreases with the increase of the mass transfer coefficient, k, which is dependent on the Reynolds Number.

When the membrane has a high retention coefficient, the permeate concentration, C_p, has a low value or even null.

$$\mathrm{J}_v = \mathrm{k} \ln\left(\frac{\mathrm{C_m}}{\mathrm{C_f}}\right) \tag{11}$$

The polarization module for this situation is then, $\frac{C_m}{C_f}$,and its value increases with the increase of the permeate flux and decreases with the decrease of the mass transfer coefficient.

The effect of concentration polarization is very noticeable in ultrafiltration membrane processes because of the high permeate fluxes and low mass transfer coefficients associated with the filtration of macromolecules. Usually, the higher the cut-off the more the concentration polarization effect is visible.

This phenomenon is noticeable in the permeation flux of the membrane, as it decreases abruptly over time. The decrease of the permeate flux effects the efficiency of the membrane separation process. The concentration polarization phenomenon can be decreased by changing operating conditions such as the feed concentration, the temperature and the transmembrane pressure (TMP).

As the solute becomes so concentrated at the membrane surface, a gel layer is formed and becomes a barrier to the flow of the desired particles through the membrane. This gel layer can be reversible or irreversible, but the relation between this fact and the limit flux, does not depend on that fact. Assuming this

model explains the limit flux, J_∞, and that the gel layer has a constant concentration, C_g, the previous equation, (11), is given by:

$$J_\infty = k \ln\left(\frac{C_g}{C_f}\right) \quad (12)$$

Fouling

Several factors are responsible for the decrease of the permeate flux over time during the filtration processes. The accumulation of particles in the membrane surface, for several reasons, prevents the particles of solvent of going through the membrane. This phenomenon is known as fouling and depends on several chemical and physical parameters such as the concentration, the feed rate, the pressure, the temperature, the pH and specific chemical and physical interactions between the molecules and the membrane (Baker 2001).

Besides from concentration polarization phenomenon, the molecule adsorption in and on the membrane surface. For some porous membranes, some solutes infiltrate in the pores and might get trapped in them temporarily or permanently. This is another factor that creates resistance to the mass transfer through the membrane (Zhu 2014).

An initial pre-treatment of the solution, such as changing the temperature and or the pH can significantly decrease the fouling in the membranes. The use of a pre-treatment can reduce the time used in membrane cleaning afterwards, but it is possible that the solution which will be filtrated can be altered by changing this type of parameters, which is a disadvantage.

The growth of bacteria and other microorganisms in the membrane surface, known as biological fouling, can affect the permeate flux and even damage the membrane. The most efficient way to fight this type of fouling is chlorination (Yu et al. 2014), in which chlorine is added to water and the membrane is “washed”. The disadvantage of this process is the membrane chemical stability in chlorine and the fact that vestigial amounts of chlorine will be in the used set-ups, which can affect the solution being filtrated.

As for methods to decrease fouling after its effects are shown, it is possible to back-flush the membrane, which is basically to do the filtration process in a reversed way, usually applying higher fluxes that the ones used in the filtration process. If this method is not enough to clean the membrane, a chemical cleanse can be done by using chemical components(Baker 2001).

When a cross-flow system is used in an ultrafiltration membrane separation process one of the most important ways to decrease the fouling effect is to modify the operating conditions, specially the transmembrane pressure and the feed flow-rate. As explained in the concentration polarization chapter, by increasing the feed flow-rate, the number of Reynolds increases (equation (8) and (9)), and so does the mass transfer coefficient, k, which decreases the polarization module. This means, that the concentration

polarization effect decreases. On the other hand, by increasing the pressure, the permeate flux, J_v, increases which based on the concentration polarization effect, described above, increases the polarization module, which means, increases the concentration polarization effect. Decreasing the transmembrane pressure is then, another way of decreasing the fouling effect (Nunes and K.-V. 2001).

2.2.5 Diafiltration

Diafiltration is a process used in membrane separation processes in which the concentrated solute is diluted using water as a solvent. This is a way of purifying the solute even further than with a single filtration. Usually, after a pre-concentration of the initial feed, the retentate is diluted by adding water one, or several times. This method is frequently used with ultrafiltration processes and works not only as a purifying method but is also known to superficially clean the membrane surface, decreasing the fouling.

2.3 Aim of the thesis

The main purpose of this thesis is to contribute to the advancement of the state of the art on the separation and purification of wheat straw nanolignin particles from its impurities by using an ultrafiltration/diafiltration separation process.

The following steps were based on previous experiments (Beisl, Loidolt, et al. 2018)) and were used as the base of the production of nanolignin particles.

1. Production of an extract solution of wheat straw using an Organosolv pre-treatment with a mixture of pure ethanol and water as solvents.
2. Precipitation of the nanolignin particles using water as an anti-solvent.

The nanolignin particles suspension produced by precipitation were processed by Ultrafiltration/Diafiltration to separate and purify the nanolignin particles from the other impurities present in the suspension. The operating conditions of feed flow-rate and transmembrane pressure were also investigated to optimize the separation and purification process.

3 Material and Methods

3.1 Experimental Procedure for Nanolignin particles production

3.1.1 Extract Production

The extraction production comprised two main steps, an Organosolv extraction in a 1L stirred autoclave (Zirbus, HAD 9/16, Bad Grund, Germany) and a mechanical separation of the reactor product. The mechanical separation is initially done using a hydraulic press to separate most of the wheat straw from the liquid solution. Then, centrifugation is used to separate smaller particles that still remain in the solution.
The preparation of approximately 350 mL of extract comprised the following steps:

1) Wheat straw with a composition of approximately 94 % of dry matter and 6% of water was weighted and mixed with an aqueous solution of 60 wt % ethanol. The final mixture had a 1:11 mass ratio of wheat straw to hydroalcoholic solution.
2) The mixture was inserted in the reactor (which had a temperature and pressure recorder connected to a computer). The temperature of the jacket was 210 °C for 45 min and afterwards 190°C for 15 min, with the goal of reaching 180ºC inside the autoclave. In the end of the reaction, the reactor was cooled down using a cooling water system.
3) The mixture was placed in the hydraulic press (Hapa, HPH 2.5, Achern, Germany) at 200 bar to separate the solid from the liquid.
4) The remaining liquid was centrifuged at 24000 g for 20 min to separate smaller particles that were still in the mixture.
5) The solution was kept in the refrigerator.
6) Approximately 3 L of extract for the next experiments were produced by using the same steps.
7) The Organosolv extract was analyzed for carbohydrates, lignin and degradation products externally to this thesis.

The extract production is the base of the experiments and the reaction conditions were chosen based on previous experiments (Beisl, Loidolt, et al. 2018).

Using a computer software to record the operating conditions of the Organosolv extraction, the temperature of the product inside the reactor and the pressure was measured for all the experiments.

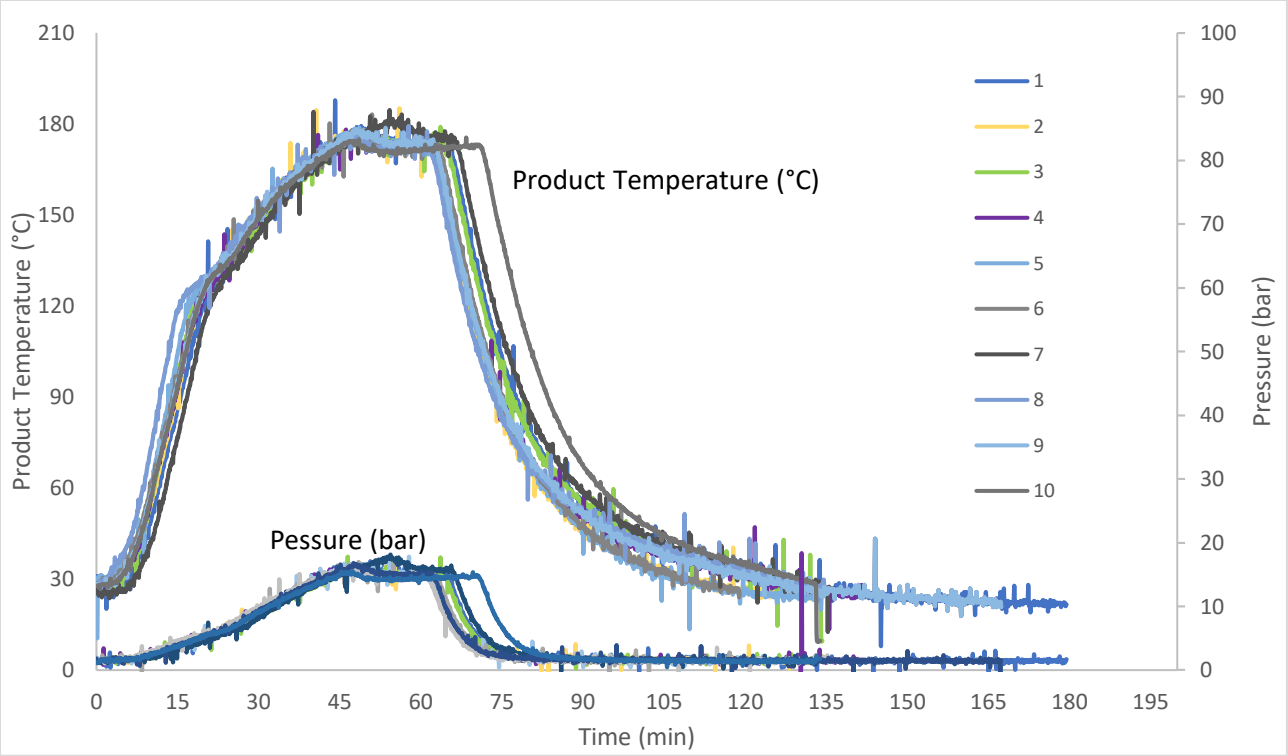

Figure 7. Product temperature (°C) and pressure (bar) for all the extract production experiments.

The graphic in Figure 7 shows the pressure (bar) inside the autoclave and the product temperature (ºC) for all the ten experiments made to produce wheat straw extract. All the conditions were approximately the same for the ten experiments, producing extract with similar characteristics.

3.1.2 Precipitation of lignin nanoparticles

The following step was to obtain lignin nanoparticles. For this purpose, a precipitation was done using water as an anti-solvent. An anti-solvent is solvent which reduces the solubility of other component in the solution, making the solution saturated, and the particles to precipitate. The choice of the anti-solvent was based on previous experiments (Beisl, Loidolt, et al. 2018). The production of suspension was made by using two Syringe Pumps (TSE Systems) to mix the solute and anti-solvent at precise flow-rates.

This suspension is used in the ultrafiltration process and it should be used as soon as possible after the precipitation to avoid unwanted agglomeration of the nanoparticles.

3.2 Ultrafiltration Process Set-ups

3.2.1 Stirred Cell

Many filtration processes use a dead end cell to perform a separation process. In this type of equipment, the feed stream is perpendicular to the membrane surface. The main disadvantage of this separation

method is the high build-up of molecules and particles in the membrane surface that forms when the concentration of particles in the solution is too high.

For the first experiments the HP0470 stirred cell from *Sterlitech* was used for the separation processes. This dead-end cell has a processing volume of approximately 300 mL and a membrane active area of 14.6 cm^2. The cell is placed on the top of a magnetic stirrer plate as there is a stirrer inside the cell which creates the necessary turbulence. This cell is suitable for reverse osmosis (RO), nanofiltration (NF), ultrafiltration (UF), microfiltration (MF) and has a maximum operation pressure of 69 bar. The body of the cell is made of stainless steel and the O-rings are made of Buna-N rubber, which is resistant to ethanol. The top of the cell is coupled to a high-pressure hose that is connected to an inert gas supply, in this case, Nitrogen (N_2). The data for the permeate mass was collected by using a digital scale connected to a computer software which recorded the mass of permeate over time.

Figure 8. HP0470 stirred cell from Sterlitech.

3.2.2 Cross flow System

The other system used to perform the membrane separation processes experiments was a cross-flow system whose set-up was built, for this purpose, in a laboratory scale. The set-up model is *Memcell* from *OSMO Membrane Systems* and allows the construction of cross-flow system with several flat modules in parallel or series. In a cross-flow filtration, the feed flow circulates tangentially to the membrane surface area. The feed is then separated into two different streams, the permeate stream, that goes through the membrane and a concentrated stream, the retentate, that does not go through the membrane. The next figure, Figure 9 , shows a simplified diagram of the cross-flow system that was used. The flat module corresponds in his hydraulic properties to a spiral wound element. On permeate side, to guarantee a steady flow, there is a porous sinter plate. This allows a reliable scale-up process possible. The set-up is made of stainless steel and can be operated with pressures up to 64 bar. The active membrane area of this single flat module used is 80 cm^2.and the feed stream is connected to a *2-Series* gear pump, from *Liquiflo*, which allows changes in the feed flow-rate. To guarantee that the solution in the feed tank was homogenous a stirrer was added. The pressure can be altered by using the globe valve inserted near the retentate stream in the set-up. Later, a second similar pump was added in parallel to allow the increase of the feed flow-rate.

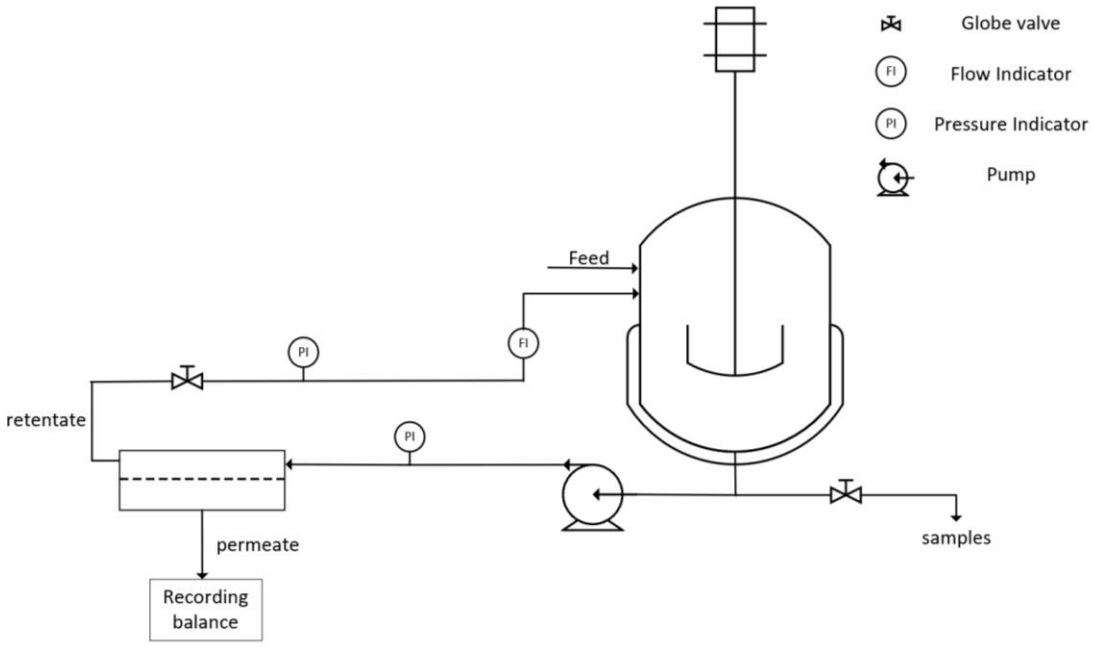

Figure 9. Diagram of the adapted Memcell (OSMO membrane systems) cross-flow system.

3.3 Membrane Selection

It was known from previous experiments (Loidolt 2017) that the average molecular weight of the dissolved lignin molecules is 10 000 g/mol. Assuming the smallest nanolignin particles have larger dimensions than the dissolved molecules, it is expected that the nanolignin particles would be retained in membranes with a cut-off equal or higher than 10 kDa. For the same reason, if the membrane molecular cut-off is too high, the nanolignin particles would pass through the membrane. For that reason, membranes with 10, 20, 30 and 50 kDa cut-offs were chosen to perform the separation processes. The solution that was going to be separated had an ethanol content of approximately 15 wt % and therefore the membrane material had to be stable in ethanol for long periods of time. On the other hand, the solution have pH value in the range between 4 and 7 (Beisl, Loidolt, et al. 2018), so the membrane material needed to be stable in those conditions too. The membrane material that was more suitable for these circumstances, based on Table 4, was polyethersulfone (PES).

Table 4. Membrane material chemical resistance to ethanol and pH stability (Merck Milipore 2015).

Material	Chemical compatibility with ethanol	pH stability
PES/PESH	Compatible	1-14
Polysulphone	Compatible	1-14
Cellulose Acetate	Not recommended	1-10

PVDF	Highly Compatible	2-11

The membranes used in the experiments were from the Nadir membrane collection supplied by Microdyn. The chosen membranes were the following: UP010 with a 10 kDa cut-off, the UP020 with 20 kDa cut-off, and the UH030 and UH050 with 30 and 50 kDa, respectively. The 10 and 20 kDa membranes were made of Polyethersulphone (PES) and the 30 and 50 kDa membranes were made of a more hydrophilic polyethersulfone (PESH).

3.4 Membrane Filtration

According to the instructions of the manufacturer (Microdyn-Nadir 2018) the membranes should be flushed for at least 30 min to get the membrane wet and remove any impurities. Based on previous experiments with nanolignin particles production (Beisl, Loidolt, et al. 2018), the nanolignin suspension is expected to have a maximum ethanol content of 15 wt%. For that reason, initially all the used membranes were flushed for the indicated time with an aqueous solution of 15 wt.% ethanol.

3.4.1 Membrane Stability using dead end stirred cell

After choosing the membranes based on MWCO and membrane material, it was still necessary to verify if the membranes were stable in ethanol for long periods of time, as this was not guaranteed by manufactures. Therefore, the membranes were flushed with 15% ethanol solution for several times in two consecutive days, using the dead end stirred cell.

A recording balance connected to a computer measured the mass of permeate over time and with this data it was possible to obtain a graphic of the mass of permeate (g) versus time (min). The transmembrane flux for each membrane is the slope of the linear regression obtained from the recorded mass of permeate per unit of membrane surface area versus time, according to equation (13):

$$\frac{\text{Mass of Permeate (g)}}{A_m} = \text{TF} \times \text{time (min)} \qquad (13)$$

Where,

TF is the transmembrane flux, $g/(cm^2.\text{min})$.

A_m = membrane active surface area, cm^2.

By calculating the average transmembrane flux for all the experiments for each membrane and the standard deviation of this value is possible to see how stable the membranes are in an aqueous solution of 15% ethanol.

3.4.2 Ultrafiltration/ Diafiltration of nanolignin particles suspension

The main goal of this thesis was to evaluate the performance of the separation and purification of a suspension of nanolignin particles when using membranes in the Ultrafiltration range as a separation process. After flushing each different membrane with the aqueous solution of 15 % ethanol and measuring the initial transmembrane flux, the suspension of nanolignin particles was produced by precipitation using the method described in chapter 3.1.2 and used in the batch filtration process.

3.4.2.1 UF/DF in the stirred cell

As the stirred cell as a smaller processing volume than the cross-flow system and is known to be more prone to fouling, due to the feed stream being perpendicular to the membrane surface, it was decided to use the nanolignin particles suspension in the ultrafiltration process in diafiltration mode only in the cross-flow system.

3.4.2.2 UF/DF in the Cross-Flow system

For the cross-flow system, which as a maximum processing volume of approximately 2L, about 1.2L of suspension was produced for each experiment. The necessary suspension volume for the cross-flow system was decided based on the amount of produced extract, which was limited.

The filtration process was performed in three different batch experiments for each different membrane. For the first batch filtration, the feed tank was filled with the nanolignin particles suspension and concentrated until a certain volume. With the goal of removing impurities and purifying the nanolignin particle suspension, a diafiltration process was used afterwards. This diafiltration process was separated in to two batch filtrations.

The first addition of water (1st diafiltration step) was after the concentration of the initial nanolignin particles suspension until a certain volume and the amount of water added for this experiment, was the same amount of permeate collected.

The second addition of water (2nd diafiltration step) was performed after the concentration of the solution of the first diafiltration experiment. The same method was used to know the necessary amount of water to add to the solution.

The following diagram, Figure 10 summarizes the membrane filtration process for the cross-flow system.

Figure 10. Diagram of the membrane filtration process for the cross-flow system.

3.4.2.3 Assessment of membrane fouling

To understand the effect of the membrane fouling in the permeate flux of the chosen membranes, after the filtration with a suspension of nanolignin particles in a cross-flow system, each membrane was flushed with the 15 wt% ethanol solution in the end of all the experiments. The mass of permeate (g) over time (min) was again recorded and the final transmembrane flux calculated based on equation (13).

The obtained TF for the experiments after filtrating the suspension of nanolignin particles was then compared with the initial transmembrane flux, measured before the suspension filtration/diafiltration process to evaluate the flux decline caused by the fouling in the membranes.

3.4.2.4 Operating Parameters

For the stirred cell, the operating parameters that could be modified were the transmembrane pressure (TMP) and the speed of the stirrer inside the cell. The TMP was kept constant at 8 bar and the stirrer speed was also kept constant.

The most important parameters for the cross-flow system was the feed flow-rate and the transmembrane pressure (TMP). The TMP was constant and with a value of 8 bar and the feed flow-rate was constant and with a value of 0.7 L/min for all the experiments. The speed of the stirrer, which guarantees the homogeneity of the feed tank solution, was also constant for all the cross-flow system experiments with a speed of 255 rpm.

The second round of experiments goal was to optimize the operating conditions (TMP and feed-flow-rate) of the membrane which got better results from the membrane comparison experiments. By optimizing the operating conditions, it is possible to reduce the fouling effects, and improve the separation process efficiency.

For the selected membrane for optimization experiments, different operating conditions of TMP and feed flow-rate were used. Firstly, the experiment at 8 bar and 0.7 L/min was repeated. After this experiment, a new one was conducted to decrease the pressure of the system to 4 bar with the same flow-rate. Finally, another pump was added in parallel with the first one, to allow the possibility of increasing the feed flow-rate without increasing the pressure. Two different experiments were performed with this new set-up, with a flow-rate of 2 L/min at 8 and 4 bar.

3.4.3 Analytics

UF/DF stream characterization

For these experiments, several samples of retentate and permeate were taken to make further analysis. For each filtration step of each membrane, besides from a sample of the initial nanolignin particles suspension, the other samples taken during the experiments are described in Figure 11.

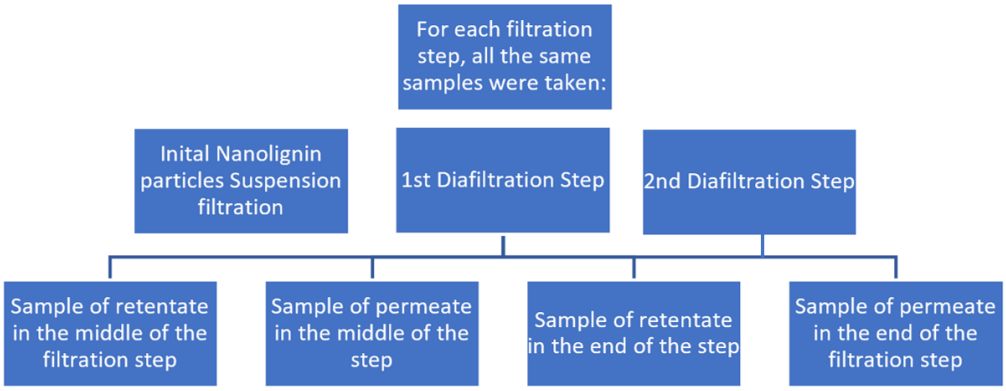

Figure 11. Diagram of the samples taken during each filtration step.

The first sample of permeate was only taken for the experiments in which a selected membrane is used to optimize the operating conditions.

The next diagram, Figure 12, shows the way each sample of initial suspension, retentate and permeate was treated.

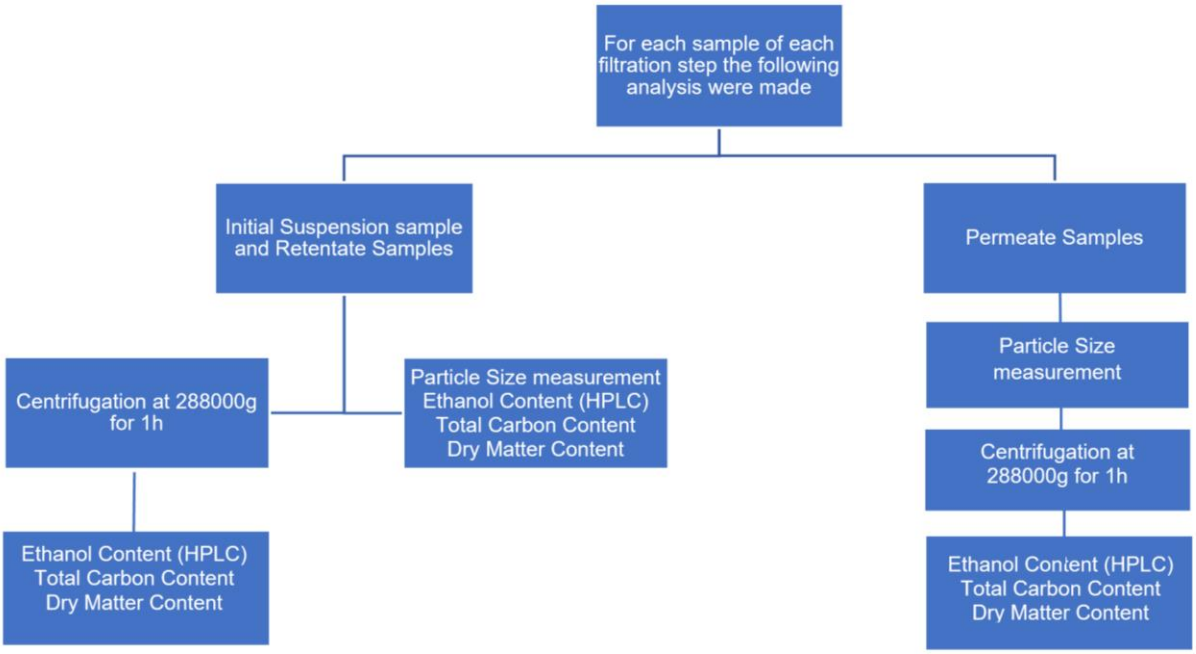

Figure 12. Diagram of sample treatment for all the samples.

Particle Size

The two main goals with the measurement of the size of the particles for all the taken samples were to verify if the nanoparticle size was constant during the UF/DF process and to verify is the collected permeates were free of nanolignin particles.

For all the samples, the particle size was measured using the ZetaPals from Brookhaven Instruments Corporation. All the samples were analyzed twice, once using the original sample that was collected and were also analyzed by diluting the original sample with deionized water in a volume ratio of 1:100 of original sample to deionized water.

Ethanol Content

The solutions of nanolignin particles over the experiments have, between other components, a large amount of ethanol. The ethanol content of the samples was measured using High Performance Liquid Chromatography (HPLC). HPLC is a method of separating and quantifying components in a solution (mobile phase), using an adsorbent material (stationary phase). The HPLC equipment used was the Nexera model from *Shimazdu Corporation* with the following components*:* Column: Sugar-SH1011 (Shodex), Guard Column: Sugar SH-G (Shodex), Detector: Refractive Index, Eluent 0.6 mL/min 0.005 molar H2SO4.

Initially, a calibration curve was made, using known concentrations of ethanol. Those concentrations were 1, 5, 10, 15, 20 and 25 g/L of ethanol solutions. The calibration curve is shown in Figure 13.

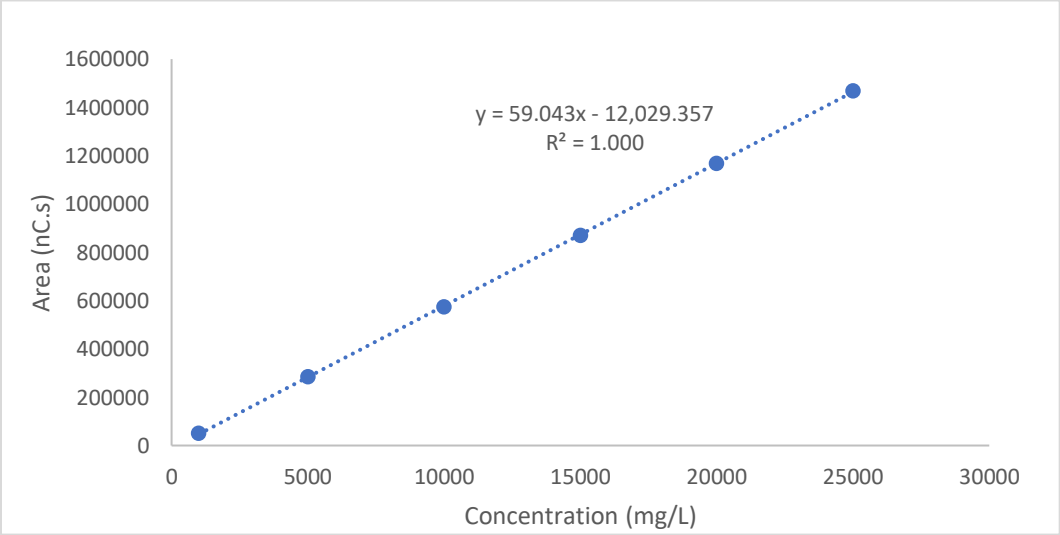

Figure 13. Calibration curve for ethanol content in HPLC.

Afterwards, all the samples taken during the experiments were diluted with water in a volume ratio of 1:5, centrifuged once more at 14000 rpm for 20 min and the supernatant placed in the HPLC tray. The concentration of these samples was obtained using the calibration curve above (Figure 13).

Total Organic Carbon Content

One of the ways to compare the membrane experiments, is to measure the total organic carbon content of the samples over the experiments. For these experiments, the analysis performed in the TOC analyzer was a Total Carbon analysis, as it is considered that only organic carbon is present in the nanolignin particle suspension, and so the total carbon concentrations will be same as the TOC concentrations. During the experiments, the collected samples of retentate and permeate have a certain carbon concentration of nanolignin particles, dissolved lignin, ethanol and other dissolved components. Based on the assumption that there are no nanolignin particles in the supernatant of the samples collected after centrifugation for 1 hour at 288000g, it is expected that:

$$\mathbf{TOC\ nanolignin\ particles} = \mathbf{TOCsample} - \mathbf{TOCsupernatant} \quad (14)$$

$$\mathbf{TOCsample} = \mathbf{TOCethanol} + \mathbf{TOCnanolignin\ \ particle} + \mathbf{TOCdis.\ components} \quad (15)$$

$$\mathbf{TOCsupernatant} = \mathbf{TOCethanol} + \mathbf{TOCdis.\ components} \quad (16)$$

Where,

$TOC\ nanolignin\ particles$, is the Total Organic Carbon (mg/L) associated with nanolignin in the solution

$TOCsample$, total organic carbon (mg/L) of retentate sample before centrifugation

$TOCethanol$, total organic carbon associated with ethanol (mg/L) in the solution

$TOCdis.components$, total organic carbon of other dissolved components in the solution

$\mathrm{TOCsupernatant}$, total organic carbon (mg/L) of supernatant of retentate sample after centrifugation

The total organic carbon (TOC) content was measured using a Total Organic Carbon Analyzer from Shimadzu Corporation, shown in Figure 14.

Figure 14. TOC analyzer from Shimadzu Corporation.

A sample is inserted in the autosampler which is then introduced in the TC combustion tube with an oxidation catalyst and heated to 680°C. The sample is then burned and the Carbon Dioxide resultant from that reaction is detected in a non-dispersive infrared (NDIR) gas analyzer. Those results are then evaluated by the TOC-Control Software. The peak area is proportional to the Total Organic Carbon concentration of

the sample (Anon 2010). From that, it is possible to know the TOC concentration by creating a calibration curve that relates the area of the peak with the TOC concentration. The calibration curve experimental procedure is explained in detail in the Appendix A.

Finally, by knowing the carbon content related with the ethanol in the samples based on the HPLC results, it would be possible, based on equation (16), to subtract the total organic carbon of ethanol from the TOC of the whole sample.

Dry Matter Content

Finally, to compare with the results obtained in the total organic carbon content analysis, a dry matter (DM) analysis was performed based on the following experimental steps:

1) Empty containers were dried in the oven for at least 4 hours, at 105°C.
2) Afterwards, the containers were placed in the desiccator for at least 1 hour to allow the containers to cool down.
3) The dry empty containers were weighted in an analytical balance.
4) The containers were filled with the samples and weighted again.
5) The full containers were placed in the oven overnight, at 105 °C.
6) In the next day, the full containers were placed in the desiccator for at least 1 hour and weighted afterwards.

Afterwards, the DM concentrations of the samples before and after centrifugation were calculated following the equation (17):

$$DM = \frac{M_{dry\ sample}}{M_{inital\ sample}} \tag{17}$$

Where,

$DM =$ dry matter concentration.

$M_{dry\ sample} =$ mass of sample after being dried, g.

$M_{inital\ sample} =$mass of initial sample taken, g.

The nanolignin particles concentration was calculated based on the assumption that no nanolignin particles were present in the supernatant of the samples that were centrifuged. The total nanolignin particles concentration is then given by equation (18).

$$\mathrm{TNL_{sample}} = \mathrm{DM_{sample\ bef.centri.}} - \mathrm{DM_{sample\ after\ \ centri.}} \tag{18}$$

Where,

TNL_{sample} =total nanolignin particles in the sample, g nanolignin particles/g of solution

$DM_{sample\ bef.centri.}$= dry matter concentration of the sample before centrifugation, g DM/g of solution.

$\mathrm{DM}_{\mathrm{sample\ after\ \ centri.}}$= dry matter concentration of the sample after centrifugation, g DM/g of solution.

Scanning Electron Microscope

To get a high-resolution image of the membranes surface, a scanning electron microscope (SEM) analysis was performed. This technique uses a beam of electrons to form a tridimensional image of a surface. The samples were prepared for the SEM by following the next steps:

1) Several small portions of each used membrane were cut and placed in the freeze dryer for two days.
2) All the samples were cut with approximately 2 mm size, placed in a specific plate and coated with gold (Au) and Paladium (Pd) mixture using a Sputter Coater from Quorum Technologies.
3) The plate was then transferred to the scanning electron microscope and the samples analyzed with a zoom of 500, 5000 and 100 000 times.

Figure 15. Membrane parts with a coat of a mixture of 40:60 of gold (Au) and Paladium (Pd)

For the membranes used in the optimization of the operating conditions experiments, the membranes were also frozen using liquid Nitrogen before being cut and the cross section of the membranes was analyzed.

4 Results and Discussion

As previously explained, there were two main goals in this experimental work. The first one was to evaluate the performance of four membranes with different MWCO in the ultrafiltration range in separating nanolignin particles from a suspension with other impurities. Then, the membrane which showed the better results in separating the nanoparticles from the rest of the suspension was used in optimization experiments by varying the operating conditions of the transmembrane pressure and the feed flow-rate. This chapter is divided in two main parts, the one that shows the results for the experiments using the different MWCO membranes (4.1) and the one that shows the results for the optimization experiments using a selected membrane (4.2).

4.1 Experiments using different MWCO membranes

4.1.1 Hydraulic Permeability

The hydraulic permeabilities indicated in the membrane specification sheets (Microdyn-Nadir 2018) give an idea of how the membranes behave when flushed with a solution of pure water at 20°C. The next table, Table 5, shows the permeability for each membrane according to the manufacturer.

Table 5. Membrane permeability for all the membranes according to product specification sheets (Microdyn-Nadir 2018).

Membrane	Permeabilities (L/$(m^2.h.bar)$)
10 kDa	≥ 50.0
20 kDa	≥ 70.0
30 kDa	≥ 35.0
50 kDa	≥ 85.0

4.1.2 Membrane stability using dead end stirred cell

For the dead end stirred cell, the membranes were flushed with the same 15 wt.% ethanol solution for several times, to guarantee that the membranes would be stable for longer periods when using solutions with maximum ethanol concentration of 15 wt.%. As previously described, (chapter 3.4.1) the transmembrane flux is the slope of the linear regression of mass of permeate per unit of membrane surface area versus time. As an example, Figure 16 shows the mass of permeate over time for one of the experiments using 15% ethanol for each membrane.

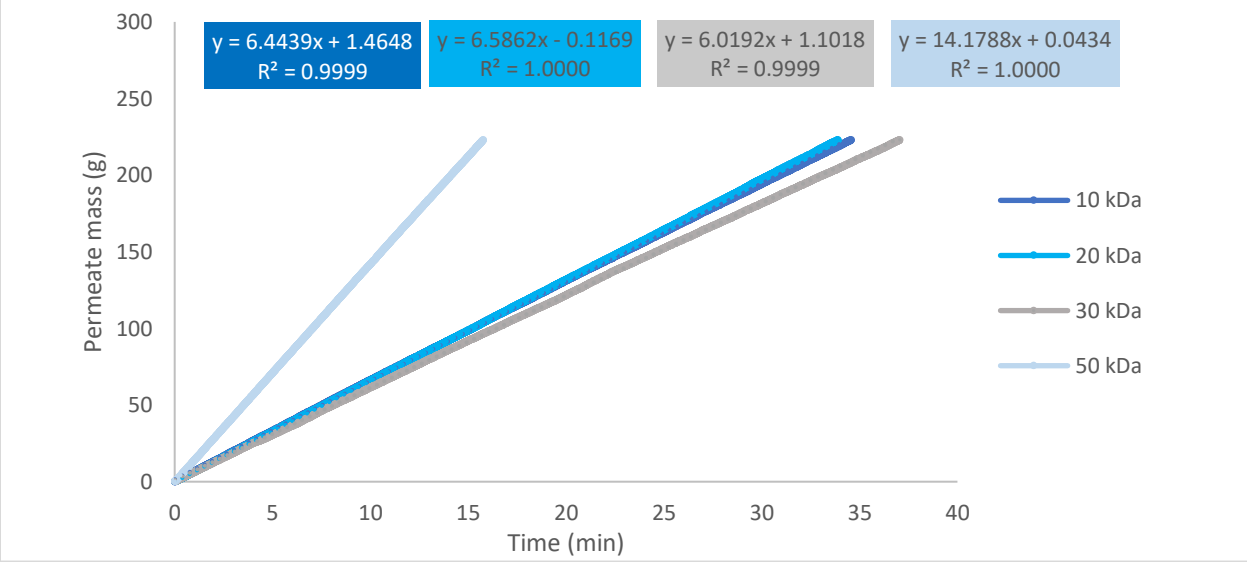

Figure 16. Permeate mass (g) over time (min) for the first experiment of each membrane.

In Figure 17 the average transmembrane flux for each membrane experiment and the standard deviation is shown. The obtained transmembrane fluxes were recalculated to the specific transmembrane flux units $(\mathrm{L}/(m^2.h))$ using the membrane surface area of 14.6 cm^2.

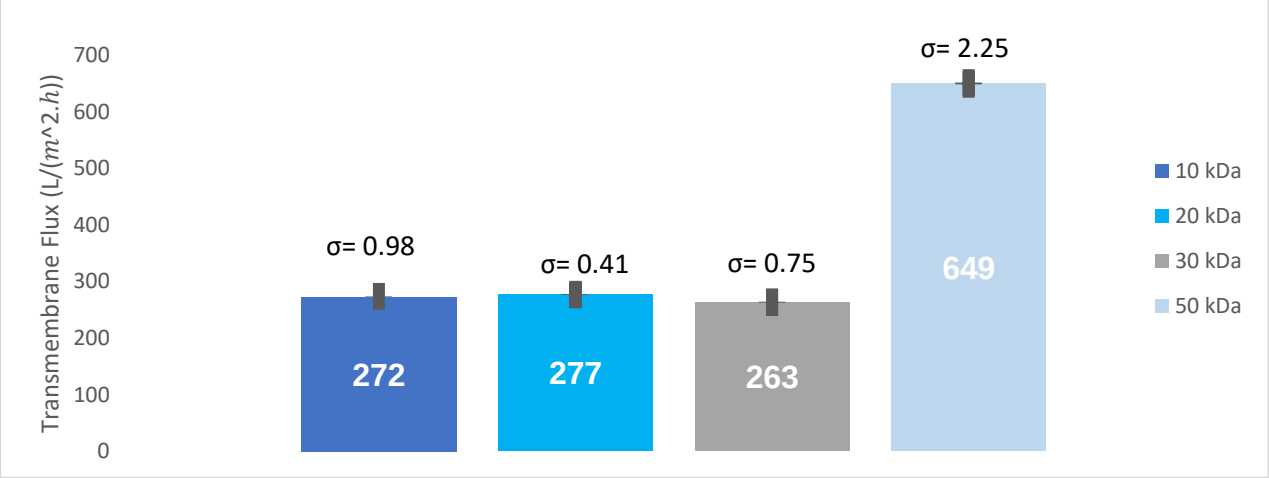

Figure 17. Average initial transmembrane flux for all different membranes.

The average transmembrane flux for 5 experiments of each different membrane was calculated as well as the standard deviation of this value. The permeate flux over the experiments is decreasing slightly, mainly because the stirred cell set-up was not in a sterile environment. This fact contributed to the accumulation of dust particles in the membrane which affected negatively the transmembrane flux over time. Nevertheless, the deviation of the transmembrane fluxes between experiments is not significant so it is possible to conclude that the membranes made of PES and PESH are stable when using a 15% ethanol

solution. It is possible to see in Figure 17, that the transmembrane flux is similar for the 10, 20 and 30 kDa membrane and higher for the 50 kDa membrane.

4.1.3 Cross-Flow system experiments

4.1.3.1 Initial Transmembrane Flux

As previously mentioned (3.4) initially, membranes with different MWCO were analyzed and tested for the separation of a nanolignin particles from the other impurities in the suspension. For the experiments with different membrane cut-offs the operating pressure was set at 8 bar and the feed flow-rate at 0.7 L/min.

For the cross-flow system, after the initial flushing with an ethanol solution, the transmembrane flux for all the membranes was obtained considering the variation of permeate mass over time. The next graph, Figure 18, illustrates the mass of permeate over time for the initial experiment with 15% hydroalcoholic solution.

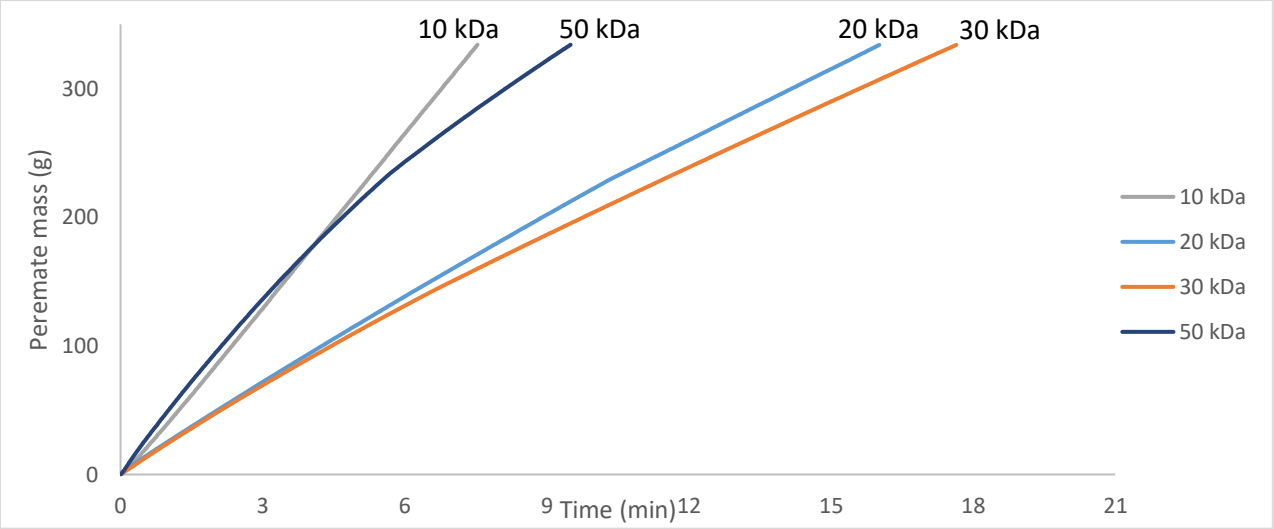

Figure 18.Permeate mass (g) over time(min) for all the membranes in the cross-flow system (8 bar and 0.7 L/min).

From the previous graphic Figure 18 it is possible to see that the variation of permeate mass(g) over time (min) is not linear for the 20, 30 and 50 kDa membranes. Comparing with the results for the stirred cell in Figure 16, it is possible to see that by changing from a dead end stirred cell to a cross-flow system already introduces differences in the results. Nevertheless, the cross-flow filtration type is the one that is usually used in the industry, so the results for the cross-flow system are more reliable when changing to a pilot or industrial scale.

4.1.3.2 Mass Balances

To have an in-depth idea of the filtration process in the cross-flow system mass balances were made over time for all the steps and all membranes used in the experiments. Some approximations and assumptions were made to facilitate the calculation of the mass balances. To begin with, it was assumed that no layer of nanolignin particles are formed in the membrane surface, which would mean that all the nanolignin particles are present in the retentate, which always allows the calculation of the total mass of nanolignin particles.

On the other hand, for the calculations of the mass balances, it was assumed that the initial amount of nanolignin particles in the suspension is not changing, either by getting dissolved or by small losses of suspension when feeding the tank or taking samples. Based on that, the total mass of the system and the total nanolignin particles mass was calculated.

Total mass of the system and total nanolignin particles mass

Considering the assumptions previously made, the Total Mass of the system is, given by equation (19), in which i, is the filtration step (initial filtration, 1st diafiltration and 2nd diafiltration) and x, is the time at which the total mass of the system is being calculated.

$$\mathrm{TMS(x)} = \mathrm{TMS_{initial}} - \sum \mathrm{M}_{permeate}(\mathrm{x}) - \sum M_{sample,i}(x) + \sum M_{water\ ,i}(x) \quad (19)$$

Where,

$TMS(x) =$ total mass of the system at time x, g.

$TMS_{initial} =$ initial mass of suspension, g.

$\mathrm{M}_{permeate}(\mathrm{x}) =$ mass of permeate collected until a certain time x, g.

$M_{sample,i} =$ mass of sample taken for each filtration step, g.

$M_{water,i}\ (x) =$ mass of water added for each diafiltration step, g.

The total amount nanolignin particles at any moment of the experiment is given by equation (20):

$$\mathrm{TSL(x)} = \mathrm{TSL_i} - \sum_{i=1}^{5} \mathrm{TSL_{sample\ i}} \quad (20)$$

Where,

$TSL(x) =$ total nanolignin particles at each time, g.

$TSL_i =$ initial nanolignin particles, g.

$TSL_{sample\ i} =$ total amount of nanolignin particles in each sample taken for analysis during experiments, g.

The initial amount of nanolignin particles was calculated based on the assumption that only 49% of the dissolved lignin in the extract precipitates (Beisl, Loidolt, et al. 2018).

The next table shows the initial mass of suspension, the initial mass of nanolignin particles and the amount of water added for each of the water steps for the four membranes used in the experiments.

Table 6. Initial mass of the total system, initial mass of suspension, the initial mass of nanolignin particles and the amount of water added for each of the water steps.

Membrane	Initial suspension (g)	Initial calculated nanolignin (g)	water added for 1st DF step (g)	water added for 2nd DF step(g)
UP010	1181	0.71	459	459
UP020	1153	0.70	465	465
UH030	1051	0.63	457	459
UH050	1358	0.82	459	460

The amount of water added to each of the experiments after the filtration of the initial suspension was approximately the same amount of permeate collected in the previous step.

The next graphic (Figure 19) shows the total mass of the system (TMS) and the total nanolignin particles (TNL) for the 50 kDa membrane experiments. The mass balances graphics for the 10, 20 and 30 kDa membrane are similar to the one showed in Figure 19. The graphics show three different colors for each UF/DF step of the experiments, for both the total mass of the system and the total nanolignin particles in the solution. That means the graphic shows the filtration with suspension step, the filtration after the first addition of water (1st Diafiltration Step) and the filtration after the second addition of water (2nd Diafiltration Step). When the amount of total nanolignin particles decreases, it means a sample was taken for further analysis. The addition of water is shown in the graphic as an increase in the total mass of the system.

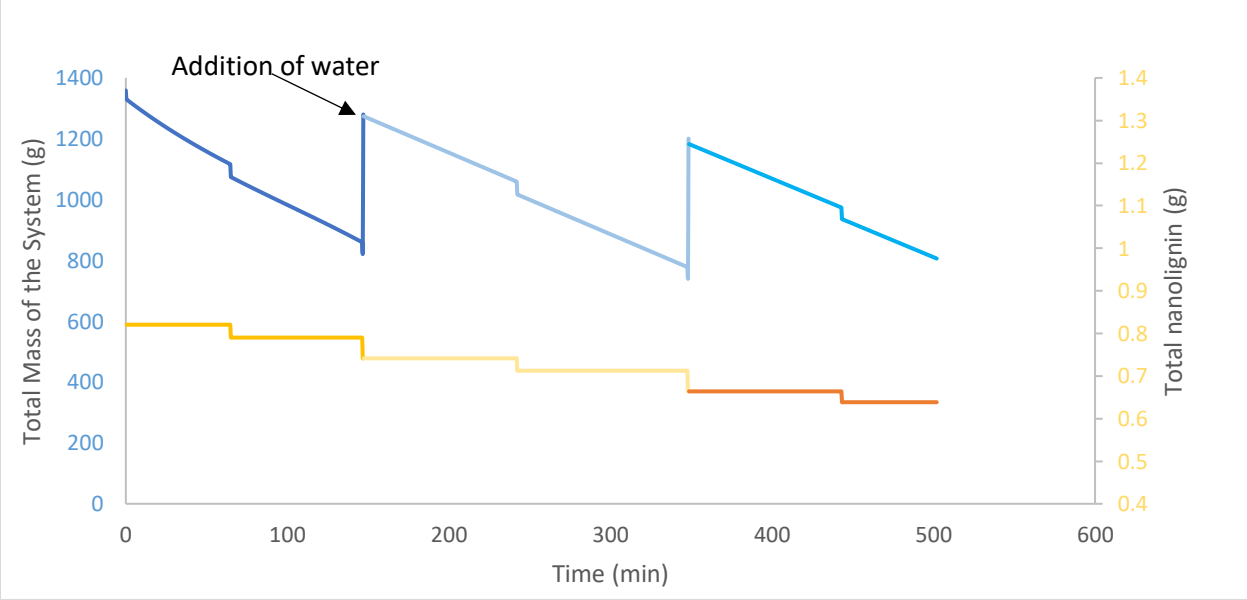

Figure 19. Total mass of the system and total nanolignin particles mass for the 50 kDa membrane. (8 bar and 0.7 L/min)

Nanolignin Particles Concentration

The lignin concentration over time for all the steps of each membrane experiment was calculated, using the following equation, (21):

$$\mathrm{LC(x)} = \frac{\mathrm{TNL(x)}}{\mathrm{TMS(x)}} \tag{21}$$

Where,

$LC(x) =$ nanolignin particles concentration at time x, g of nanolignin/g of solution.

$TMS(x) =$ total mass of the system at time x, g.

$TNL(x) =$ total mass of nanolignin at time x, g.

The next graphic (Figure 20) shows the nanolignin concentration over time for all the steps of the experiments with the 50 kDa membrane. The graphics for the lignin concentration over time for the rest of the membranes are similar to the one showed in Figure 20.

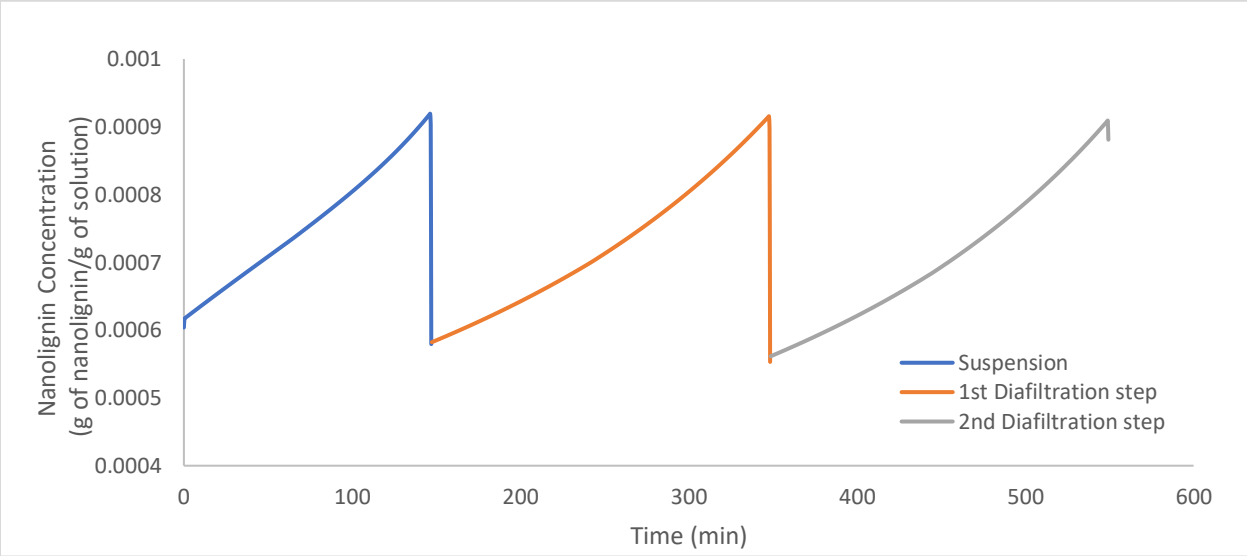

Figure 20. Lignin concentration for all the steps with the 50 kDa membrane.

From Figure 20 it is possible to see that the lignin concentration increases over time for all the three steps of the experiment and it decreases instantaneously after the addition of water, as expected. The lignin concentration does not decrease when samples are taken, because both the total mass of the system and the total nanolignin particles decrease in the same proportion.

4.1.3.3 UF/DF of Nanolignin Particles Suspension

After the assessment of the Initial Transmembrane flux using a hydroalcoholic solution with 15% ethanol, the nanolignin particles suspension was inserted into the feed tank and concentrated until a certain volume. Afterwards, water was added to the tank to begin with the first diafiltration step that was stopped when the same amount of permeate as in the previous step was collected. Finally, the second water step was initiated by adding water once more and the diafiltration process was repeated. Figure 21 to Figure 24 show the permeate mass (g) over time (min) for the three UF/DF steps for each different membrane and Table 7 to Table 10 show the mean transmembrane flux for each of the different steps of each different membrane experiment.

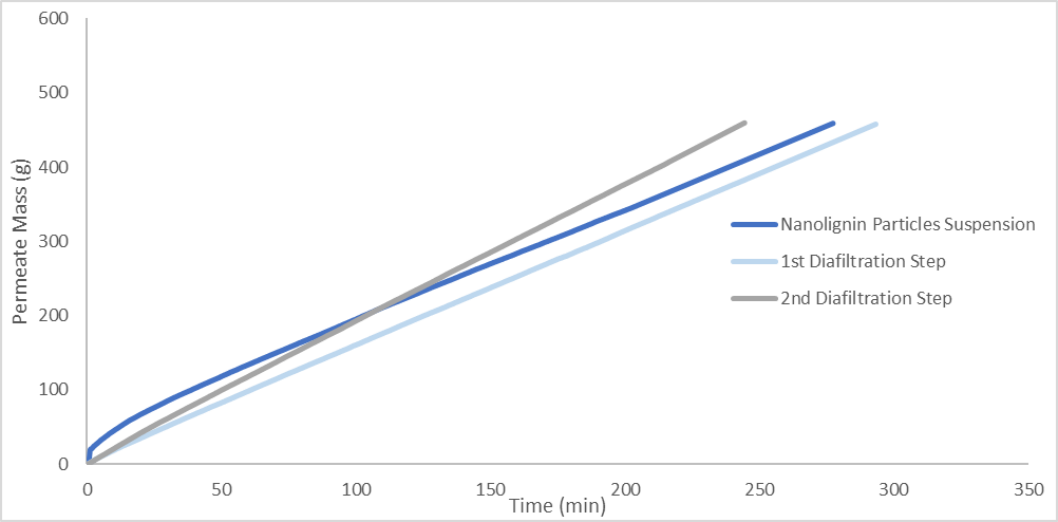

Figure 21. 10 kDa membrane experiments (8 bar and 0.7 L/min).

Table 7. Mean transmembrane fluxes for each filtration step of 10 kDa membrane.

UF/DF Step	Mean Transmembrane Flux (L/(m^2.h))
Initial Suspension Filtration	11.94
1st Diafiltration Step	11.89
2nd Diafiltration Step	14.41

For the 10 kDa membrane experiments (Figure 21 and Table 7) , initially, for the concentration of the initial nanolignin particles suspension, the plot of permeate mass (g) vs time (min) does not show a linear trend for approximately the first hour of filtration, which shows that the amount of dissolved components going through the membrane for the first hour is not even. For the concentration of the nanolignin particles suspension after the first addition of water (1st Diafiltration Step), the permeate mass over time has a linear trend, but the transmembrane flux decreases slightly when compared with the initial suspension filtration step. This phenomenon can be explained by the increase of the fouling effect over time, in the 10 kDa membrane. Finally, the second addition of water (2nd Diafiltration Step) shows an increase in the transmembrane flux when compared with the first two batch filtrations, which shows that the fouling decreased with the second addition of water, allowing a higher TF than the initial one.

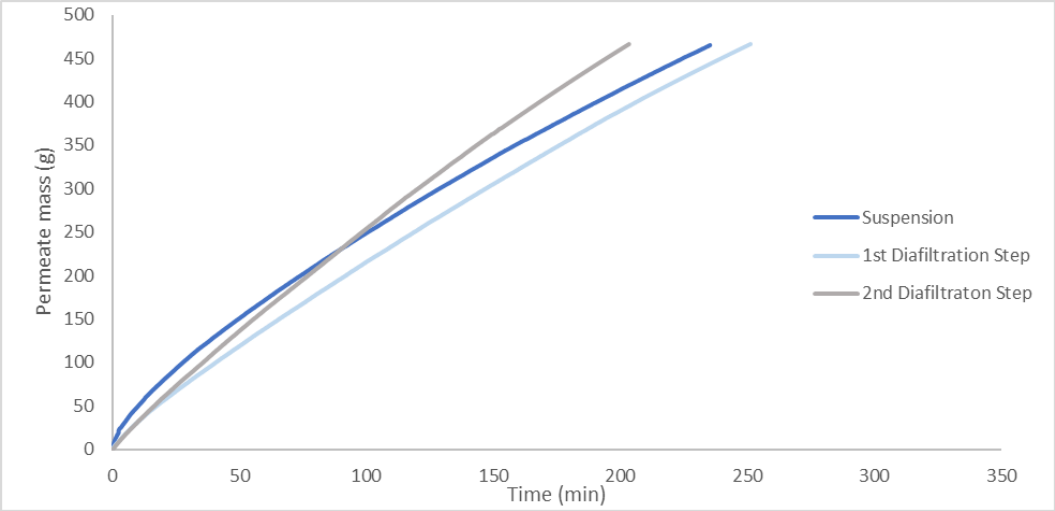

Figure 22. 20 kDa membrane experiments (8 bar and 0.7 L/min).

Table 8. Mean transmembrane fluxes for each filtration step of 20 kDa membrane.

UF/DF Step	Mean Transmembrane Flux (L/(m^2.h))
Initial Suspension Filtration	14.06
1st Diafiltration Step	13.94
2nd Diafiltration Step	17.46

In Figure 22 the permeate mass over time for the three batch experiments using the 20 kDa membrane is shown. Table 8, shows the transmembrane fluxes for the different UF/DF steps and when compared to the 10 kDa membrane (Table 7) it is possible to see that all the three experiments already have a great increase in the transmembrane flux, which can mean that this membrane is less affected by fouling. On the other hand, for the 20 kDa membrane none of the filtration steps show a linear trend, which means that the passage of molecules and dissolved components through the membrane does not occur at even rates over each experiment period.

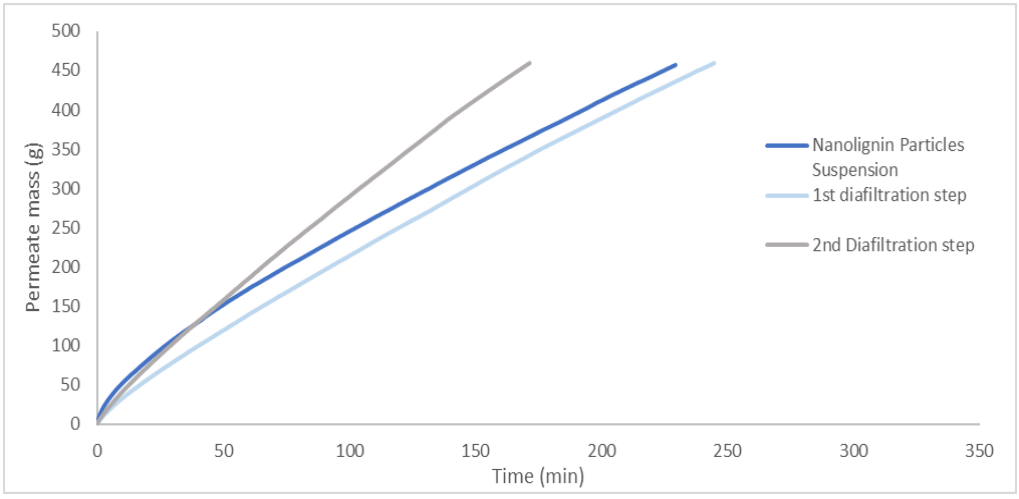

Figure 23. 30 kDa membrane experiments (8 bar and 0.7 L/min).

Table 9. Mean transmembrane fluxes for each filtration step of 30 kDa membrane.

UF/DF Step	Mean Transmembrane Flux (L/(m^2.h))
Initial Suspension Filtration	13.98
1st Diafiltration Step	13.99
2nd Diafiltration Step	20.11

For the 30 kDa membrane (Figure 23 and Table 9), the transmembrane fluxes for the initial suspension step and the 1st Diafiltration step are similar to the ones from 20 kDa membrane (Table 8). On the other hand, the transmembrane flux for the 2nd Diafiltration Step is higher than the ones for the 10 and 20 kDa membranes. This shows, that the second addition of water as a more prominent effect in the transmembrane flux than for the previous membrane.

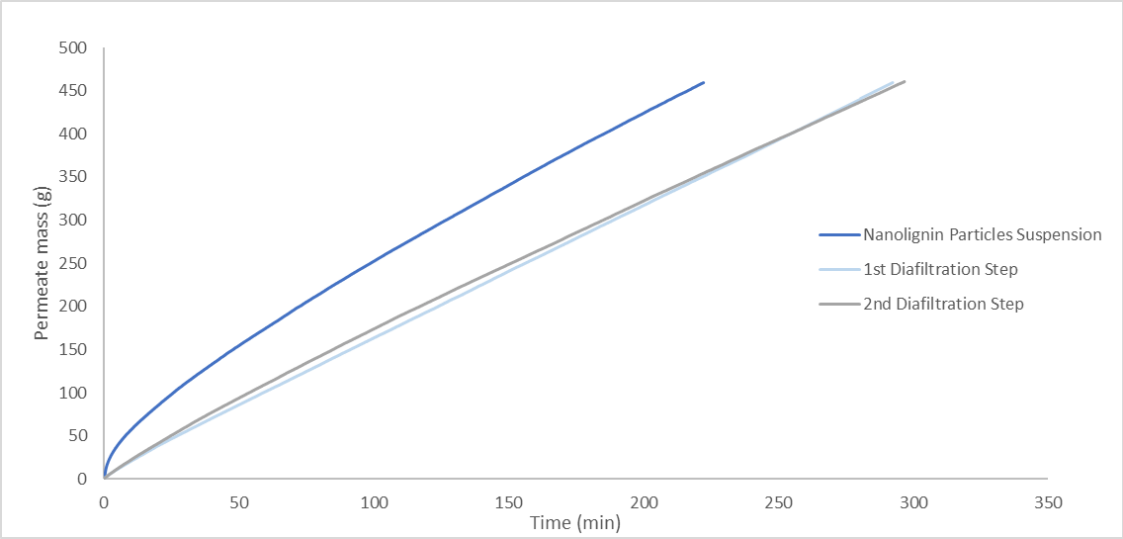

Figure 24. 50 kDa membrane experiments (8 bar and 0.7 L/min).

Table 10. Mean transmembrane fluxes for each filtration step of 50 kDa membrane.

UF/DF Step	Mean Transmembrane Flux (L/(m^2.h))
Initial Suspension Filtration	14.5
1st Diafiltration Step	11.9
2nd Diafiltration Step	11.6

In Figure 24 and Table 10 , are represented the three batch filtration steps for the 50 kDa membrane and the respective transmembrane fluxes. The transmembrane flux for the nanolignin particle suspension for the 50 kDa membrane is slightly higher than for the 20 and 30 kDa membranes. In contrast with that, the 1st and 2nd diafiltration have lower transmembrane fluxes than the ones from the 10, 20 and 30 kDa membranes. This might be explained by the fact that the addition of water when using the 50 kDa membrane does not have such a significant effect in cleaning the membrane fouling and so increasing the transmembrane flux than for the other membranes. On the other hand, unlike the other three membrane experiments, the 2nd diafiltration step does not show an increase in the amount of permeate mass over time, which means, the transmembrane flux does not increase with the second addition of water.

4.1.3.4 Assessment of membrane fouling

The final transmembrane flux was measured for the cross-flow system after all the filtration experiments using the nanolignin particles suspension were finished, with the goal of evaluating the effect of fouling in the transmembrane flux. For that reason, a 15 % ethanol hydroalcoholic solution was used to measure the permeate flux in each of the membranes used. The permeate mass (g) over time for each of the membranes used is shown in Figure 25.

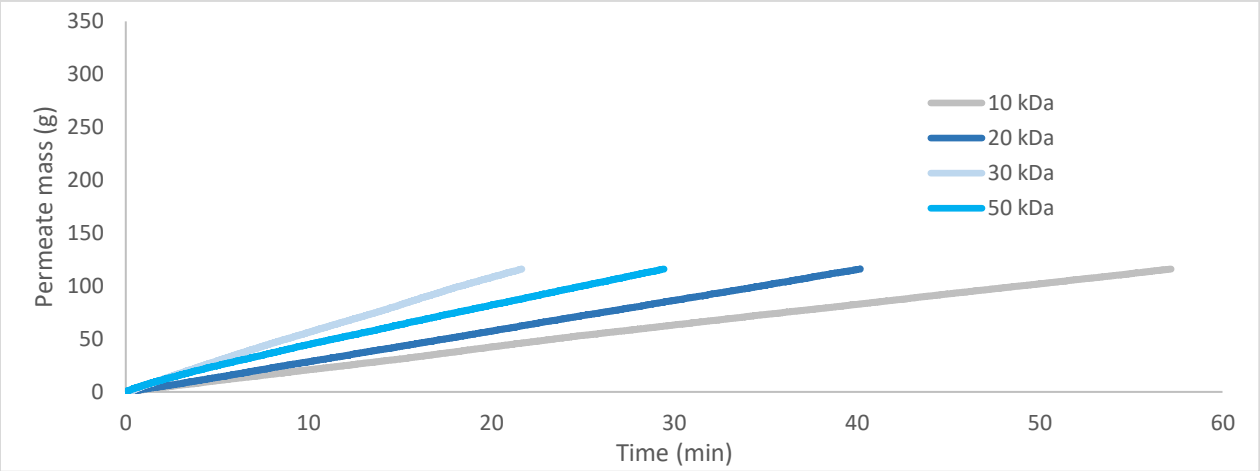

Figure 25. Permeate mass (g) over time (min) for the measurement of the final permeate flux of each membrane.

The permeate mass over time for all the membranes shows a linear trend. As expected, the 10 kDa membrane is the one with the lowest slope, which means, the lowest final transmembrane flux. The experiment that took least time to reach the final permeate mass content was the 30 kDa membrane.

The difference between the initial and the final transmembrane flux for each of the membranes is represented in Figure 26.

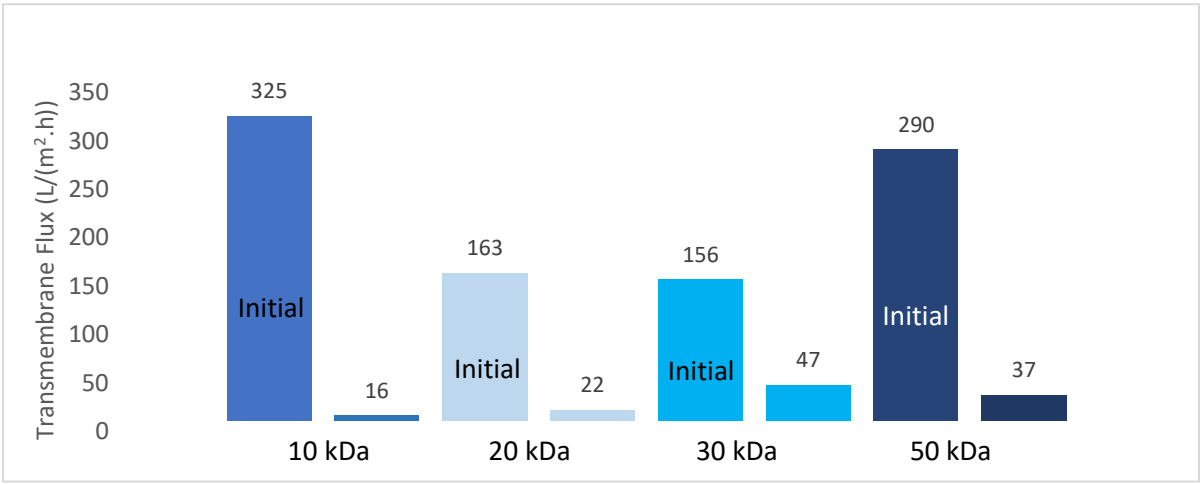

Figure 26. Initial and final Transmembrane Flux for membranes with different cut-offs.

Comparing the initial transmembrane flux for the cross-flow system (Figure 26) with the experiments using the stirred cell (Figure 17) it would be expected, since the membrane active surface area is smaller (14.6

cm^2) than for the cross-flow system (80 cm^2), that the initial transmembrane fluxes would be higher for all the experiments when using the cross-flow system. Since the membranes were not used in a sterile environment this could influence the fluxes as dust particles get on the membrane surface.

For the final transmembrane flux, two different comparisons can be made. First, it is expected that the smaller the cut-off, the thicker the layer formed in the surface of the membrane (fouling), which means, the smaller the final transmembrane flux. On the other side, the 30 and 50 kDa membranes are made of hydrophilic PES, which means, that these membranes should be more resistant to fouling (Nunes and K.-V. 2001). Having in account these two points, it makes sense that the final transmembrane flux increases from the smallest to the biggest cut-off.

For the 50 kDa membrane, the final transmembrane flux is lower than for the 30 kDa membrane. For the same operating conditions, the initial transmembrane flux is expected to be higher for membranes with bigger cut-offs, resulting in a bigger number of dissolved components going through the membrane. However, according to equation (7) in page 13, as the permeate flux through the membrane increases, so does the concentration polarization module, which translates into an increase in the concentration polarization effect. This effect will contribute to the membrane fouling which leads to a lower final transmembrane flux for the 50 kDa membrane when compared with the 30 kDa membrane, which have a lower concentration polarization effect. According to this evaluation, the best membrane should be the one where the difference between the initial and the final transmembrane flux is smaller because it means the filtration process will be less affected by fouling and other conditions over time. As seen in Figure 26, the 30 kDa membrane is the one in which the difference between the initial and the final transmembrane flux is lower, making this membrane the one that shows the best performance in this separation process. It is also possible to notice that all the membranes have a reduction in the transmembrane flux after experiments, varying from 70 % to 95 % of TF reduction depending on the membrane which might be explained by the thick layer of nanolignin particles that forms on the membrane surfaces.

4.1.4 Analytics

The samples taken for further analysis were labeled according to the code indicated in Table 11, to simplify the results analysis. The letter X corresponds to the membrane cut-off used in each experiment (10, 20, 30 and 50 kDa).

Table 11. Samples labeling code.

Code name	Type of sample	Step of filtration when sample was taken
SX	Initial suspension	Before filtration starts
R1X	1st retentate	Middle of the suspension step
R2X	2nd retentate	End of the suspension step
W1R1X	3rd retentate	Middle of 1st diafiltration step
W1R2X	4th retentate	End of 1st diafiltration step
W2R1X	5th retentate	Middle of 2nd diafiltration step
W2R2X	6th retentate	End of 2nd diafiltration step
P1X	1st Permeate	Middle of the suspension step
P2X	2nd permeate	End of the suspension step
W1P1X	3rd permeate	Middle of 1st diafiltration step

W1P2X	4th permeate	End of 1st diafiltration step
W2P1X	5th permeate	Middle of 2nd diafiltration step
W2P2X	6th permeate	End of 2nd diafiltration step

As a lapse, the first sample of retentate (R1) for the 30 kDa membrane experiments was not taken, so only the final retentate (R2) of the first filtration step was analyzed.

4.1.4.1 Particle Sizing

As previously described (chapter 3.4.3) all the samples taken during the concentration and purification of the nanolignin particles suspension for each of the membrane experiments, before being ultra-centrifuged, were evaluated for their particle size using the ZetaPals from Brookhaven Instruments Corporation.

The next graphic (Figure 27) shows the obtained particle size for all initial nanolignin particle suspension and retentate samples taken before centrifugation, in their diluted form. Since the samples were diluted at a ratio of 1:100 of sample to deionized water, the viscosity and refractive index selected in the equipment parameters were the ones from water, which means a viscosity of 0.890 cP and a refractive index of 1.330.

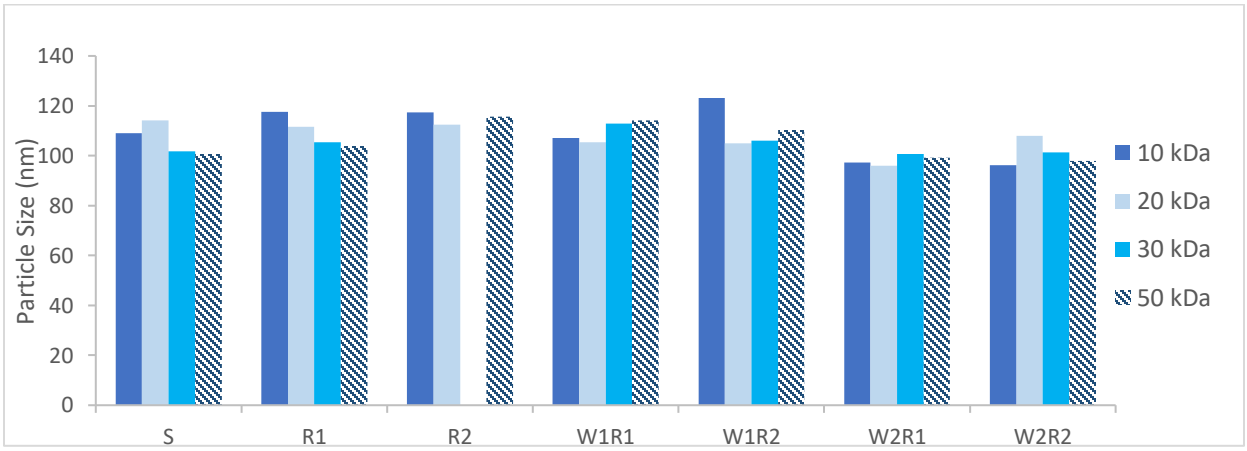

Figure 27. Particle size for each sample of all different membranes.

Even though the particle size measurements vary between 97 and 123 nm, those values are in the expected range of particle size for nanolignin particles based on previous experiments (Beisl, Loidolt, et al. 2018). So, it is possible to conclude that the particle size is approximately constant over time within all the experiments.

4.1.4.2 Ethanol Content

As explained before in chapter 3.4.3, High Performance Liquid Chromatography was used to determine the ethanol content of the samples taken during the experiments with the nanolignin particle suspension. All the samples of retentate and permeate before centrifugation and the supernatant of the samples after centrifugation were analyzed. The initial assumption was that the total amount of ethanol in the solution over the filtration process would decrease in the same proportion as the total volume of solution. This would mean that the ethanol concentration should be approximately the same, for each filtration step of each different membrane experiment.

The ethanol content of the samples after centrifugation, is expected to be slightly higher, since the ultra-centrifugation at 288000g separates a small quantity of solids from the solution, decreasing the total volume of solution and consequently increasing the concentration of ethanol.

Based on the initial assumption that all the ethanol molecules would pass through the membrane at the same rate as water does and considering that the samples taken do not change the concentration of ethanol in the solution, it would be expected that the ethanol concentration would be constant within each filtration step and decrease only with the addition of water for each of the different diafiltration steps.

The next graphics (Figure 28 to Figure 31) show the ethanol content variation over the three steps of the filtration process, for both the samples before and after centrifugation, for all the four different membranes. In addition to that, the graphics show the expected ethanol concentrations based on the assumptions made.

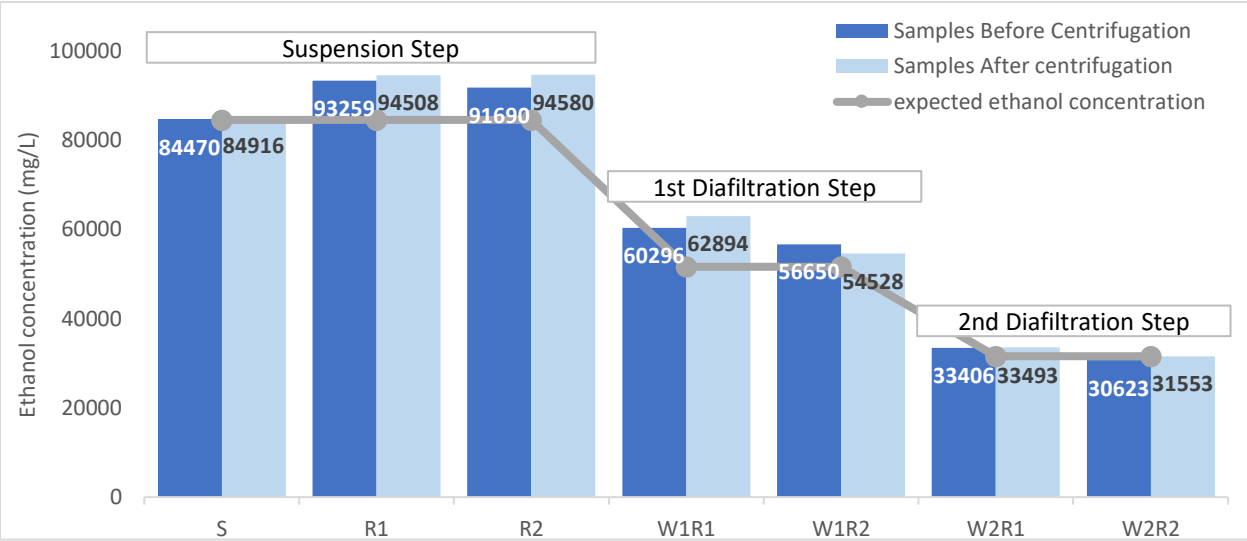

Figure 28. Ethanol Concentration (mg/L) for samples before and after centrifugation for 10 kDa membrane.

For the 10 kDa membrane, one thing that could justify the difference between the initial suspension and the first sample of retentate (R1), is that as the thick layer of nanolignin and other components is formed on the membrane surface, it is possible that the dissolved lignin molecules with bigger dimensions (such as 10 kDa), are also retained on the membrane surface, leading to an increase or decrease of the total volume of suspension and therefore, changing the ethanol concentration. On the other hand, the small difference between the first sample of retentate (R1) and the final retentate sample for the first filtration step (R2), can be due to small ethanol evaporation or errors associated with the analysis methods. With the addition of water, for the first and second diafiltration steps, the ethanol concentration decreases, as expected, since there is more volume of solution for the same amount of ethanol.

For the different retentates of each diafiltration step, it would also be expected that the concentration of ethanol would not change within the same diafiltration step. As seen in Figure 28, this does not occur, once again, this can be due to fluctuations within the dissolved lignin trapped on the membrane surface, which could change the overall concentrations and also the errors of the measurements.

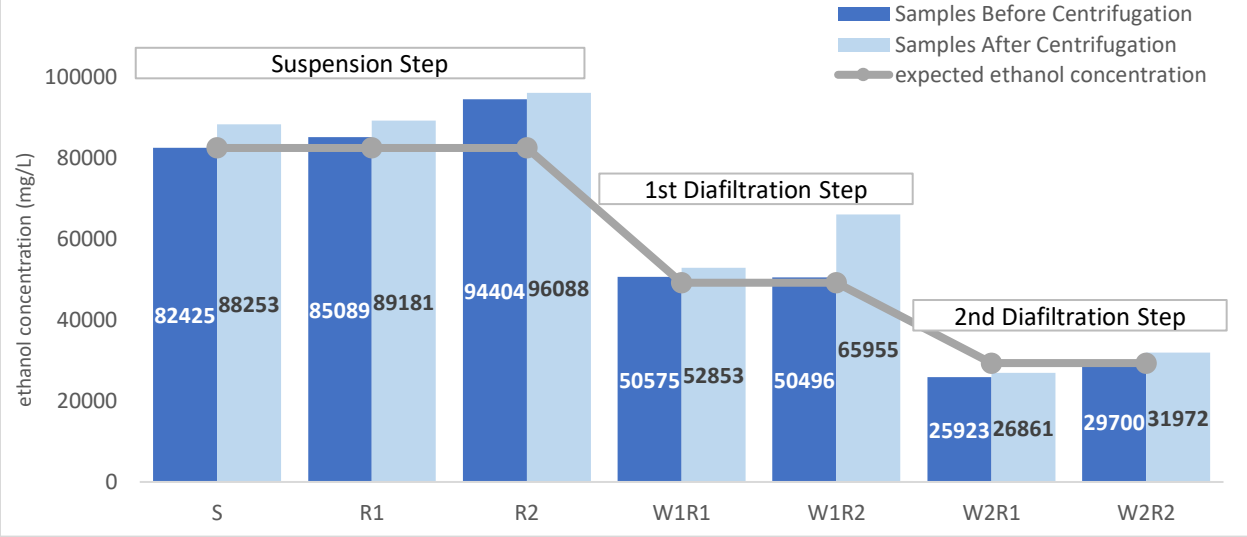

Figure 29. Ethanol Concentration (mg/L) for samples before and after centrifugation for 20 kDa membrane.

In Figure 29, the ethanol concentration for all the samples of the experiment using the 20 kDa membrane is shown. The increase of the membrane cut-off from the previous experiment, may justify the difference in the ethanol concentration of the retentate samples of the first filtration step (suspension step). Since the cut-off is bigger than the previous one (10 kDa), initially, the dissolved lignin molecules, (which size is about 10 kDa) will not be retained on the membrane surface. After a while, as a thick layer of nanolignin particles forms on the membrane surface it is possible that also the dissolved lignin molecules are trapped on the membrane surface, decreasing their concentration in the retentate and consequently increasing the ethanol concentration. For the sample labeled as W1R2, the high difference between the ethanol concentration of the sample before and after centrifugation is probably because of errors associated with the analysis methods, as explained before.

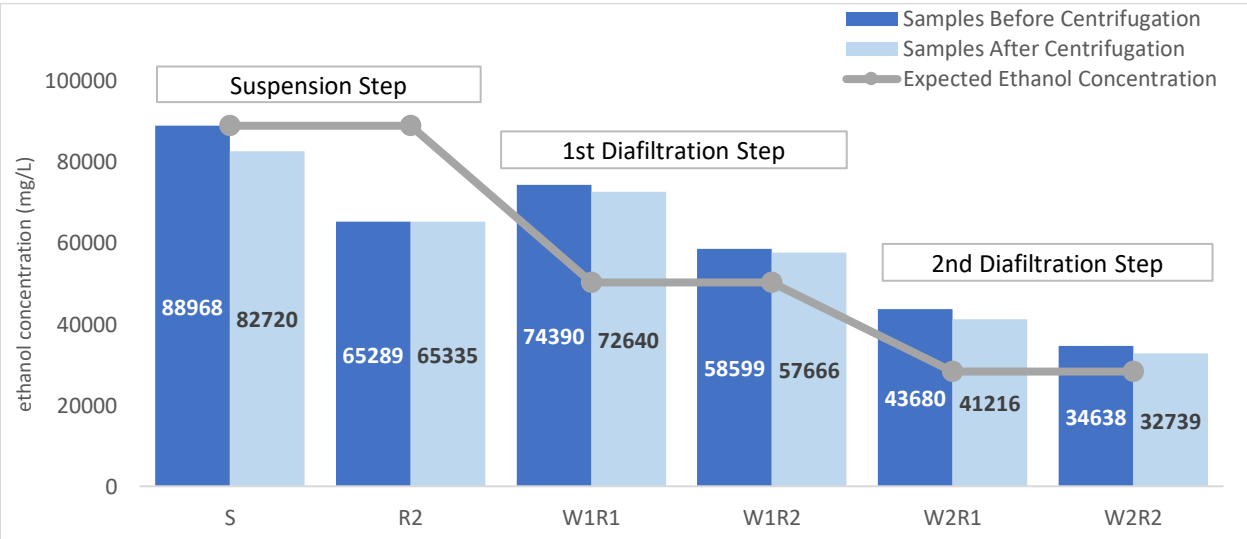

Figure 30. Ethanol Concentration (mg/L) for samples before and after centrifugation for 30 kDa membrane.

The ethanol concentration for the 30 kDa membrane experiments is represented in Figure 30. As previously said, (p. 12) as a lapse, the first sample of retentate in the initial filtration step was not taken. For this

membrane the obtained results are not clear. It is possible to see the ethanol concentration decreases with the addition of water but, it was expected, that this value would be much lower than the results show, at least for the sample W1R1.

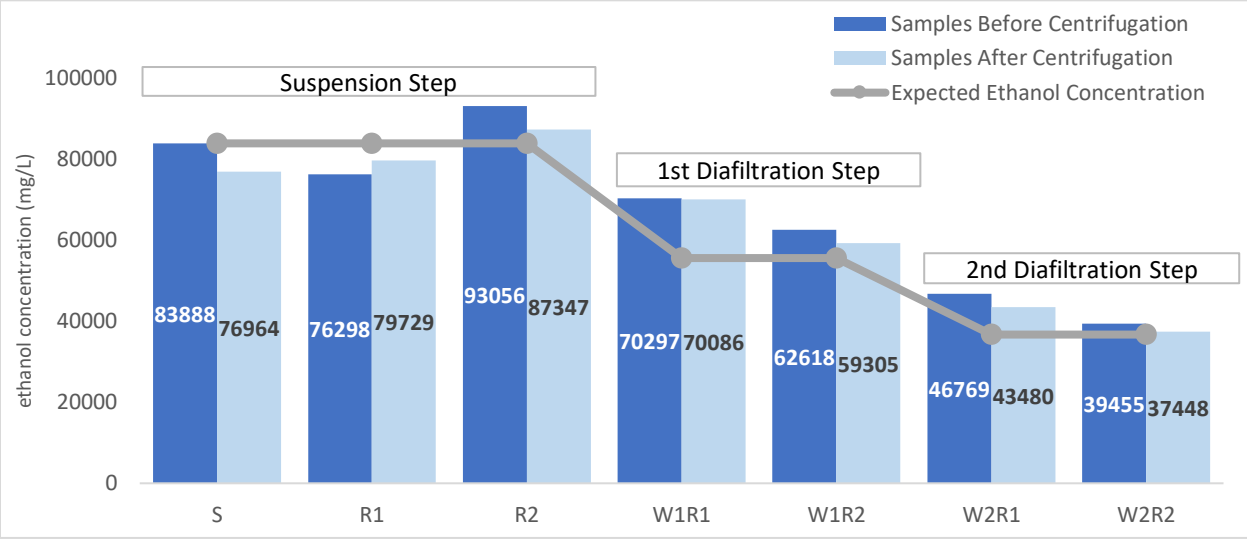

Figure 31.Ethanol Concentration (mg/L) for samples before and after centrifugation for 50 kDa membrane.

In Figure 31, are represented the results for the 50 kDa experiments. It is possible that the concentration of ethanol increases slightly as the nanolignin particles layer forms on the membrane surface, decreasing the total volume, leading to fluctuations of the ethanol concentration within the first filtration step. The addition on water decreases the ethanol concentration but not as much as expected. On the other hand, these differences might be explained by the errors associated with the analysis which means that the repeatability and confidence of the analysis is not reliable, especially for the 30 and 50 kDa.

The next figure, Figure 32, shows the ethanol content of all the permeate samples for each different experiment using different membranes.

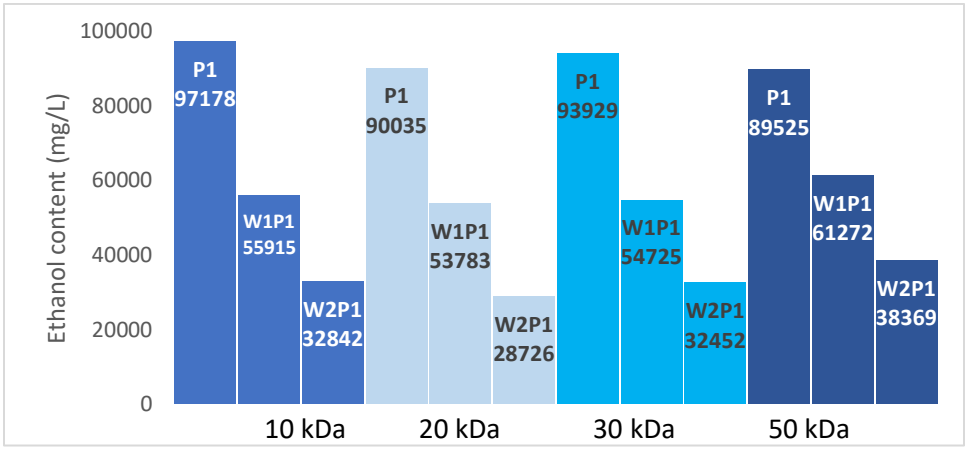

Figure 32. Ethanol concentration for all the permeates of all membranes used.

The best membrane should be the one that initially in the first filtration step is less affected by the fouling, which means, the one in which the ethanol concentration seems constant (between the retentates). On the other hand, should be the one that shows the highest concentration decrease between the initial and the

final retentate (W2R2). All the membranes seem to have a similar efficiency in separating ethanol from the nanolignin particles, since the difference between initial and final ethanol concentration is similar. The 50kDa membrane experiment as a lower difference in the initial and final ethanol concentration but there was a higher amount of initial suspension for the same collected permeate, which justifies that difference.

4.1.4.3 Total Organic Carbon Content

As explained in Chapter 3.4.3, all the samples were analyzed for their total Organic carbon (TOC) content, with the goal of calculating the difference between the TOC of the samples before centrifugation and the supernatant of the samples after centrifugation and getting the exact amount of nanolignin particles concentration in the solutions. The TOC concentration of the initial suspension and retentate samples, before and after centrifugation for all the different membrane experiments are shown in the following graphics (Figure 33 to Figure 36).

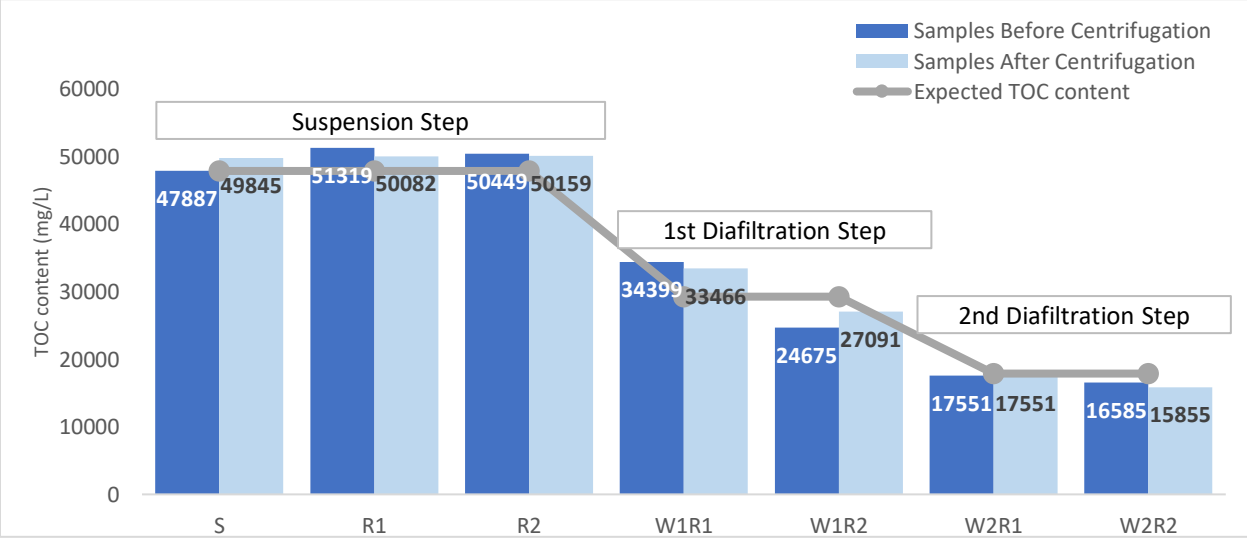

Figure 33. TOC concentrations for the 10 kDa membrane experiments.

For the 10 kDa membrane experiments (Figure 33), the total organic carbon concentration seems to increase slightly from the initial suspension (S) to the first retentate sample (R1) but it seems approximately the same than the second retentate (R2). This might be explained by the accumulation of nanolignin particles on the membrane surface, which decreases the total volume, increasing the concentration of the TOC in the retentates or by errors associated with the measurements. Within the 1st Diafiltration Step the concentration decreases between W1R1 and W1R2 due to errors associated with the analysis and the samples preparation.

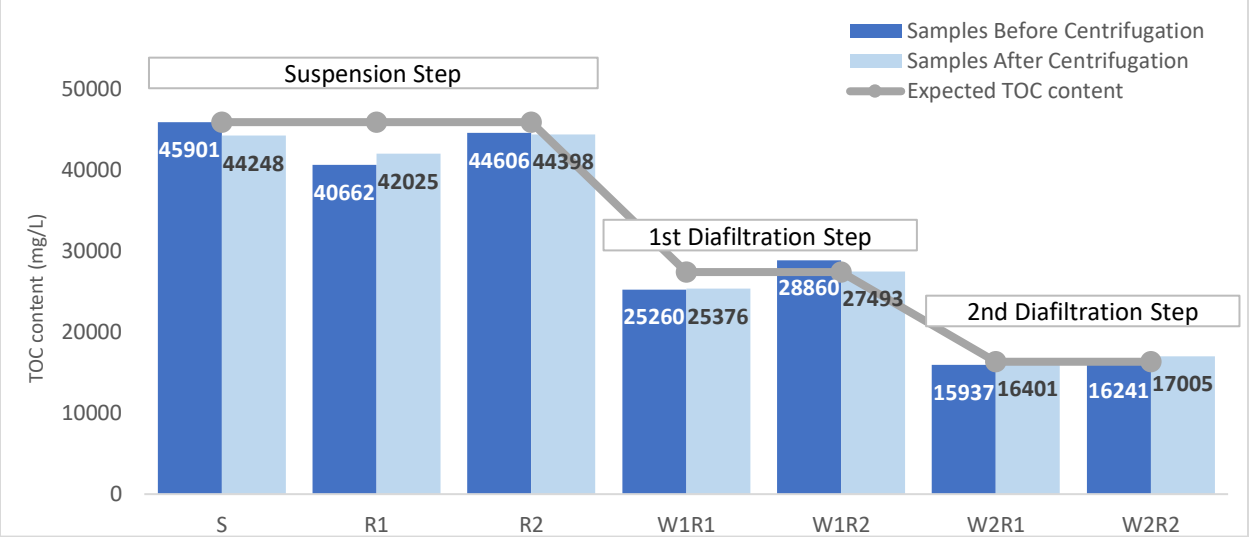

Figure 34. TOC concentrations for the 20 kDa membrane experiments.

For the 20 kDa membrane experiments (Figure 34) the TOC concentration slightly increase within the first filtration step, can be due to accumulation of nanolignin particles on the membrane surface and due to errors associated with the analysis. The TOC content decreases in the same range as expected, and the differences within samples of the same diafiltration step, change due to errors of the analysis.

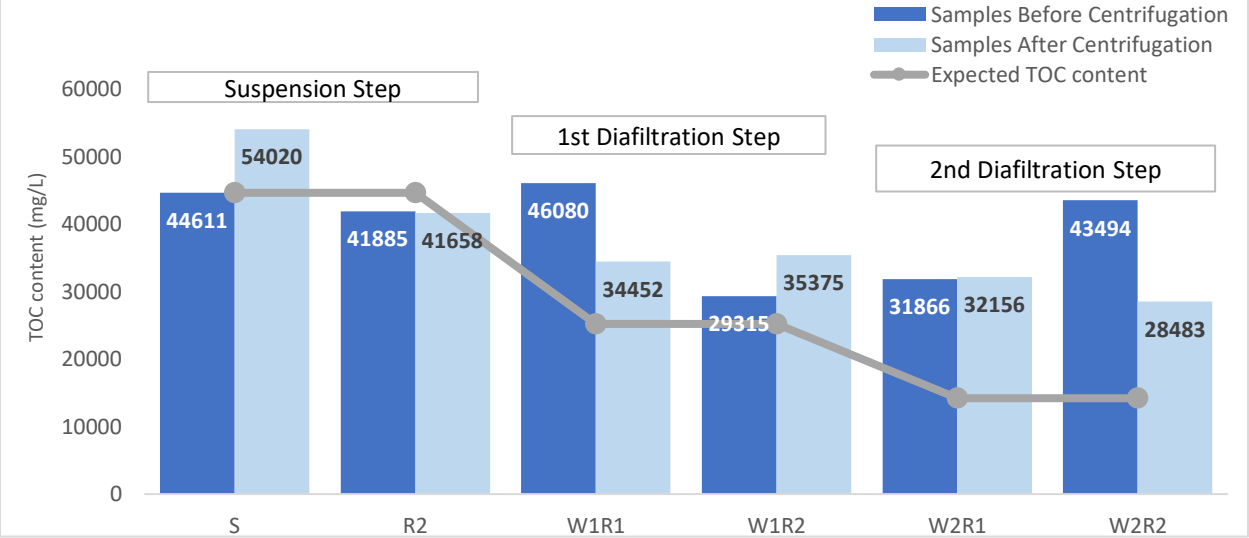

Figure 35. TOC concentrations for the 30kDa membrane experiments.

For the 30kDa membrane, Figure 35, the retentate sample taken for the first filtration step (R2) shows results closer to what was expected contrary to ethanol concentration results (Figure 30), which could mean that something happened in the preparation of the same sample for the HPLC analysis. On the other hand, the expected results for the samples of W2R1 and W2R2 do not give reliable results, since the TOC concentration is way higher than expected, this might be due to errors in the measurements.

In Figure 36, the results for the TOC analysis of the 50 kDa experiments are represented. As for the other experiments, these results are highly affected by the measurements errors and are not reliable.

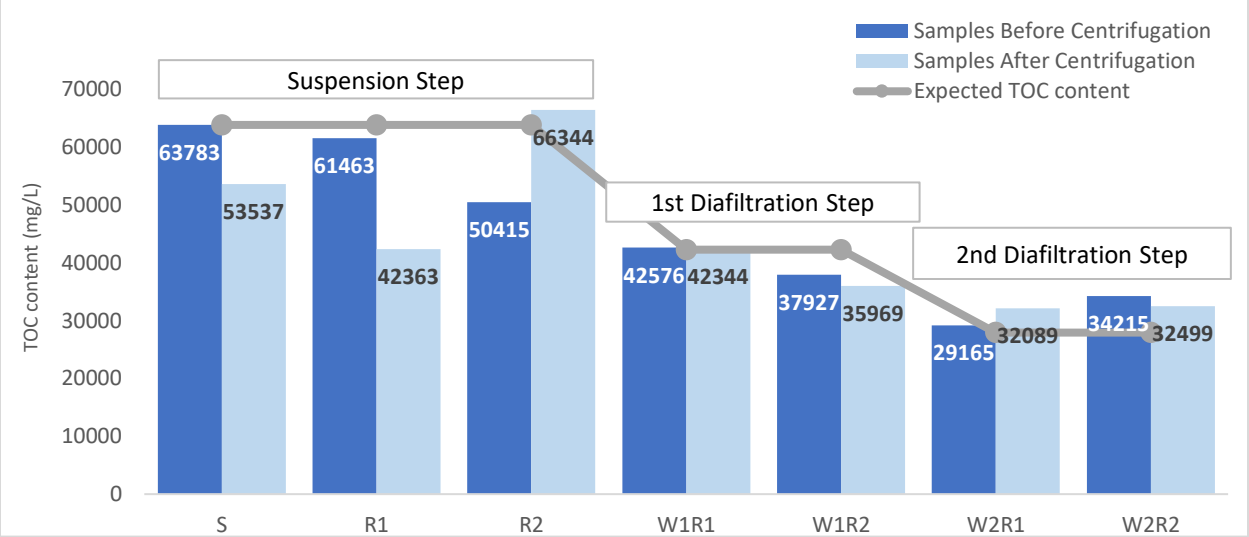

Figure 36. TOC concentrations for the 50 kDa membrane experiments.

Several difficulties made it impossible to use this method to obtain the exact amount of nanolignin particles. To begin with, the unreliability of the HPLC results made it impossible to calculate the correct amount of carbon content in the samples that was from ethanol contribution. Moreover, a thick layer of nanolignin particles is formed on the membrane surface, which makes it impossible to close the mass balances for the nanolignin particles. Furthermore, the suspensions before centrifugation have nanolignin particles which can settle at the bottom of the flask and affect the results of the TOC analysis, as the analysis time takes at least 30 minutes. Finally, deionized water is always used for the preparation of the samples and in the machine for the analysis itself, but it is not possible to guarantee that this water is not contaminated with small amounts of other components, affecting the results. Based only on the TOC concentrations of the retentate samples and considering our measurement errors, it is not possible to conclude which membrane is better in separating and purifying the nanolignin particles from the dissolved components.

4.1.4.3.1 Removal efficiency of dissolved components

A mass balance of the TOC mass in the system at the end of all UF/DF experiments can be made, based on equation (22).

$$TOC_{initial\ suspension} = TOC_{W2R2} + \sum_{i=1}^{3} TOC_{samples} + \sum_{i=1}^{3} TOC_{permeates} \quad (22)$$

Where,

$TOC_{initial\ suspension}$ = TOC amount of the initial suspension, mg.

TOC_{W2R2} = TOC amount of the final retentate (W2R2), mg.

$TOC_{samples}$ = TOC amount of each of the samples taken (R1, R2, W1R1, W1R2, W2R1), mg.

$TOC_{permeates}$ = TOC amount of each of the collected permeates (P1, W1P1, W2P1), mg.

Table 12. TOC amount (mg) used for the mass balance of TOC for each membrane experiment.

Membrane	10kDa	20kDa	30kDa	50kDa
TOC initial suspension (mg)	59794	52012	57261	74121
TOC final retentate (W2R2) (mg)	5997	8098	15523	22754
TOC all samples taken (mg)	13289	10632	3273	8679
TOC all permeates (mg)	40537	36116	55696	51641
Mass Balance result (equation (22))	-31	-2836	-17232	-8956

The mass balances for the TOC amount do not close, which can be due to the accumulation of nanolignin particles on the membrane surface, which vary within the all UF/DF experiment and can influence the concentration at a certain moment and errors associated with the measurements.

To find the removal efficiency of the dissolved components from the initial nanolignin particle suspension, the ratio of TOC amount from the permeates and TOC amount of dissolved components in the initial suspension was calculated, following the equation (23). The total organic carbon amount used for the initial suspension is the supernatant from the suspension after centrifugation to use only the TOC related with the dissolved components and not with the nanolignin particles.

$$RE = \frac{\sum_{i=1}^{3} TOC_{permeates}}{TOC_{initial}} \quad (23)$$

Where,

$TOC_{permeate}$ = TOC amount in each permeate (P1, W1P1, W2P1), mg.

$TOC_{initial}$ = TOC amount of dissolved components in the initial suspension, mg.

The results obtained for this comparison method are shown in Table 13.

Table 13. removal efficiency of dissolved components in permeate based on TC results.

Membrane	RE of dissolved components (%)
10kDa	67.7%
20kDa	69.4%
30kDa	97.3%
50kDa	69.7%

Based on the mass balances results from Table 12, the results are not accurate, particularly for the 30 and 50kDa membrane which showed more errors for the mass balances calculations. The total amount of

organic carbon in the permeate samples was calculated using the TOC concentration of permeates over experiments. These concentrations are shown in Figure 37.

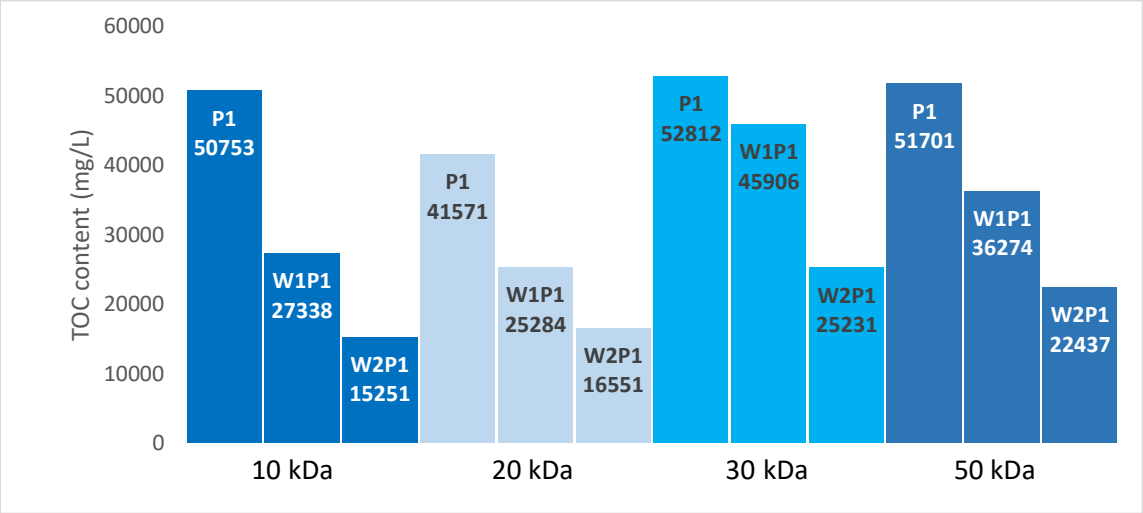

Figure 37. TOC concentration for all the permeates of all membranes used.

4.1.4.4 Dry Matter Content

As previously mentioned in chapter 3.4.3, the dry matter content of the samples before and after centrifugation was obtained. The dry matter concentration for the retentate samples before and after centrifugation is presented in Figure 38 to Figure 41.

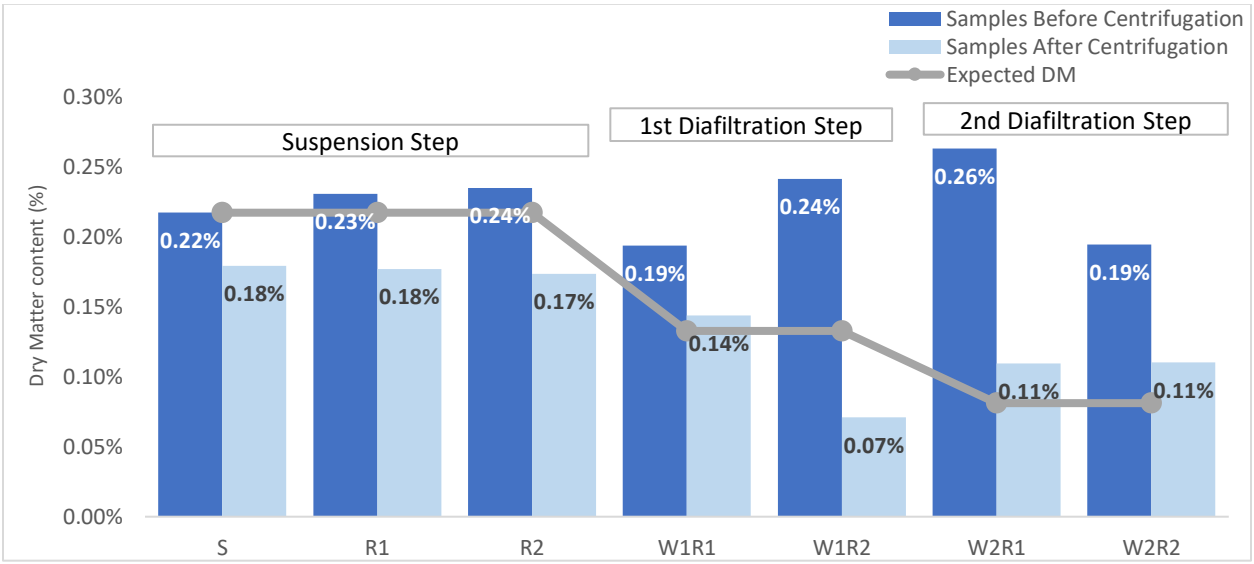

Figure 38. Dry matter content for 10 kDa membrane experiments.

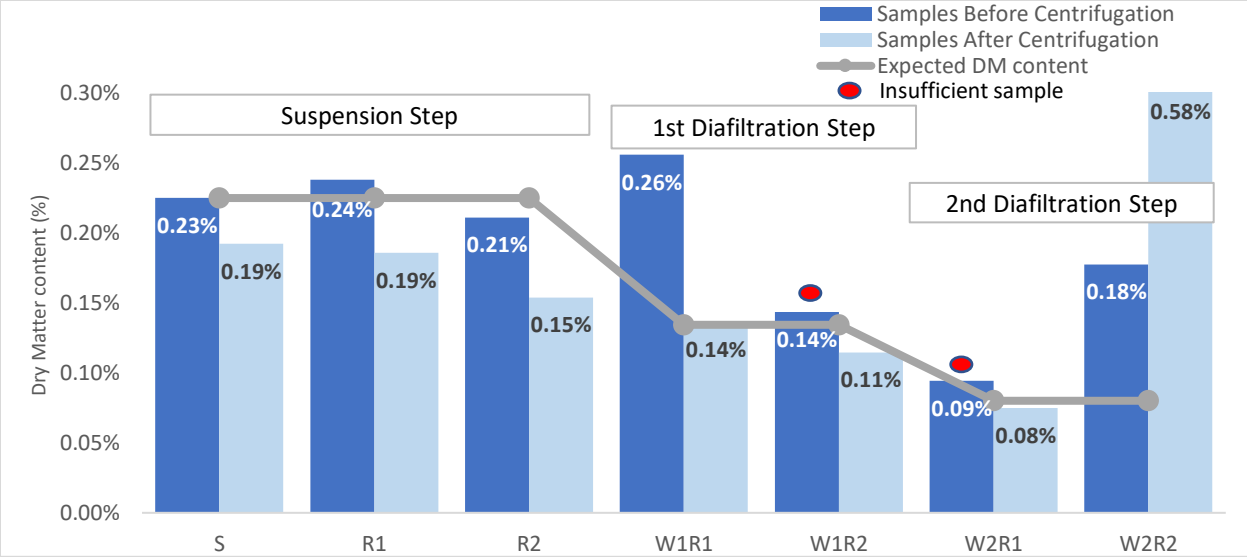

Figure 39. Dry matter content for 20 kDa membrane experiments.

In Figure 38 and Figure 39 the dry matter content for all steps of the 10 kDa and 20 kDa membrane experiment is shown, respectively. As expected, the dry matter content of the supernatant of the samples after centrifugation decreases with the addition of water for each new filtration step, as the suspension becomes less concentrated. The addition of water can also help clean the membrane surface, allowing the nanolignin particles trapped in the membrane to go back to the bulk solution, increasing the DM concentration in the samples before centrifugation. It was considered, that a minimum mass of 0.005g of dry matter was needed for each sample to have reliable results. For that reason, some of the samples in the graphics from Figure 38 to Figure 41 have an indication (red circle) that shows that not enough amount of sample was available to get a reliable result. Finally, the last sample of retentate (W2R2) for the 20 kDa membrane experiments,should not be considered since it was stored for a considerate amount of time prior to the DM analysis, which changed the sample considerably.

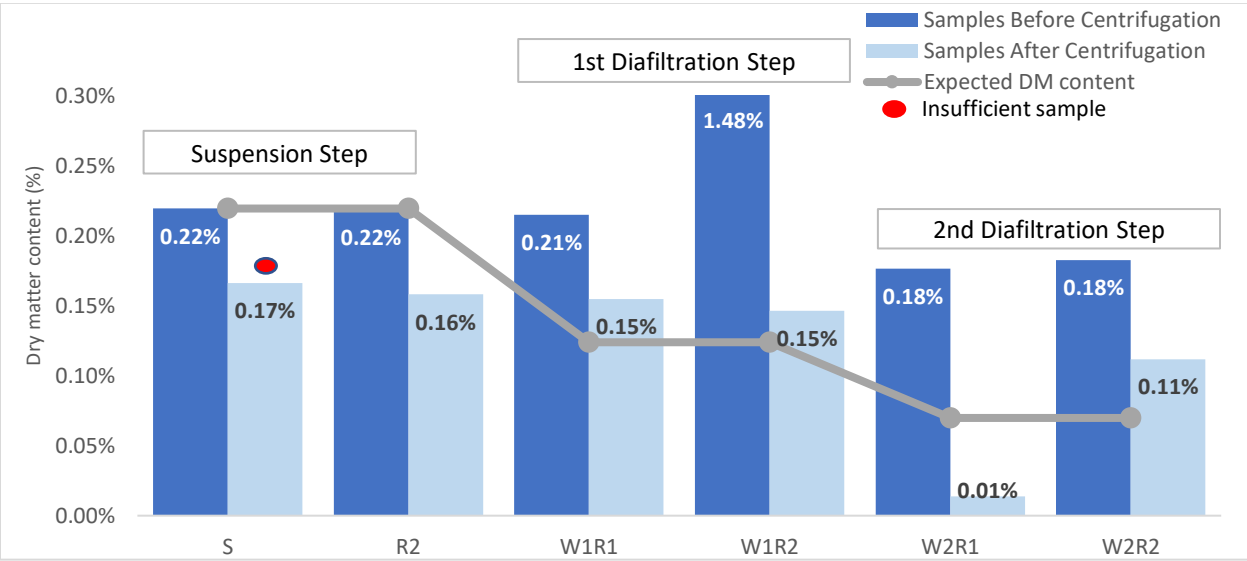

Figure 40. Dry matter content for 30 kDa membrane experiments.

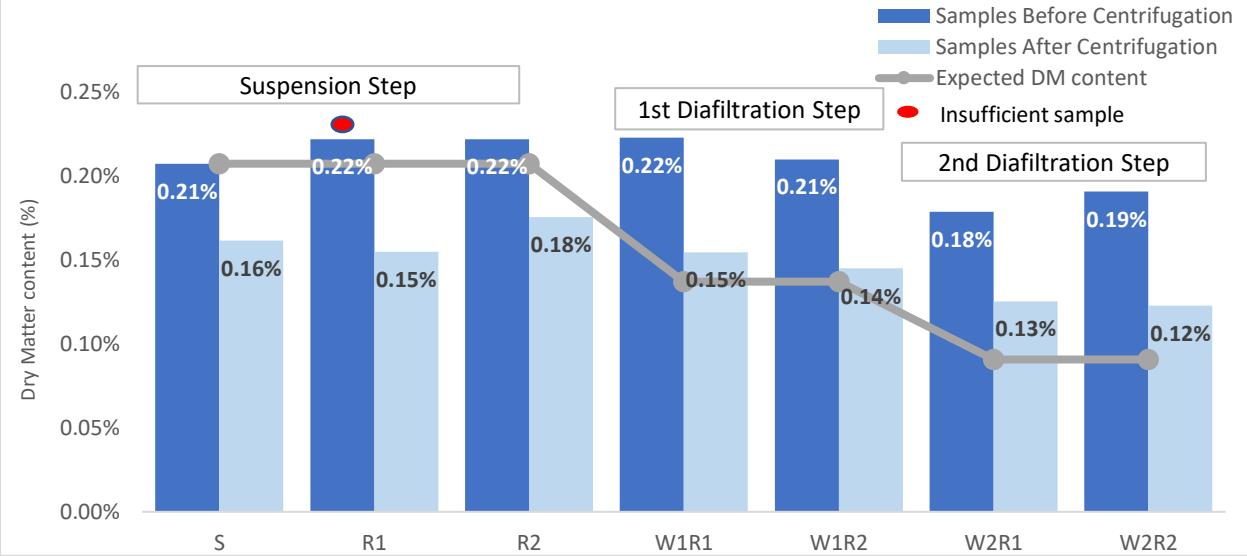

Figure 41. Dry matter content for 50 kDa membrane experiments.

In Figure 40 and Figure 41 is represented the dry matter concentration over the experiments for the 30 and 50 kDa membranes, respectively. As the results for the Total Organic Carbon analysis show (chapter 4.1.4.3), the dry matter concentration for the 30 and 50 kDa membranes seems to be overall stable between all UF/DF experiments (excluding W1R2 and W2R1 from 30kDa membrane). The addition of water should decrease the DM concentration initially, but by the time the first retentate sample of each diafiltration step (W1R1 and W2R1) is taken, several hours of diafiltration have already been done, which can cause significant changes in the DM concentration. If the addition of water is also responsible for partially cleaning the membrane, then the DM concentration of the samples before centrifugation can increase has more nanolignin particles return to the bulk solution.

These clean membranes also have higher permeation fluxes and the addition of water can allow a higher rate of water and other dissolved components that do not contribute for the DM content to go through the membrane while the same quantity of components that contribute to the DM content go through the membrane at the same rate. For the 30 kDa membrane, Figure 40, the samples of W1R2 before centrifugation and W2R1 after centrifugation are not usable, since there was not enough sample to get reliable results.

Most of the errors associated with this method are caused by not having enough quantity of sample to get reliable results. It was expected that the dry matter content before centrifugation was higher than the dry matter content of the samples after centrifugation, since the nanolignin particles were removed from the suspension. For some of the samples, only the result before or after centrifugation can be analyzed as some of the values are not accurate. On the other hand, some of the samples were stored for a considering amount of time, it is not possible to evaluate the changes that can occur to this type of solution during that time and how they affect it.

Although the results are not completely accurate, it is still a more reliable method than the TOC analysis, at least for this type of suspension. The best membrane should be the one in which the concentration of

components that contribute to DM content is constant over the experiments within each filtration step, only changing with the addition of water. On the other hand, it should be the membrane in which the results show a lower DM concentration on the last retentate (W2R2) when compared with the initial suspension DM concentration. Since the results of this difference are similar for the samples after centrifugation for the 10, 20 and 50 kDa membranes and since the 3kDa W2R2 sample was unreliable, it is necessary to analyze the DM in terms of exact amounts for the permeate samples. These samples DM content were made with a significant amount of permeate sample, which makes these results more reliable.

4.1.4.4.1 Removal efficiency of dissolved components for DM results

A mass balance of the Dry Matter mass in the system at the end of all UF/DF experiments can be made, based on the equation (24).

$$DM_{initial\ suspension} = DM_{W2R2} + \sum_{i=1}^{5} DM_{samples} + \sum_{i=1}^{3} DM_{permeates} \quad (24)$$

Where,

$DM_{initial\ suspension}$ = DM amount of the initial suspension, mg.

DM_{W2R2} = DM amount of the final retentate (W2R2), mg.

$DM_{samples}$ = DM amount of each of the samples taken (R1, R2, W1R1, W1R2, W2R1), mg.

$DM_{permeates}$ = DM amount of each of the collected permeates (P1, W1P1, W2P1), mg.

Table 14. DM amount (mg) used for the mass balance of DM for each membrane experiment.

Membrane	10kDa	20kDa	30kDa	50kDa
DM initial suspension (mg)	2.120	2.218	1.750	2.195
DM final retentate (W2R2) (mg)	0.414	2.706	0.606	0.852
DM all samples taken (mg)	0.543	0.453	0.135	0.296
DM all permeates (mg)	0.642	0.625	0.822	0.839
Mass Balance result (equation (22))	0.521	-1.565	0.187	0.208

The mass balances for the DM amount do not close, which can be due to the accumulation of nanolignin particles on the membrane surface, which vary within all UF/DF experiment and can influence the concentration at a certain moment and errors associated with the measurements.

Figure 42 shows the DM concentration for all the collected permeates for the experiments with each different membrane.

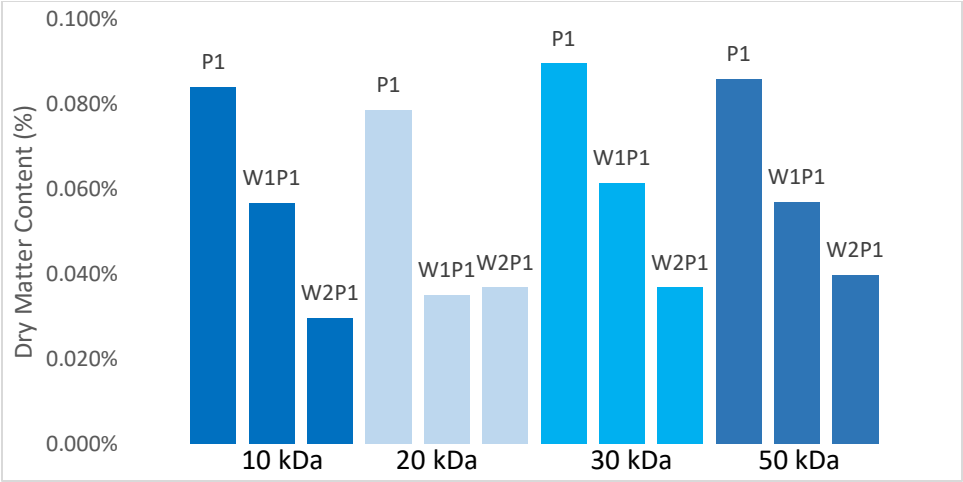

Figure 42. Dry Matter content for all the permeates of all different membranes.

All the permeates DM content results are considered reliable, since a great amount of sample was used for these analyses which allows the calculation of the removal efficiency (RE) of the dissolved components from the nanolignin particles. As it was previously made for the TOC analysis, the ratio of DM amount from the permeates and DM amount of dissolved components in the initial suspension was calculated, following the equation (25). The DM sample used for the initial suspension is the supernatant from the suspension after centrifugation to use only the DM related with the dissolved components and not with the nanolignin particles.

$$RE = \frac{\sum_{i=1}^{3} DM_{permeates}}{DM_{initial}} \quad (25)$$

Where,

$DM_{permeate}$ = DM amount in each permeate (P1, W1P1, W2P1), mg.

$DM_{initial}$ = DM amount of dissolved components in the initial suspension, mg.

The results obtained for this comparison method are shown in Table 15.

Table 15. Removal efficiency of dissolved components in permeate based on DM results.

Membrane	RE of dissolved components (%)
10 kDa	30.3%
20 kDa	28.2%
30 kDa	47.0%
50 kDa	38.2%

Based on Table 15 the membrane which is more efficient in separating the dissolved components from the nanolignin particle suspension is the 30kDa membrane, followed by the 50 kDa membrane.

4.2 Optimization UF/DF process using 30kDa membrane

Since the 30 kDa membrane showed better results in separating the nanolignin particles from the rest of the dissolved components in the suspension and as the results from the transmembrane flux analysis show this membrane is less prone to fouling, the 30 kDa membrane was chosen to do optimization experiments by varying the transmembrane pressure and the feed flow-rate in the cross-flow system.

One of the main problems in the previous experiments was the thick layer of nanolignin particles and other dissolved components that was formed on the membrane surface. As it is known, decreasing the pressure of the system and increasing the feed flow-rate usually decreases the fouling in the membrane surfaces. For this reason, three different experiments were made using the 30 kDa membrane. First, the previous experiment made with the 30 kDa membrane was repeated using 8 bar and a feed flow-rate of 0.7 L/min. Then, an experiment at 4 bar and 0.7 L/min was performed. Finally, the pressure was kept at 4 bar and the flow-rate increased for 2 L/min.

4.2.1 Initial Transmembrane Flux

As previously done for the experiments using membranes with different MWCO, the permeate mass (g) over time (min) was measured initially using an aqueous solution of 15 wt% ethanol. The results are in the graphic represented in Figure 43 and Table 16.

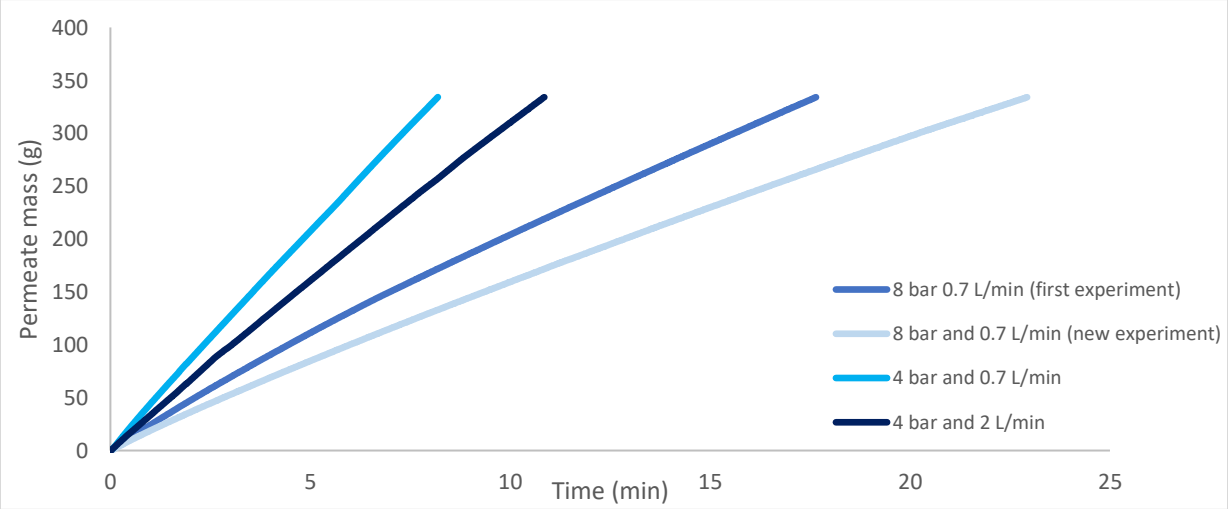

Figure 43. Permeate mass (g) over time (min) for the initial 15% ethanol solution experiments using different operating conditions.

Table 16. Mean transmembrane fluxes for each initial experiment using 15 % ethanol solution.

UF/DF Step	Mean Transmembrane Flux (L/(m^2.h))
8 bar and 0.7 L/min (previous experiment)	156
8 bar and 0.7 L/min	118
4 bar and 0.7 L/min	324
4 bar and 2 L/min	233

The results show a linear trend for the experiments using 4 bar but not for the experiments using 8 bar. On the other hand, the two experiments at 8 bar and 0.7 L/min show a great difference when using the hydroalcoholic solution with 15% ethanol, so more experiments were needed to further investigate this difference. Finally, the slope for the experiment at 4 bar and 0.7 L/min is higher than at 4 bar and 2 L/min, which means that the initial transmembrane flux for the experiment with lower flow-rate is higher. The opposite result was expected, but the increase in the transmembrane pressure could lead to membrane compaction, which would explain the difference in the initial transmembrane fluxes. Further experiments would have to be conducted with these conditions to verify this. Later, more conclusions regarding the initial transmembrane flux will be made when explaining the assessment of membrane fouling results.

4.2.2 UF/DF of Nanolignin Particles Suspension

After the assessment of the initial transmembrane flux the feed tank was filled with the nanolignin particles suspension and UF in DF mode was performed to separate and purify the nanolignin particles from the rest of the impurities. The permeate mass over time for the three filtration batches using different operating conditions is shown in Figure 44 to Figure 46. Furthermore, Table 17 to Table 19 show the mean transmembrane fluxes for all the experiments using the 30 kDa membrane.

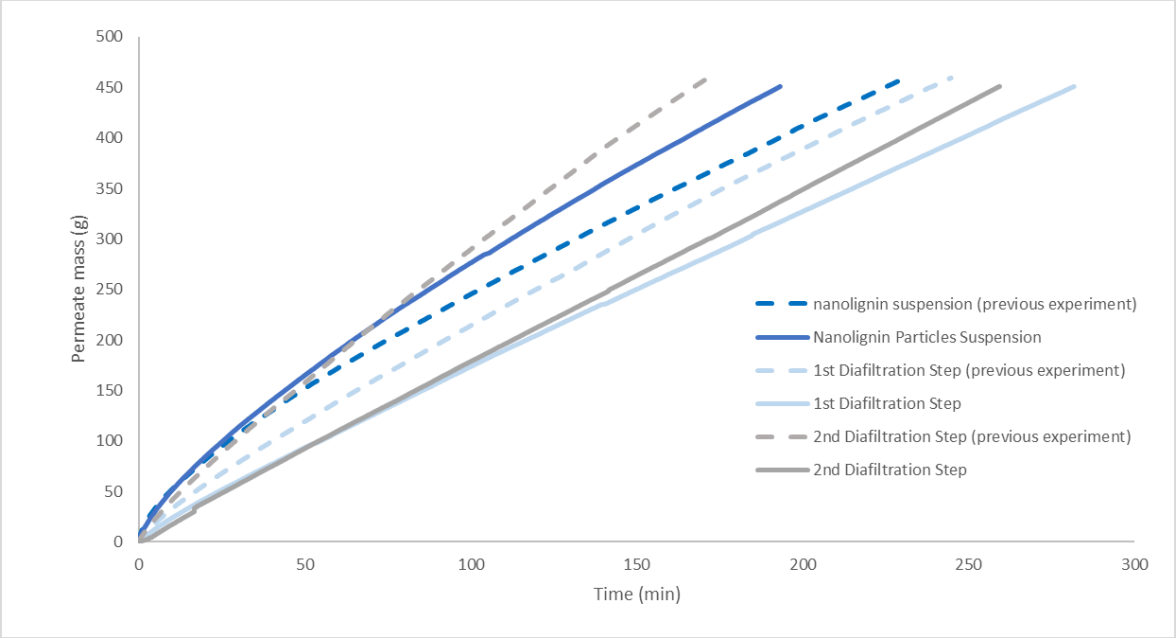

Figure 44. Permeate mass (g) over time (min) for the new experiment at 8 bar and 0.7 L/min.

Table 17. Mean transmembrane fluxes for each filtration step of both experiments at 8 bar and 0.7 L/min.

UF/DF Step	Mean Transmembrane Flux (L/(m^2.h))	
	8 bar and 0.7 L/min (previous experiment)	8 bar and 0.7 L/min
Initial Suspension Filtration	13.98	16.69
1st Diafiltration Step	13.99	12.01
2nd Diafiltration Step	20.11	13.24

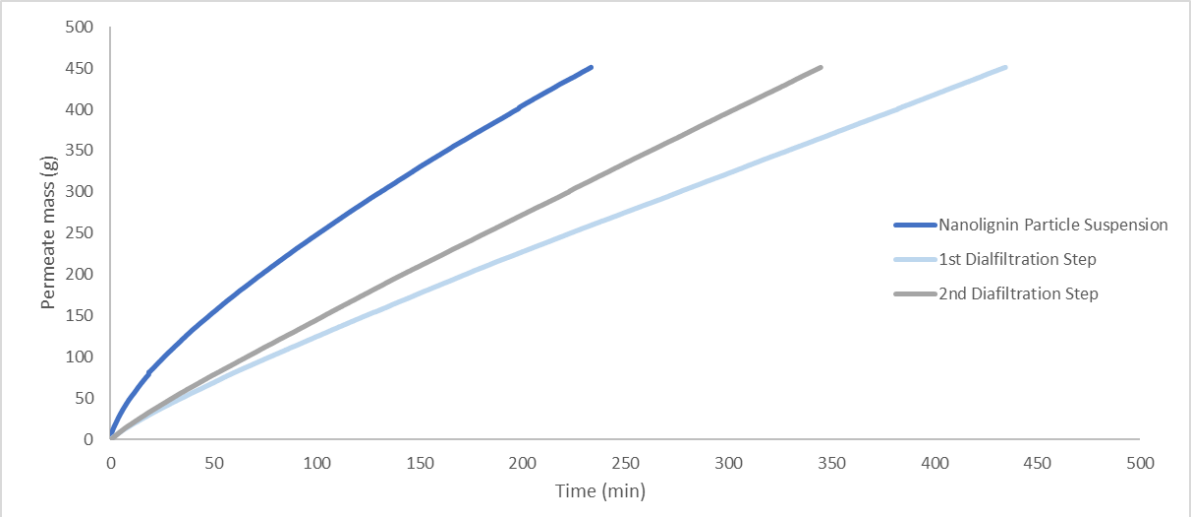

Figure 45. Permeate mass (g) over time (min) for the experiment at 4 bar and 0.7 L/min.

Table 18. Mean transmembrane fluxes for each filtration step of of experiment at 4 bar and 0.7 L/min.

UF/DF Step	Mean Transmembrane Flux (L/(m^2.h))
Initial Suspension Filtration	13.51
1st Diafiltration Step	7.71
2nd Diafiltration Step	9.84

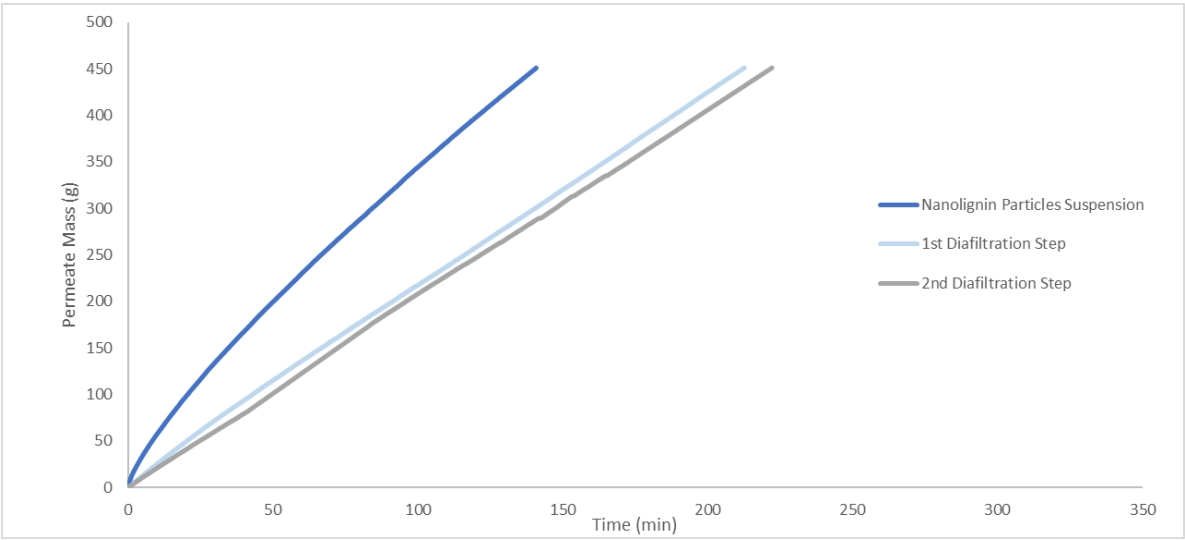

Figure 46. Permeate mass (g) over time (min) for the experiments at 4 bar and 2 L/min.

Table 19. Mean transmembrane fluxes for each filtration step of of experiment at 4 bar and 2 L/min.

UF/DF Step	Mean Transmembrane Flux (L/(m^2.h))
Initial Suspension Filtration	23.28
1st Diafiltration Step	16.00
2nd Diafiltration Step	15.59

To begin with, there is a significant difference between the transmembrane fluxes for both experiments at 8 bar and 0.7 L/min for all the different UF/DF steps. These experiments were performed using a different membrane sheet which can explain these differences. More experiments using the same conditions needed to be conducted in order to take conclusions about the repeatability of the experiments When comparing the results for the three different experiments using different transmembrane pressures and feed flow-rates it is shown that the nanolignin particle suspension takes less time to be concentrated until a certain volume (based on the amount of collected permeate) when using a pressure of 4 bar and 2 L/min of feed flow-rate. For the experiments at the same feed flow-rate (0.7 L/min), the experiment at 4 bar took longer to collect the same amount of permeate for the 1st and 2nd Diafiltration Steps, this might show that the fouling effect is more intense at lower pressures when using the same feed flow-rate, decreasing the transmembrane fluxes. On the other hand, for the experiments at 0.7 L/min, the difference in the transmembrane fluxes of the 1st and 2nd Diafiltration steps is bigger at 4 bar than at 8. This might mean that the second addition of water has a more prominent effect in cleaning the membrane at 4 bar than at 8.

Finally, for the experiment at 4 bar and 2 L/min of feed flow-rate it is possible to see that the slope decreases for each filtration step, which means the addition of water does not have a noticeable effect in cleaning the membrane, and consequently increasing the transmembrane flux. Nevertheless, these are the experimental conditions that give higher transmembrane fluxes for all the DF/UF steps.

The operating conditions that allow an optimization in the separation and purification of nanolignin particles should be the one that shows higher transmembrane fluxes in the first ultrafiltration step, as higher fluxes mean the membrane is less affected by fouling phenomena in the first filtration step. On the other hand, the difference between the flux decrease from the first suspension step to the first diafiltration step should be the smallest. The transmembrane flux decrease for these two steps is 28% for the new experiment at 8 bar and 0.7 L/min, 42% for the experiment at 4 bar and 0.7 L/min and 31% for the experiment at 4 bar and 2 L/min. Only with the transmembrane fluxes it is not possible to verify the best experimental conditions and it is also necessary to evaluate the membrane fouling effect.

4.2.3 Assessment of membrane fouling

As previously done for the experiments using different MWCO membranes, the final transmembrane flux was calculated by flushing a 15 % ethanol solution through the membrane after all the UF/DF experiments using the nanolignin particles suspension were done and measuring the permeate mass over time.

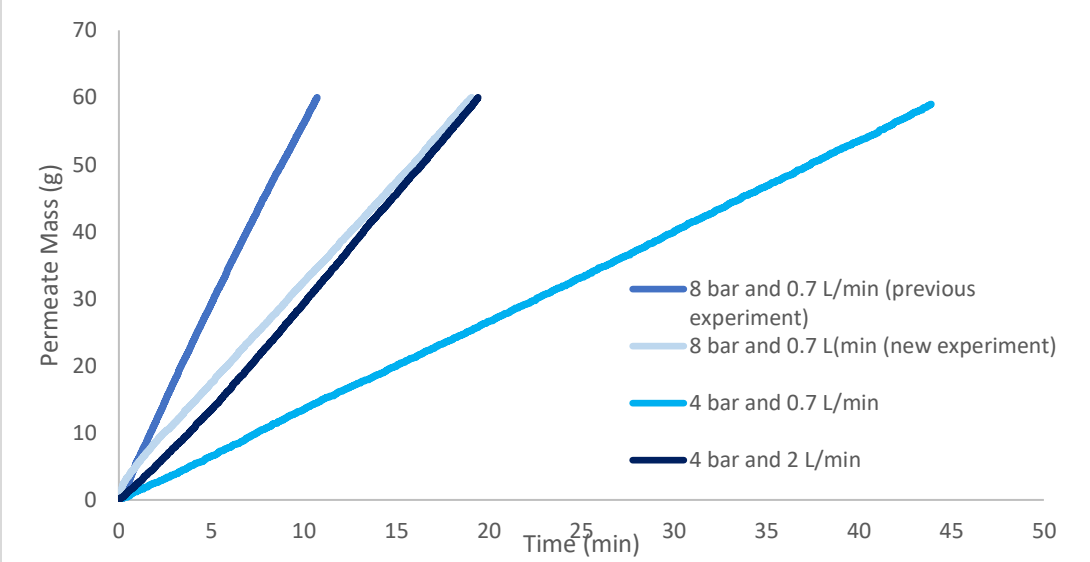

Figure 47. Permeate mass (g) over time (min) for a 15 % ethanol solution after all the UF/DF experiments using the nanolignin particle suspension.

The results in Figure 47 show that the experiments at 4 bar show the lowest slope which means the lowest transmembrane flux, specially the experiment at 4 bar and 0.7 L/min. Figure 48 shows the initial and final calculated transmembrane flux for the optimization experiments. The first column of each color represents the initial transmembrane flux and the second represents the final transmembrane flux for each different experiment.

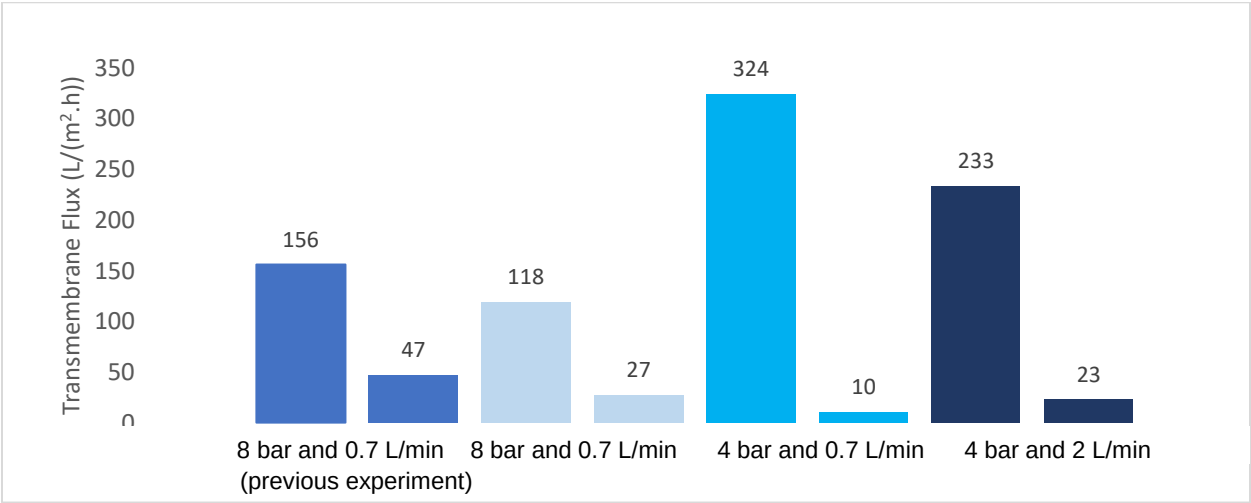

Figure 48. Initial and final transmembrane flux for the 30 kDa performance experiment.

Table 20. % of flux decline for each experiment.

Experiment	% of flux decline
8 bar and 0.7 L/min (previous experiment)	69.9%
8 bar and 0.7 L/min	77.1%
4 bar and 0.7 L/min	96.9%

4 bar and 2 L/min	90.1%

In Figure 48 and Table 20 is possible to see that the first experiment made in the new series of experiments with the 30 kDa membrane gives different results when compared with the previous experiment made in the same conditions. The initial transmembrane flux for the experiment repetition has a difference of approximately 24 % when compared with the first experiment. On the other hand, the final transmembrane flux for both experiments at 8 bar and 0.7 L/min is also relatively different. As the membranes used for the experiments were cut from different membrane sheets, it is expected that they would behave slightly different. Furthermore, prior to the measurement of the initial transmembrane flux the cross-flow system was cleaned. As it is not possible to guaranteed that the cleaning process was as efficient in one experiment as it was for the other, that can also affect the mass of permeate that goes through the membrane over time. Further experiments are necessary to evaluate how membranes with the same MWCO and composition behave when using the same operating conditions.

Another result that was not expected, was the difference in the initial transmembrane flux between the 8 bar and 0.7 L/min experiment and the 4 bar and 0.7 L/min experiment. Usually, increasing the pressure of the system, increases the transmembrane flux. There is the possibility that increasing the pressure, will compress the membrane, which reduces the membrane volume and consequently the permeate flux. On the other hand, using a hydroalcoholic solution with 15% ethanol is completely different than using pure water, which can explain the difference to the results expected from using water. Further experiments with the same conditions needed to be done to conclude if this type of membrane is compressible and what is the effect of the pressure and the feed flow-rate in the passage of ethanol molecules through the membrane.

Finally, the experiment at 4 bar and different flow rates also shows a difference in the initial transmembrane flux of 28 %, which is in the acceptable range expected between different sheets of membranes. For these two experiments the results show what was expected. The final transmembrane flux is higher in the experiment with flow-rate of 2 L/min, as increasing the feed flow-rate, increases the turbulence of the fluid which decreases the concentration polarization effect (explained in detail in chapter 2.2.4), which decreases the fouling.

As for the comparison of all the experiments, it is possible to see in Figure 48 that even with decreasing the pressure and increasing the flow-rate, the experiment that shows the smaller difference between the initial and the final transmembrane flux is the experiment at 8 bar and 0.7 L/min.

On the other hand, Figure 49, shows photographs of the membranes used, for each experiment after each filtration step. Based on the images, the experiment at 4 bar and 2 L/min show a less evident layer of lignin on the membrane surface. This result, shows, that even if the transmembrane flux decline is higher for the experiments at 4 bar and 2 L/min, the fouling effect does seem less evident with these experimental conditions.

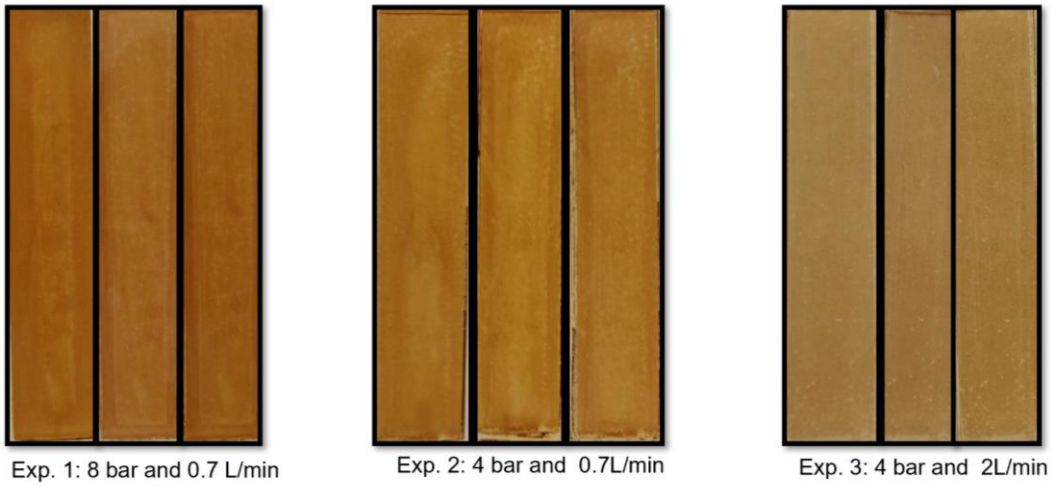

Figure 49. Membrane photos at the end of each UF/DF for the different experiments.

4.2.4 Analytics

4.2.4.1 Particle Sizing

As it was made for the first membrane experiments, the particle size of all the samples (retentates and permeates) was measured. Once again it was proved that the particle size of the nanolignin particles over time and over experiments was kept approximately constant and in the expected range (Beisl, Loidolt, et al. 2018). No particles were detected in the permeate samples which concludes once again that there are no nanolignin particles in the permeate. The next graphic (Figure 50) show the particle size for all the optimization experiments.

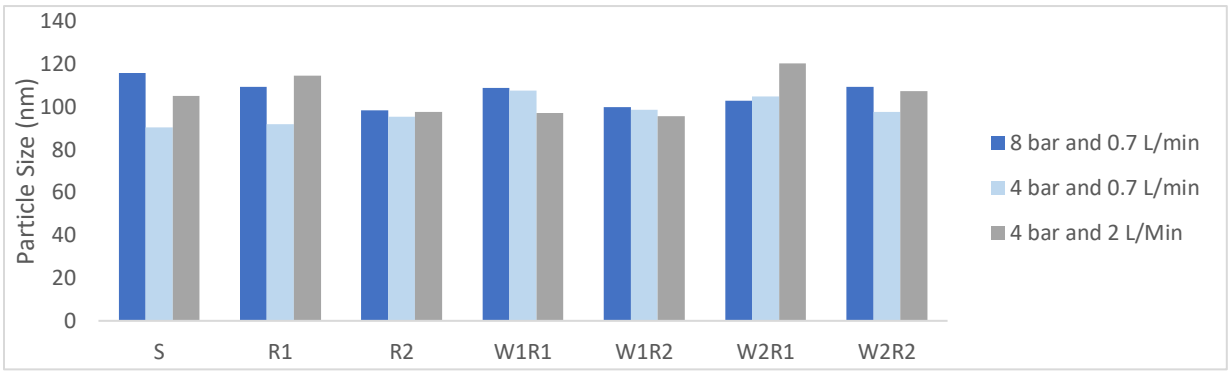

Figure 50. Particle Size measurement for performance experiments with 30 kDa membrane.

4.2.4.2 Ethanol Content

The same method used in the previous experiments to measure the ethanol concentration in the samples over the filtration process was used for the 30 kDa membrane performance experiments. The graphics below (Figure 51 to Figure 53), show the ethanol concentration variation for all the steps of the filtration process for the three experiments. It was expected that the ethanol concentration for the samples after

centrifugation was slightly higher than in the samples before centrifugation, as with the centrifugation at 288000g, the ethanol amount does not change, only the total volume of the solution changes.

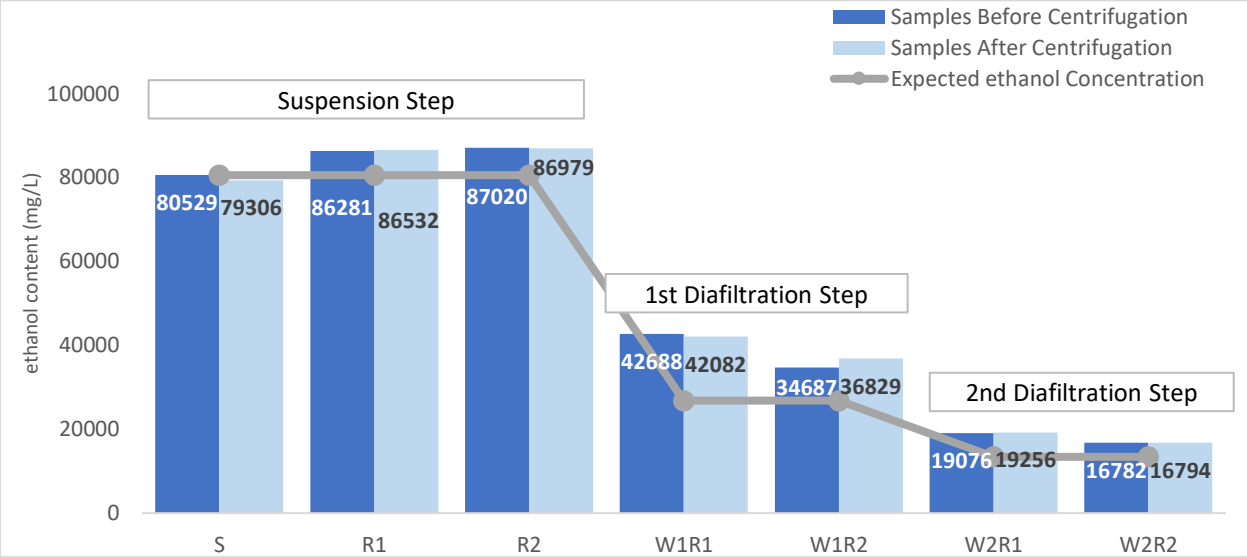

Figure 51. Ethanol concentration (mg/L) for the 8 bar and 0.7 L/min experiment.

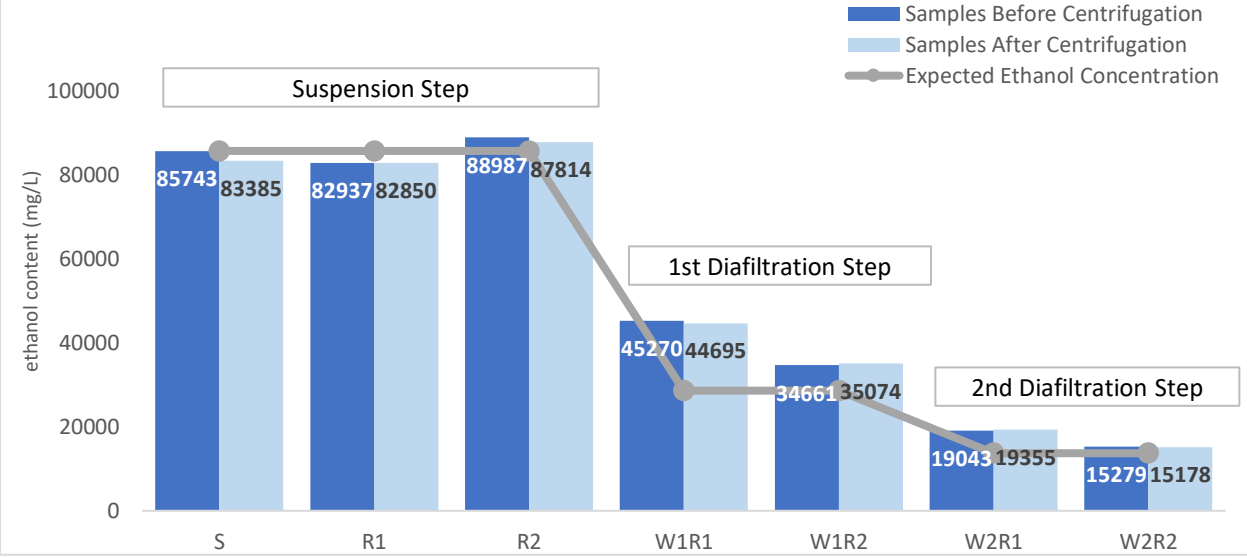

Figure 52. Ethanol concentration (mg/L) for the 4 bar and 0.7 L/min experiment.

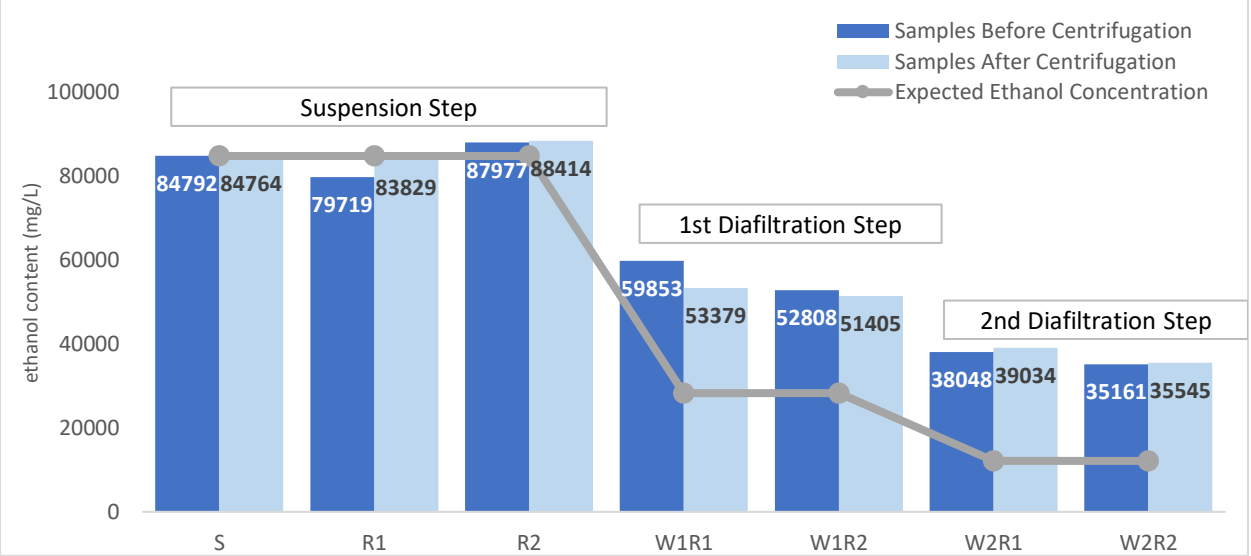

Figure 53. Ethanol concentration (mg/L) for the 4 bar and 2 L/min experiment.

According to the graphics above (Figure 51 to Figure 53), the ethanol concentration varies between the first filtration step retentates, this could be due to errors associated with the measurements. For the two experiments at 0.7 L/min it seems that the addition of water as approximately the same effect in both experiments. When comparing the ethanol concentration profiles of these experiments using the 30kDa membrane with the previous one made using the 30kDa membrane (Figure 30) , the decrease in the concentration after the addition of water is more evident, which could imply that something went wrong with the first experiment. For the optimization experiments, it is expected that the better conditions are the ones in which the ethanol concentration in the final retentate (W2R2) is lower for the same final volume of concentrated nanolignin suspension. Based on that, the operating conditions that seems to be more efficient are 4 bar and 0.7 L/min.

4.2.4.3 Total Organic Carbon Content

The TOC results for the optimization experiments using the 30kDa membrane is shown in Figure 54 to Figure 56.

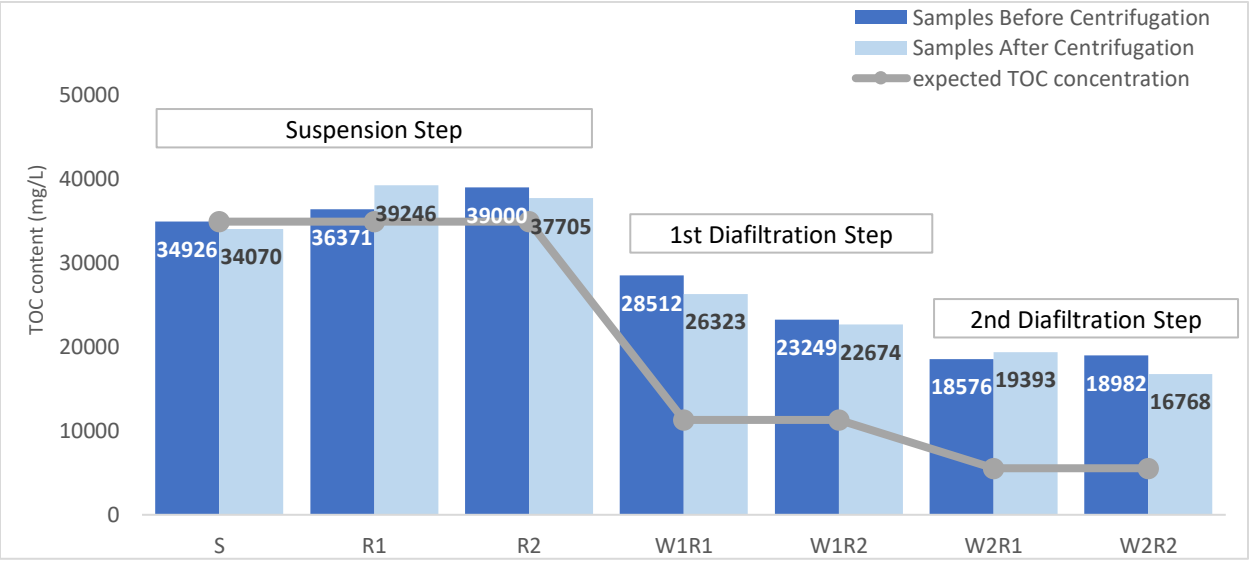

Figure 54. TOC concentration (mg/L) for the 8 bar and 0.7 L/min experiment.

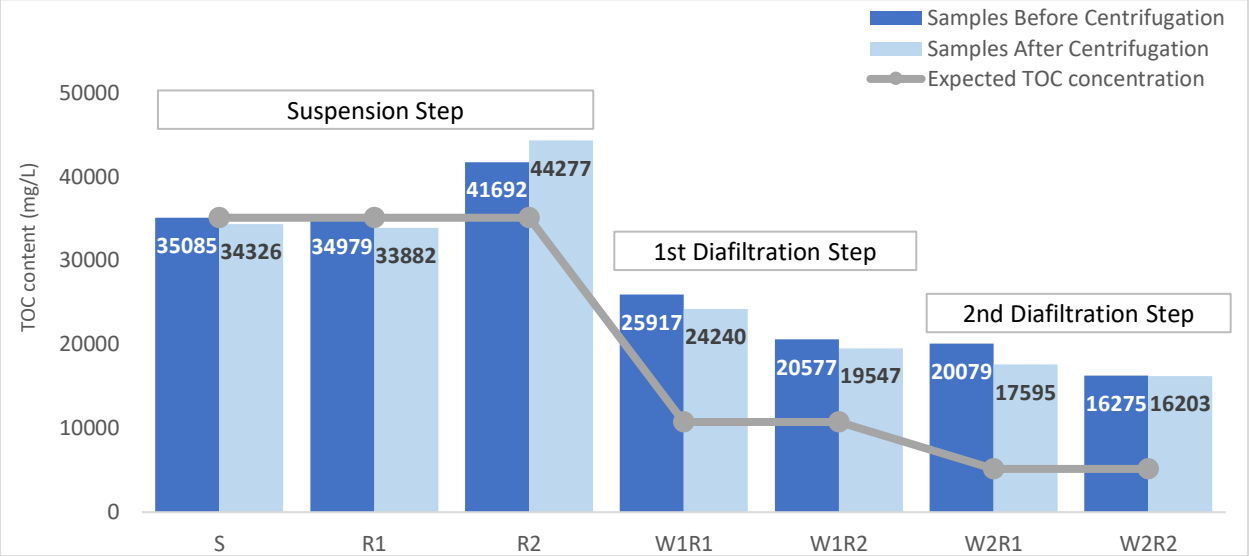

Figure 55. TOC content (mg/L) for experiment at 4 bar and 0.7 L/min.

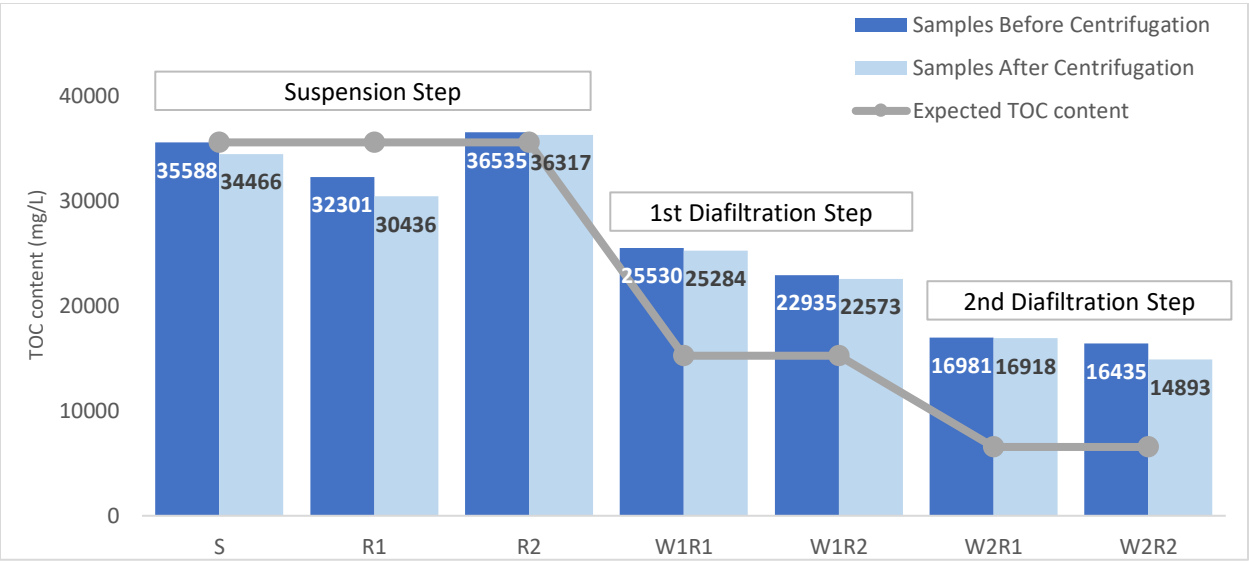

Figure 56. TOC concentration (mg/L) for experiment at 4 bar and 2 L/min.

The TOC concentration includes not only the ethanol content but other components, such as the nanolignin particles and the dissolved lignin. For all the experiments, the TOC content variation within the first filtration step could be mainly due to errors associated with this analytical method and fluctuations in the amount of nanolignin particles in the membrane that go back to the bulk solution, varying the TOC concentration. The second retentate after the addition of water for both diafiltration steps (W1R2 and W2R2) indicates that over time, the addition of water slightly cleans the membrane, increasing the rate of the dissolved components that go through the membrane, decreasing the concentration but it is not possible to prove this, has it can be also associated with errors. Based on the expected TOC contents calculated using the amount of water added for each filtration steps, these experiments can still be improved to decrease the final amount of TOC in the nanolignin particle suspension.

The best operating conditions for this separation process should be the ones in which the concentration of TOC in the last retentate (W2R2) for the same volume of concentrated nanolignin suspension is lower when compared to the initial nanolignin suspension. To conclude which experimental conditions are the best, the removal efficiency of the dissolved components was calculated, as it is more accurate to compare based on the TOC amount instead of concentrations.

4.2.4.3.1 Removal efficiency of dissolved components for TC analysis

The TOC mass balances used in the optimization experiments are the same used for the experiments using different MWCO membranes, which is based on equation (22). The results for these mass balances are shown in Table 21.

Table 21. TOC amount (mg) used for the mass balance of TOC for each membrane experiment.

Experiment	8 bar and 0.7 L/min	4 bar and 0.7 L/min	4 bar and 2 L/min
TOC initial suspension (mg)	41518	41970	42139
TOC final retentate (W2R2) (mg)	10473	8533	11563
TOC all samples taken (mg)	5898	5690	5329
TOC all permeates (mg)	53571	65229	40812
Mass Balance result (equation (22))	-28426	-37483	-15566

The mass balances for the TOC amount do not close, which can be due to errors associated with the measurements. Since the mass balances results are not reliable the calculation of the removal efficiency (RE) of the dissolved components for this membrane gives dubious results, with values higher than 100%, which once again proves the unreliability of this analytical method for this type of suspension. The RE for these experiments was calculated based on equation (26). The total organic carbon amount used for the initial suspension is value obtained from the supernatant of the initial suspension after centrifugation to use only the TOC related with the dissolved components and not with the nanolignin particles.

$$RE = \frac{\sum_{i=1}^{6} TOC_{permeates}}{TOC_{initial}} \quad (26)$$

Where,

$TOC_{permeate}$ = TOC amount in each permeate (P1, P2, W1P1, W1P2, W2P1, W2P2), mg.

$TOC_{initial}$ = TOC amount of dissolved components in the initial suspension, mg.

The results obtained for this comparison method are shown in Table 22.

Table 22. Removal efficiency (%) of dissolved components for TOC analysis.

Experiment	RE of dissolved components (%)
8 bar and 0.7 L/min	129.0%

4 bar and 0.7 L/min	155.4%
4 bar and 2 L/min	96.9%

The TOC concentration of all the permeates collected during the experiments is shown in Figure 57.

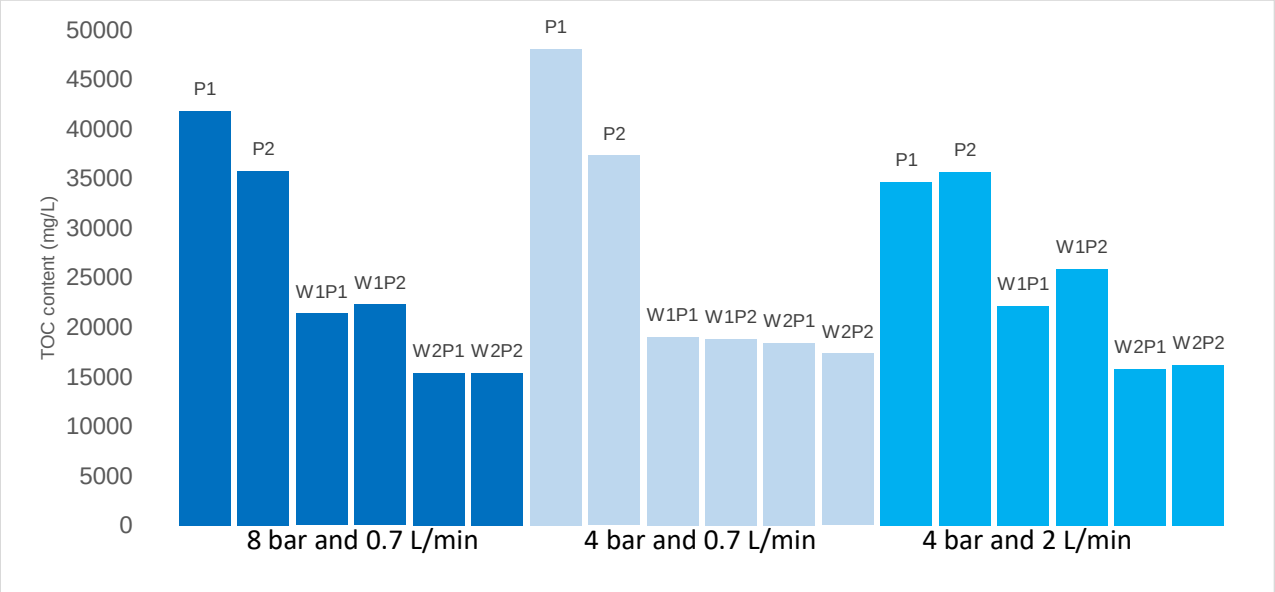

Figure 57. TOC concentration (mg/L) for all the permeates of all experiments.

Since the results were once again unreliable for this experiment, the dry matter content was analyzed since it is a more dependable method of comparison.

4.2.4.4 Dry Matter Content

The dry matter concentration was measured for all the retentate and permeate samples of the different experiments. The graphics below (Figure 58 to Figure 60), show the results obtained for the three different experiments made for the 30 kDa membrane performance experiments.

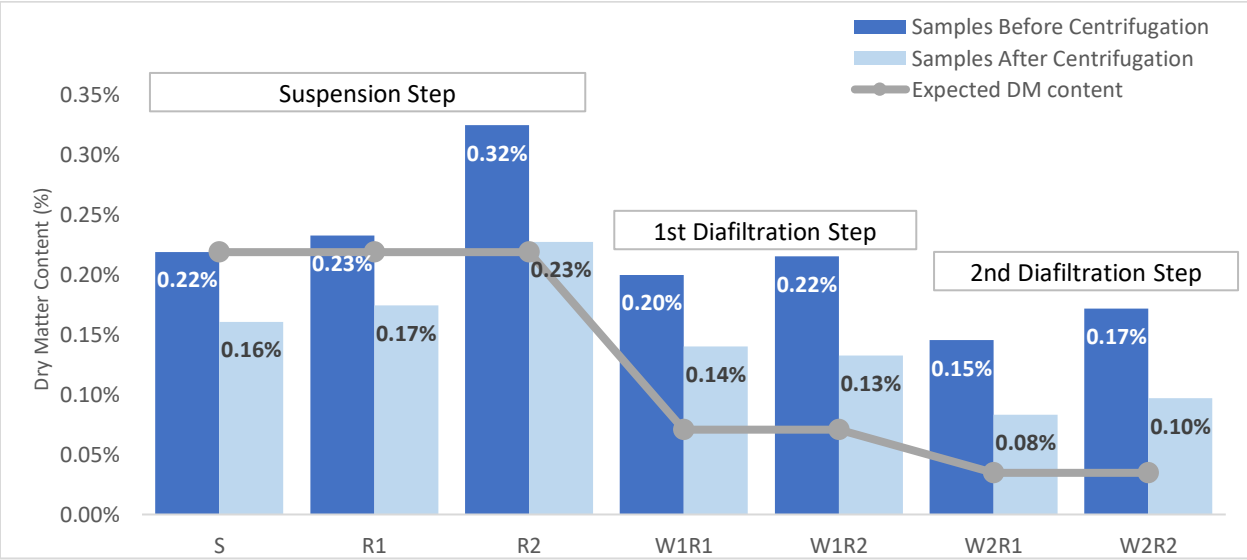

Figure 58. Dry matter concentration (g of lignin/g of solution) for 8 bar and 0.7 L/min experiment.

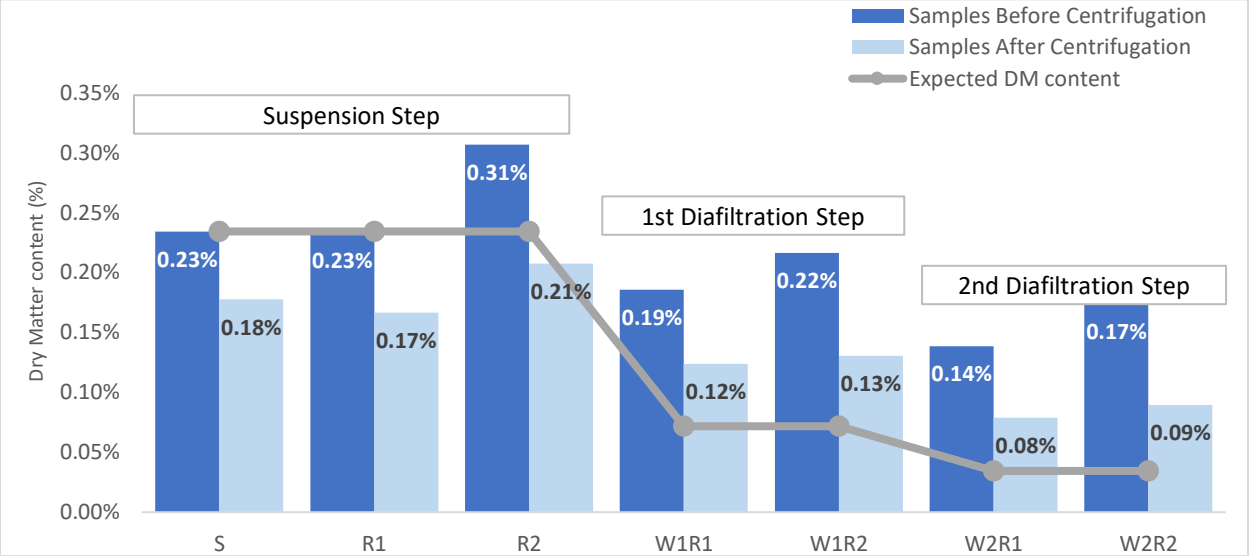

Figure 59. Dry matter concentration (g of lignin/g of solution) for 4 bar and 0.7 L/min experiment.

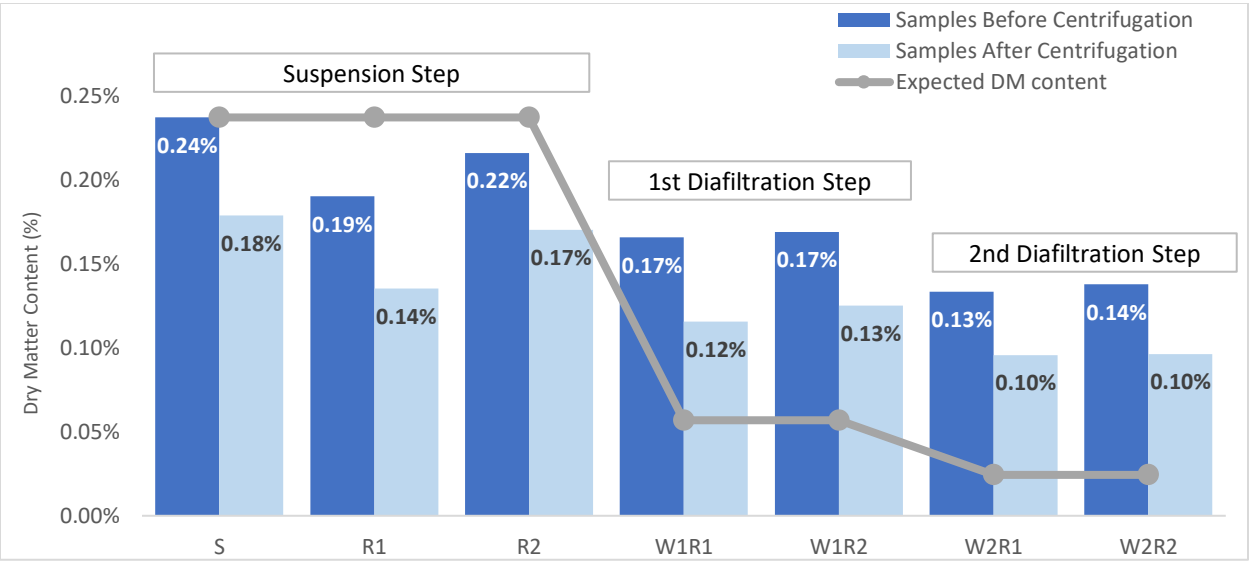

Figure 60. Dry matter concentration (g of lignin/g of solution) for 4 bar and 2 L/min experiment.

For both the experiments at 0.7 L/min (8 and 4 bar) (Figure 58 and Figure 59) the DM concentration before centrifugation is higher at the end of the first filtration step. It is possible that, for these experiments, the volume of solution decreases faster, for the same amount of nanolignin in the retentate, increasing the DM concentration. The same result would be expected for the experiment at 4 bar and 2 L/min, since this is the experiment with highest transmembrane flux in the first filtration step.

Based on the expected DM content, calculated based on the amount of water added in the diafiltration steps, the DM content of the samples was expected to be lower for all experiments for the two diafiltration steps. If the addition of water helps cleaning the membrane, which reduces the nanolignin particle layer on the membrane surface, this will, over time, increase the DM concentration of samples before centrifugation, has more nanolignin particles are back into the bulk solution.

As for the experiment at 4 bar and 2 L/min (Figure 60), the initial dry matter concentration decreases from the initial suspension to the first retentate of the first filtration step. This proves, that the dissolved components that contribute to the dry matter are not passing through the membrane at the same rate as the total volume decreases. From the first retentate (R1) to the second one (R2) the concentration increases slightly as the membrane layer of nanolignin particles and other components is formed on the membrane surface. With the addition of water, the dry matter concentration decreases, as expected, but it is constant between retentate of the same filtration step, which means the layer formed on the membrane, is stable and not increasing in thickness.

The best operating conditions should be the ones in which the final DM concentration (W2R2) is lower, when compared with the one from the initial suspension, as the volumes of collect permeates are the same. Based on the DM results, it seems to be the experiment at 4 bar and 0.7 L/min. To confirm if these operating conditions are indeed the ones that allow better results, the removal efficiency of the dissolved components, which is based on the exact amounts of DM was calculated.

4.2.4.4.1 Removal efficiency of dissolved components for DM analysis

For the calculation of the removal efficiency of the dissolved components the mass balance previously described in equation (24) was used. The DM concentrations used, are the ones for the supernatant of the samples after centrifugation. Table 23 shows the results for the mass balances of the DM quantity.

Table 23. DM amount (mg) used for the mass balance of DM for each membrane experiment.

Membrane	8 bar and 0.7 L/min	4 bar and 0.7 L/min	4 bar and 2 L/min
DM initial suspension (mg)	1.926	2.129	2.145
DM final retentate (W2R2) (mg)	0.601	0.466	0.741
DM all samples taken (mg)	0.303	0.283	0.257
DM all permeates (mg)	1.151	1.300	1.145
Mass Balance result (mg)	-0.129	0.080	0.002

The mass balances for the DM amount do not close, which can be due to the accumulation of nanolignin particles on the membrane surface, which vary within all UF/DF experiment and can influence the DM concentration at a certain moment and errors associated with the measurements. Nevertheless, the mass balances for the DM seem more reliable than the TOC mass balances. The removal efficiency of dissolved components from the initial nanolignin particle solution was calculated based on equation (25). The results of these calculations are shown in Table 24.

Table 24. Removal efficiency of dissolved components for the experiments at different conditions.

Membrane	RE of the dissolved components (%)
8 bar and 0.7 L/min	59.8%
4 bar and 0.7 L/min	61.1%

4 bar and 2 L/min	53.4%

Based on the results shown on Table 24, the operating conditions that show highest removal efficiency of dissolved components from the initial suspension are at 4 bar and 0.7 L/min.

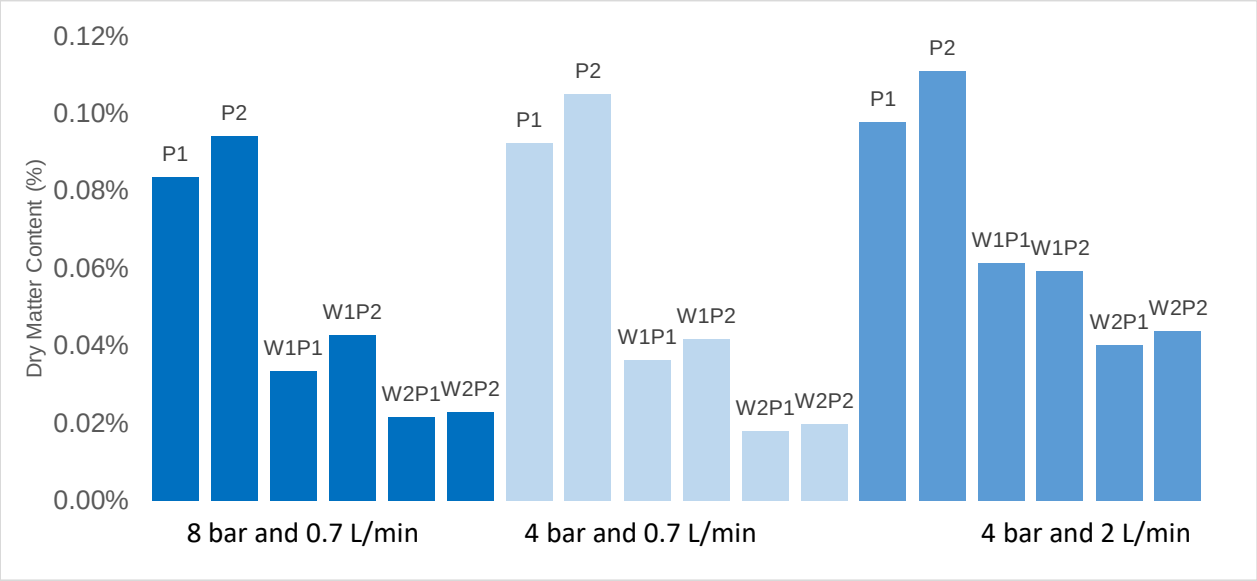

Figure 61. Dry matter concentration for all the permeates for all different conditions experiments.

The results from the removal efficiency of the dissolved components show, that the lowest pressure and lowest flow-rate were the most efficient experimental conditions to separate the nanolignin particles from the dissolved components present in the suspension, as this experiment shows the lowest removal efficiency dissolved components that do not go through the membrane. Nevertheless, the obtained results are quite similar, so it would be important to repeat each experiment several time to guarantee the repeatability of the results.

4.3 Scanning Electron Microscopy

As previously mentioned in chapter 3.4.3, SEM analysis was performed to all the membranes after UF/DF experiments. For the membranes used in the experiments using different MWCO membranes the membrane surface was scanned and for the 30 kDa membranes used in the performance experiments cross-sections of the membrane sheets were scanned.

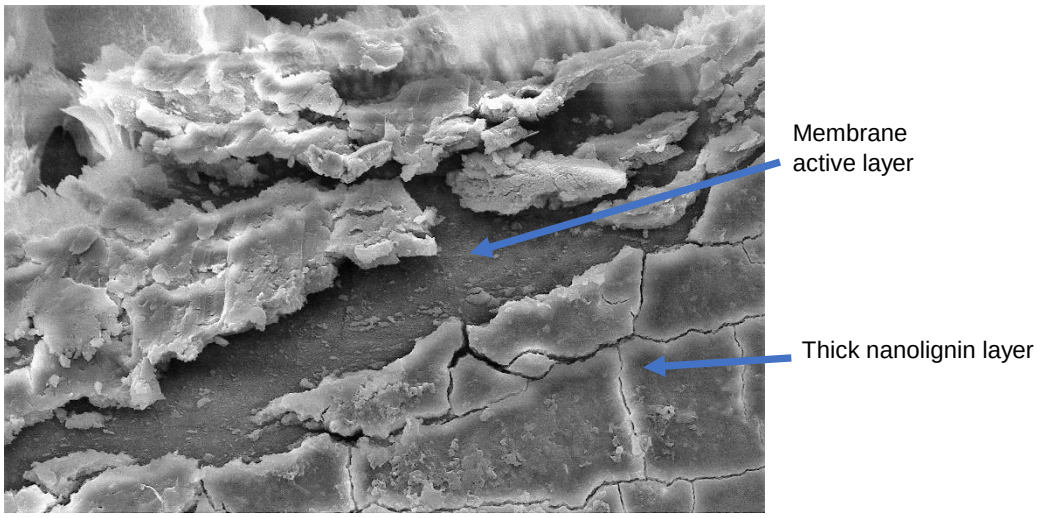

Figure 62. 10 kDa membrane surface with a zoom of 5000x.

In Figure 62 is shown a SEM picture of the 10 kDa membrane surface in which is possible to see the membrane active layer and the thick nanolignin particles layer that is formed on the membrane surface.

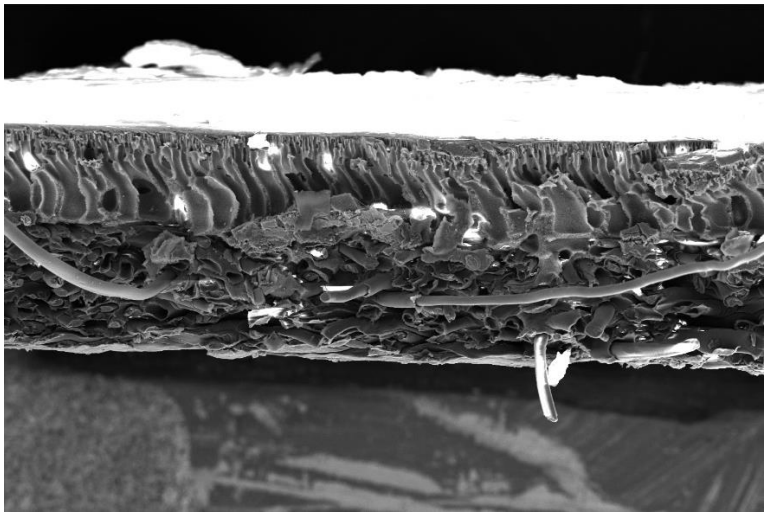

Figure 63. 30 kDa membrane cross-section with a zoom of 500x.

In Figure 63 it is shown a SEM picture of the 30 kDa membrane cross-section. It is possible to see the membrane is made of a support material, which is polypropylene (Microdyn-Nadir 2018). On the other hand, ultrafiltration membranes are usually anisotropic. This membrane characteristic shows the porous layer of the membrane is divided in two layers, the top layer is made of small pores while the lower layer has bigger pore sizes and works as a support layer of the membrane.

5 Conclusions/ Outlook

The conclusions related with this work are made only for wheat straw lignin that was pre-treated with Organosolv technique using ethanol as an organic solvent. Also, the precipitation method using only water as anti-solvent at a specific ratio produces specific shapes and particle sizes different than other precipitation methods. The literature review showed that depending on the source of lignin and the pre-treatment made to this molecule, the results can be completely different. Since this happens, the precipitation of nanolignin particles is also dependent on the same parameters.

The particle size analysis showed that all the membranes from 10 kDa to 50 kDa were able to retain the produced nanoparticles of lignin, since no nanolignin particles were found in the collected permeates. Also, the particle size was constant over the filtration process for all the membranes, which shows that during the ultrafiltration process there is no nanolignin particles agglomeration.

Regarding the ethanol content analysis, it was possible to conclude that the transmembrane flux through the membrane is not even during the experiments, which affects the ethanol concentration at different stages of the UF/DF experiments. It is influenced by the membrane MWCO and by the addition of water in the Diafiltration steps. Concerning the optimization experiments, when using the 30 kDa membrane, the least efficient operating conditions are 4 bar and 2 L/min, as these are the conditions in which the expected concentration differs more from the obtained results (for the diafiltration steps).

The Total Organic Carbon (TOC) analysis showed, that the amount of nanolignin particles in the initial suspension was approximately the amount that was expected, since only 49 % of the dissolved lignin in the solution precipitates and forms nanolignin particles. Regarding the results of the retentate and permeate samples for the TOC analysis, it is not possible to take accurate conclusions, as this measurement method is subject to a lot of errors making it impossible to rely on the exact obtained values.

In conclusion, both the ethanol and TOC content analysis results are subject to a lot of errors and were not considered a reliable method for comparing the removal efficiency of dissolved components of a nanolignin particles suspension when using membranes with different MWCO and different operating conditions.

A more simplistic and yet reliable method for the analysis of the removal efficiency of dissolved components was the dry matter method which showed better results for the 30 kDa membrane with a value of approximately 47 %, showing that this membrane is the one that retains the least quantity of dissolved components.

To decrease the number of particles deposited on the membrane surface (fouling), several experiments were performed by changing the pressure and the feed flow-rate parameters. For the optimization experiments using the 30 kDa membrane the operating conditions that showed the most promising results was when using 4 bar and 0.7 L/min which had a removal efficiency of dissolved components of 61% but further experiments should be made to verify the reproducibility of this results. The next table, Table 25, summarizes all the results obtained for the experimental work performed on this thesis.

Table 25. Summary of all experimental conclusions.

Membrane MWCO	Operating conditions	Initial T.Flux (L/(m^2.h))	Final T.Flux (L/(m^2.h))	% flux decrease	DM initial suspension (%)	DM last retentate (W2R2) (%)	RE of dissolved components (%)
10kDa	8 bar and 0.7 L/min	325	16	95.1%	0.22	0.11	30.3%
20kDa	8 bar and 0.7 L/min	163	22	86.5 %	0.23	0.58 (not reliable	28.2%
30kDa	8 bar and 0.7L/min (1stexp.)	156	47	69.9%	0.22	0.11	47.0%
50kDa	8 bar and 0.7 L/min	290	37	87%	0.21	0.12	38.2%
30kDa	8 bar and 0.7L/min (2ndexp.)	118	27	77.1%	0.22	0.10	59.8%
30kDa	4 bar and 0.7 L/min	324	10	96.9%	0.23	0.09	61.1%
30kDa	4 bar and 2 L/min	233	23	90.1%	0.24	0.1	53.4%

For future work, firstly, it is necessary to repeat the experiments with the same conditions for several times, to verify if the results between the same experiments are reproduceable. In addition to that, it is important to find a way of thoroughly cleaning the cross-flow system set-up, as it was not possible to guarantee there were no particles left in the set-up that could give slightly different results. On the other hand, the fouling effect was prominent in all the different membranes, decreasing the efficiency of the separation and purification of the nanolignin particles. For future experiments it is necessary to find a way of cleaning the membrane and decreasing the fouling during the experiments, since the used techniques to decrease the fouling phenomenon did not work as good as expected.

Regarding the samples taken during the experiments, and additional sample of the nanolignin particle suspension immediately after the addition of water for each of the diafiltration step should be taken to better understand the difference of the addition of water.

As for the diafiltration steps, other experiments using more diafiltration steps could be performed to see if it is possible to improve the removal efficiency of the dissolved components from the nanolignin particle suspension.

6 References

Anon. 2010. *Total Organic Carbon Analyzer Manual*. Shimadzu Corporation.

Baker, Richard W. 2001. *Membrane Technology and Applications*. 2nd Editio. edited by T. Ennals. California: John Wiley & Sons.

Beisl, Stefan, Anton Friedl, and Angela Miltner. 2017. “Lignin from Micro- To Nanosize: Applications.” *International Journal of Molecular Sciences* 18(11):2367.

Beisl, Stefan, Anton Friedl, and Angela Miltner. 2018. “Lignin from Micro- To Nanosize: Production Methods.” *International Journal of Molecular Sciences* 18(6):1244.

Beisl, Stefan, Petra Loidolt, Angela Miltner, Michael Harasek, and Anton Friedl. 2018. “Production of Micro- and Nanoscale Lignin from Wheat Straw Using Different Precipitation Setups.” *Molecules* 23(3):633.

Bhongsuwan, Darunee and Tripob Bhongsuwan. 2008. “Preparation of Cellulose Acetate Membranes for Ultra- Nano- Filtrations.” *Kasetsart J. (Nat. Sci.)* 317:311–17.

FitzPatrick, M., P. Champagne, M. F. Cunningham, and R. A. Whitney. 2010. “A Biorefinery Processing Perspective: Treatment of Lignocellulosic Materials for the Production of Value-Added Products.” *Bioresour. Technol* 101(23):8915–22.

Gellerstedt, Göran and Gunnar Henriksson. 2008. “Major Sources, Structure and Properties.” in *Monomers, Polymers and Composites from Renewable Resources*, edited by M. N. Belgacem and A. Gandini. Netherlands.

Gordobil, Oihana, Rosana Moriana, Liming Zhang, Jalel Labidi, and Olena Sevastyanova. 2016. “Assesment of Technical Lignins for Uses in Biofuels and Biomaterials: Structure-Related Properties, Proximate Analysis and Chemical Modification.” *Industrial Crops and Products* 83:155–65. Retrieved (http://dx.doi.org/10.1016/j.indcrop.2015.12.048).

Liu, Fu, N. Awanis Hashim, Yutie Liu, M. R. Moghareh Abed, and K. Li. 2011. “Progress in the Production and Modification of PVDF Membranes.” *Journal of Membrane Science* 375(1–2):1–27.

Loidolt, Petra. 2017. “Master Thesis (Diplomarbeit), Herstellung von Lignin-Nanopartikeln Durch Direkte Ausfällung Aus Organosolv-Aufschlusslösungen.”

Lora, J. 2008. “Industrial Commercial Lignins: Sources, Properties and Applications.” in *Monomers, Polymers and Composites from Renewable Resources*, edited by M. . Belgacem and A. Gandini. Amsterdam: Elsevier.

Lora, Jairo H. and Wolfgang G. Glasser. 2002. “Recent Industrial Applications of Lignin: A Sustainable Alternative to Nonrenewable Materials.” *Journal of Polymers and the Environment* 10(1–2):39–48.

Luque, Susana, Daniel Gómez, and José R. Álvarez. 2008. “Industrial Applications of Porous Ceramic Membranes (Pressure-Driven Processes).” in *Inorganic Membranes: Synthesis, Characterization and Applications*, edited by R. Mallada and M. Menéndez. Amsterdam: Elsevier.

Merck Milipore. 2015. *Chemical Compatibility of Filter Components*. Retrieved (http://www.merckmillipore.com/INTERSHOP/web/WFS/Merck-PT-Site/en_US/-/EUR/ShowDocument-Pronet?id=201510.400).

Microdyn-Nadir. 2017. “Membrane Chemistry (Acetate Cellulose vs. Thin Film Composite.” Retrieved (https://static1.squarespace.com/static/54e2b7aee4b0902efd671f90/t/5a6f7afbc830254f3362aba2/1517255420924/TB-017+Membrane+Chemistry+-+Cellulose+Acetate+%26+Thin-Film+Composite+RevB.pdf).

Microdyn-Nadir. 2018. “NADIR UH030 Flat Sheet.” 639233. Retrieved (https://www.microdyn-nadir.com/fileadmin/user_upload/UH030_P_Flat_Sheet_Membrane.pdf).

Mohan, D., C. U. Pittman, and P. H. Steele. 2006. “Single, Binary and Multi-Component Adsorption of Copper and Cadmium from Aqueous Solutions on Kraft Lignin - a Biosorbent.” *Jornal of Colloid and Interface Science* 297(2):489–504.

Mosier, Nathan et al. 2005. “Features of Promising Technologies for Pretreatment of Lignocellulosic Biomass.” *Bioresource Technology* 96(6):673–86.

Mulder, M. 1996. *Basic Principles Of Membrane Technology,*. Dordrecht: Kluwer Academic Publishers.

Nunes, S. P. and Peinemann K.-V. 2001. *Membrane Technology in the Chemical Industry*. edited by S. P. Nunes and P. K.-V. Geesthacht: Wiley-VCH.

Ragauskas, Arthur J. et al. 2014. “Lignin Valorization: Improving Lignin Processing in the Biorefinery.” *Science* 344(6185).

Rana, D., T. Matsuura, R. M. Narbaitz, and C. Feng. 2005. “Development and Characterization of Novel Hydrophilic Surface Modifying Macromolecule for Polymeric Membranes.” 249:103–12.

Rastogi, S. and U. N. Dwivedi. 2008. “Manipulation of Lignin in Plants with Special Reference to O-Methyltransferase.” *Plant Science* (174):264–77.

del Río, José C., Jorge Rencoret, and Pepijn Prinsen. 2013. “Structural Characterization of Wheat Straw Lignin. Evidence for a Novel Monomer in Grasses.”

Strathmann, H. 1986. *Synthetic Membranes: Science, Engineering and Applications*. edited by P. . Bungay, H. Lonsdale, and M. N. Pinho. NATO ASI Series.

Vishtal, A. and A. Kraslawski. 2011. “Challenges in Industrial Applications of Technical Lignins.” 6(3):3547–68.

Xu, Feng, Jin-xia Sun, Runcang Sun, Paul Fowler, and Mark S. Baird. 2006. “Comparative Study of Organosolv Lignins from Wheat Straw.” 23:180–93.

Xu, T., N. Zhang, H. L. Nichols, D. Shi, and X. Wen. 2007. “Modification of Nanostructured Materials for Biomedical Applications.” *Mater. Sci. Eng.* 27(3):579–594.

Yebo, Li and Samir Kumar Khanal. 2016. *Bioenergy:Principles and Applications*. New Jersey, USA: Wiley-Blackwell.

Yu, Wenzheng, Lei Xu, Nigel Graham, and Jiuhui Qu. 2014. “Pre-Chlorination on Membrane Fouling.”

Zhu, LP. 2014. “Adsorption onto Membrane Surfaces.” in *Encyclopedia of Membranes*, edited by E. Drioli and L. Giorno. Berlin: Springer, Berlin, Heidelberg.

Appendix

A. Total Organic Carbon Content calibration methods

For the measurement of the total organic carbon, two different calibration curves methods were created. Firstly, a calibration curve method using different aqueous standard solutions of Potassium Hydrogen Phthalate ($C_8H_5KO_4$) with a carbon content of 47% was made, according to the TOC Analyzer Manual (Anon 2010). Afterwards, a calibration curve using know concentrations of ethanol content was made so it was possible to know the TOC associated with the ethanol content in the analyzed samples, based on equation (16). it is important for the calculation of the TOC associated with the nanolignin particles, to know the TOC amount associated with the ethanol in the sample Potassium Hydrogen Phthalate is one of the correct components for preparing calibration curves for TC analysis. For that purpose, the following steps were performed:

1) The needed amount of Potassium Hydrogen Phthalate was placed in the oven at 105-120 ºC for 1 hour and cooled in a desiccator for another hour.
2) 6.3765 g Potassium Hydrogen Phthalate were weighted in a glass watch.
3) The weighted mass was transferred to a volumetric flask of 1L and filled up with deionized water. (TOC concentration of approximately 3 g/L).
4) A dilution of 1:10 of the stock solution (approximately 0.3 g/L of TOC) and a dilution of 1:100 (approximately 0.03 g/L of TOC) were made.
5) The three different solutions were placed in the autosampler of the TC analyzer and auto-diluted to several levels.

Auto-dilutions with a factor of 3, 4, 6, 11 and 30 were made for all the three calibration curves to get carbon concentrations between 1000 mg/L and 1 mg/L of TOC.

The first calibration curve used the 3 g/L of total organic carbon solution, that was auto-diluted to be in a concentration range between 1000 and 100 mg/L of TOC. For this calibration an injection volume of 20 µL of Potassium Hydrogen Phthalate solution was used for each measurement. The obtained calibration curve is represented in Figure 64.

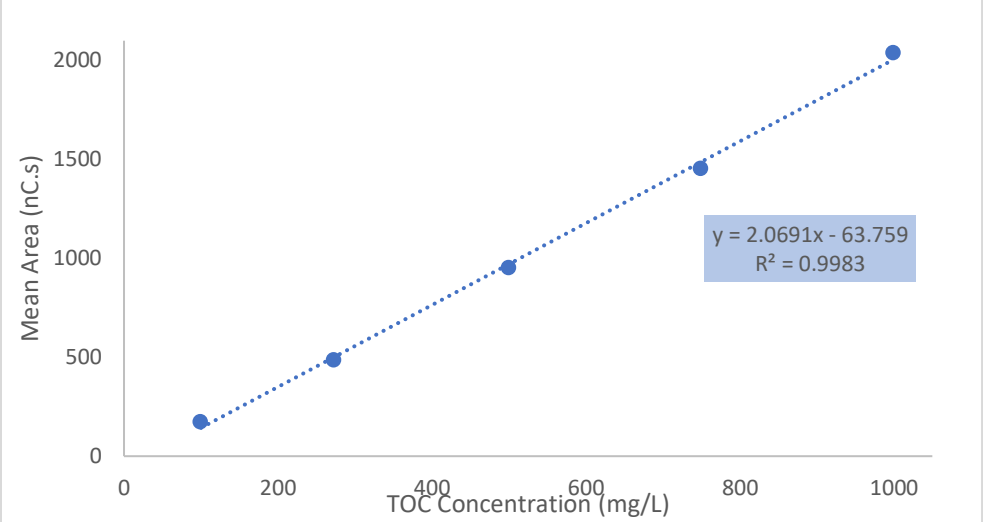

Figure 64. Calibration curve for TOC with a range between 1000 and 100 mg/L

The second and third calibration curves were made using the solutions with a TOC concentration of 0.3 and 0.03 g/L, respectively.

For these calibration curves an injection volume of 50 µL of solution was used for each measurement.

The obtained calibration curves are represented in Figure 65.

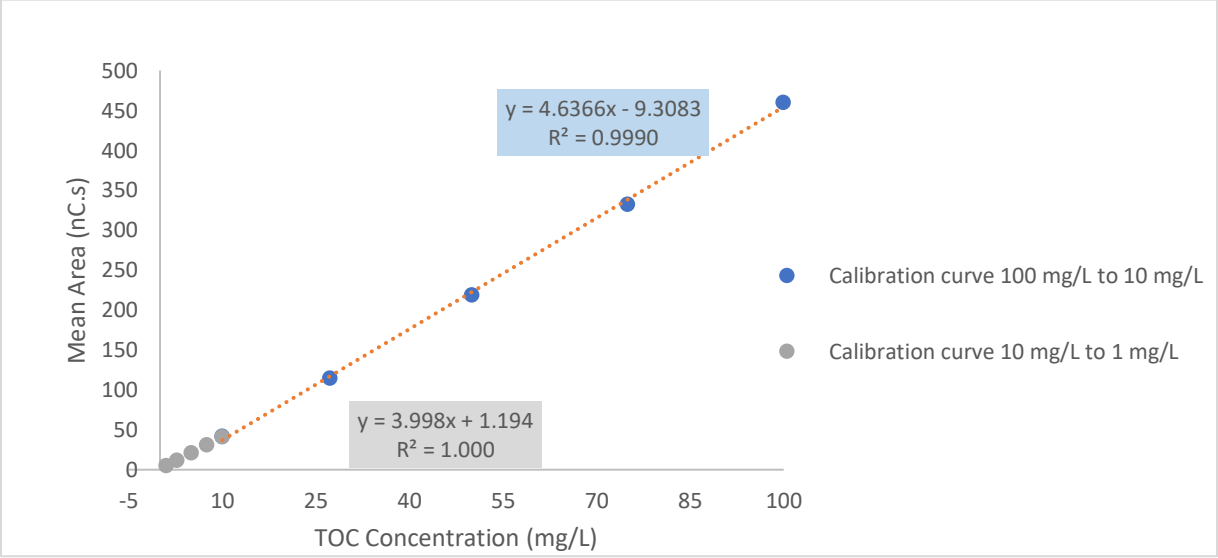

Figure 65. Calibration curves for TOC concentration with a range between 100 and 1 mg/L.

Based on equation (16), it is important for the calculation of the TOC associated with the nanolignin particles, to know the total organic carbon amount associated with the ethanol in the sample. For that purpose, an ethanol stock solution of 3 g/L of total organic carbon content was prepared. Then, the stock solution was placed in the autosampler and auto-diluted with a factor of 3,4,6,11 and 30 with deionized water (Ethanol has a carbon content of approximately 52%). Afterwards, a calibration curve that relates the carbon content of ethanol expected based on the initial solution prepared and the carbon content measured

with the TOC analyzer was created. This allowed to recalculate the carbon content associated with the ethanol for each sample that was expected in the TC analyzer, based on the carbon content results expected from the solutions. The calibration curve that relates the calculated TOC with the results from the TC analyzer are represented in Figure 66.

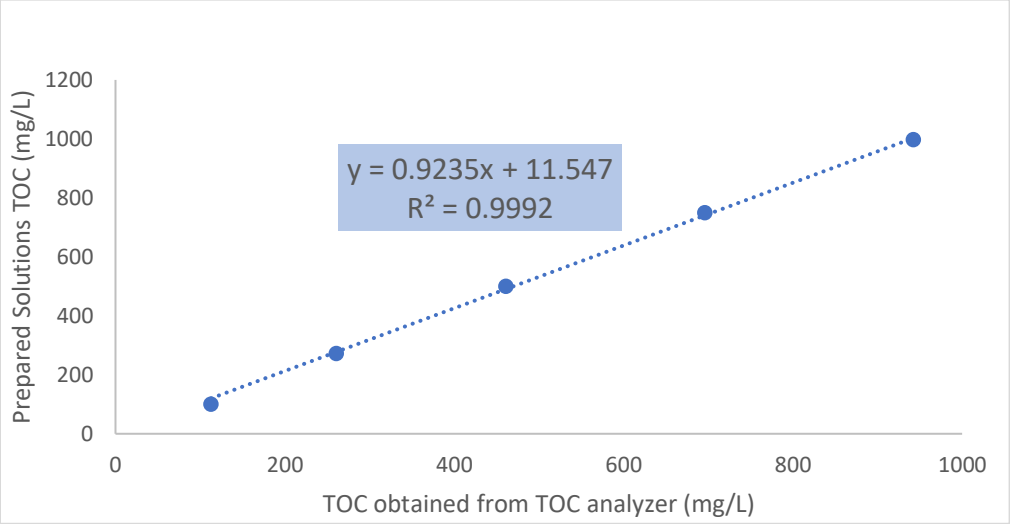

Figure 66. Calibration curve that relates expected ethanol TOC with ethanol TOC from calibration made in TOC analyzer.